UNIVERSITÀ DI PARMA

UNIVERSITA' DEGLI STUDI DI PARMA

DOTTORATO DI RICERCA IN

Scienze del Farmaco

CICLO XXXV

PARTICLE ENGINEERING APPLIED FOR DEVELOPMENT OF DRY POWDERS FOR INHALATION CONTAINING BIOTECHNOLOGICAL DRUGS

Coordinatore:

Chiar.mo Prof. Marco Mor

Tutore:

Chiar.ma Prof.ssa Francesca Buttini

Co-Tutore:

Chiar.mo Prof. Fabio Sonvico

Dottorando: Davide D'Angelo

Anni Accademici 2019/2020 – 2021/2022

INDEX

1. GENERAL INTRODUCTION 4

2. AIM 16

3. An Enhanced Dissolving Cyclosporin-A Inhalable Powder Efficiently Reduces SARS-COV-2 Infection *In Vitro* 17

3.1 Introduction 17

3.2 Materials 19

3.3 Methods 19

3.4 Results and Discussion 28

3.5 Conclusions 43

4. Calcium Phosphate Coated Liposome loaded with Cyclosporin-A as Inhalable Powder Improved the Anti-inflammatory Effect 50

4.1 Introduction 50

4.2 Materials 55

4.3 Methods 55

4.4 Results and Discussion 64

4.5 Conclusions 79

5. **Selection of Promising Bulking Agent for Pramlintide Respirability and Stability** 80

5.1 Introduction 80

5.2 Materials 83

5.3 Methods 83

5.4 Results and Discussion 87

5.5 Conclusions 105

6. REFERENCES 108

Abbreviations

API= Active Pharmaceutical Ingredient

BOS= Bronchiolitis Obliterative Syndrome

CaP=Calcium Phosphate

COVID-19= Coronavirus disease 2019

CQAs= Critical Quality Attributes

Cryo-TEM=Cryogenic Transmission Electron Microscopy

CsA= Cyclosporine A

DLS= Dynamic light scattering

DoE=Design of Experiment

DPI = Dry powder inhaler

DSC= Differential Scanning Calorimetry

ED= Emitted Dose

EF=Emitted Fraction

ELISA= Enzyme-Linked Immunosorbent Assay

FPD=Fine Particle Dose

FSI=Fast screening impactor

HA= Sodium Hyaluronate

HPLC= High Performance Liquid Chromatography

LOD= Loss on Drying

MMAD= Mass Median Aerodynamic Diameter

NGI= Next Generation Impactor

PDI = Polydispersity Index

RF= Respirable Fraction

rm= raw material

SARS-CoV-2= Severe Acute Respiratory Syndrome Coronavirus 2

SD=Spray Dried

SEM= Scanning Electron Microscopy

TGA= Thermogravimetric Analysis

WDT= Weibull Dissolution Time

XRPD= X-Ray Powder Diffraction

1. GENERAL INTRODUCTION

1.1 Inhalation therapy

Inhalation therapy has its roots about 4000 years ago for the inhalation of the alkaloids contained *in Datura stramonium* preparations [1–3]. To date, inhalation therapy, commonly used for pathologies such as asthma and chronic obstructive pulmonary disease, is attracting growing interest in the treatment of less common pathologies such as idiopathic pulmonary fibrosis, pulmonary arterial hypertension, bacterial infections associated with cystic fibrosis caused by *Pseudomonas aeruginosa and* non-tuberculous mycobacteria [4].

In general, the lung is characterized by a large contact surface area that is around 1 m^2/kg of body weight and low enzymatic activity [5]. Moreover, this route of administration reduces the effect of hepatic first-pass metabolism [6]. Because of the highly dispersed nature of an aerosol, good epithelial permeability and small aqueous volume at the absorbent surface, small molecules deposited in the lungs are absorbed very rapidly into the systemic circulation, with the fastest absorption of any delivery route other than intravenous [7]. Besides, drug-metabolizing enzymes are in much lower concentrations in the lungs than in the gastrointestinal tract and liver, and inhaled molecules that enter the circulation are less likely to be degraded than if they had been administered orally.

1.2 Local and systemic delivery

Inhalation administration allows the carrying of therapies with local or systemic effects. Local action is desirable to treat specific lung diseases, whose systemic treatment would result in an increase in dosage and associated side effects. The local effect is, for example, desirable for treatments with beta-2 agonist as *salbutamol* and formoterol or muscarinic antagonists, *e.g. tiotropium*, *glycopyrronium* or *aclidinium*, corticosteroids such as *beclomethasone*, *budesonide*, *fluticasone* and *mometasone*, used in

the treatment of asthma and chronic obstructive pulmonary disease (COPD) and antibiotics to treat local infections, whose higher pulmonary concentration would increase therapeutic efficacy [8, 9]. The use of broad-spectrum antibiotics in the treatment of pulmonary infections associated with cystic fibrosis has seen *Arykace®*, containing *amikacin* in liposomal form and administered by aerosolization, an interesting therapeutic strategy, to reduce the systemic toxicity of the antibiotic compared to the oral route thanks to the local action directed to the lung.

However, the lung represents an important access route to systemic circulation and represents a non-invasive route of administration. In particular, it would allow the absorption of macromolecules, which would otherwise require the parenteral administration and the subsequent use of needles, with the possible reduction of patient compliance. Moreover, the lung presents less enzymatic degradation or macromolecules is expected, with a significant increase in bioavailability [10].

1.2.1 Anatomical features of the lung

One of the main difficulties in the delivery of drugs to the lungs is the overcoming of some important obstacles due to peculiar anatomical and physiological characteristics of the lung. One of the main challenges is reaching the pulmonary periphery. The classic model of the airways of Weibel, states that starting from the trachea, with each division of the respiratory tree, 24 in total according to this model, two new smaller airways are formed, passing from about 1.8 cm of the trachea to about 0.04 cm [11]. Despite its complexity, the respiratory system can be simply divided into the conductive zone from generation 0 to 16 and the respiratory zone from generation 17: the conductive zone is involved in the transport of gas through the lung and therefore includes the main bronchi, its branches (bronchioles), and the main blood vessels or pulmonary veins and arteries [11]. The epithelium of the conductive zone of the lung consists of goblet cells, mucous glands, ciliated and brush cells covered by a mucous layer [6, 12]. Together, these cells form an initial barrier against airborne particles such as pollen and pathogens, and it is in these regions that mucociliary clearance occurs.

Mucociliary clearance, therefore, has the purpose of removing insoluble particles or any pathogens introduced with the air that have remained trapped in the mucous layer protecting the delicate lung epithelium and transported out of the respiratory tract by the coordinated movement of the cilia of the hair cells. This mechanism, in the case of inhalation powders, also acts in the removal of particles which have not rapidly passed the mucous layer and which, once trapped, will be eliminated [12].

The respiratory zone starts with the terminal bronchioles, which branch out in respiratory bronchioles to reach the alveolar ducts and alveolar sacs [6, 13]. Inhalable particles with an aerodynamic diameter between 1 and 5 μm have the ability to overcome this first barrier when they reach the pulmonary periphery. In particular, particles with an aerodynamic diameter out of this range if higher than 5 μm tend to deposit in the upper airways, while particles smaller than <0.5 μm, although they reach the pulmonary periphery, their deposition may not occur and may be exhaled [14].

The alveolar epithelium is characterized by a single layer of cells called type I and type II pneumocytes. The former are large, flat cells that make up the alveolus, which makes up about 95% of the alveoli, whose function falls within the gas exchange.

The gaseous exchanges take place in the alveoli not only due to the peculiar anatomy and vascularization of these cavities but also thanks to the important presence of substances that decrease the air-liquid surface tension. These substances, produced by type II alveolar cells, are mainly phospholipids and amphiphilic molecules, which therefore act as surfactants (Figure 1). These molecules will orient the hydrophilic portion towards the alveolar lining fluid while the hydrophobic alkyl chains towards the air, thus reducing the number of water molecules at the interface. In particular, about 80% of the phospholipids produced is represented by phosphatidylcholine (PC), which includes (dipalmitoyl-phosphatidylcholine, palmitoyl-myristoyl-phosphatidylcholine and palmitoyl-palmiteoyl-phosphatidylcholine [13, 15–17]. However the interaction of the drug with these molecules can limit the effect of the surfactant on the surface tension leading in some cases to the collapse of the alveoli and edema; furthermore, in the case of peptides and proteins, this layer containing surfactant can lead to the aggregation of the molecules [10].

Here the mucociliary clearance present in the upper airways does not occur and the removal of pathogens or any particles that have reached the respiratory bronchioles and alveoli depends on the action of alveolar macrophages. They represent about 1% of the alveolar cells; according to some estimates, between 12 and 14 macrophages are found in each alveolus [6]. The important presence of immunity cells makes pulmonary administration an interesting route of administration also for vaccines, although currently there are no vaccines administered by inhalation [18, 19]. However, the phagocytic action of macrophages is also influenced by the size of the inhaled particles as well as by the composition of the particles themselves. In particular, this activity seems to be lower for particles below 200 nm, while more efficient for particles between 3 and 6 μm [13]. The choice of excipients and particle size, therefore, play an essential role in the development of an inhalation formulation.

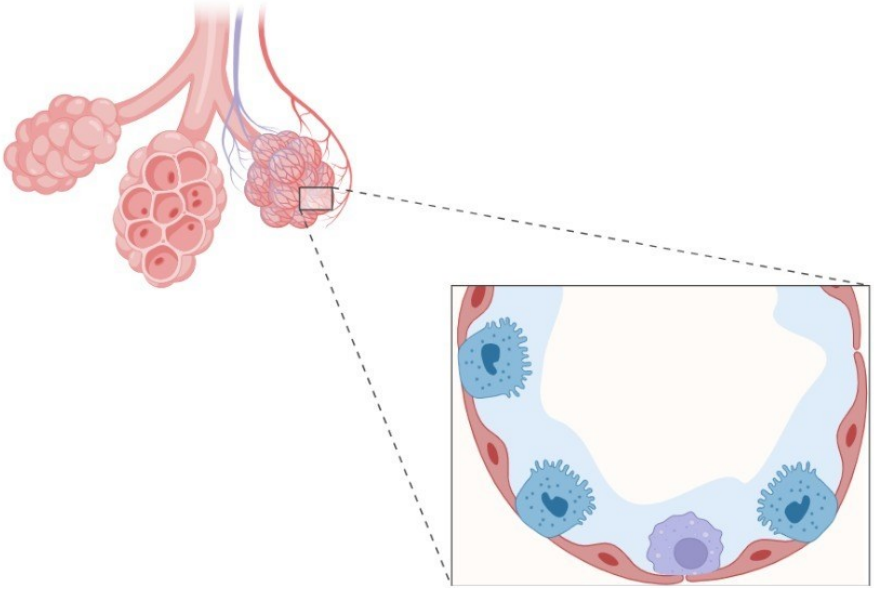

Figure 1. Schematic representation of a pulmonary alveolus. In the enlarged section red cells represent type I pneumocytes, blue cells represent type II pneumocytes, purple cell represents an alveolar macrophage. Created with BioRender.com

1.3 Delivery of biologics to the lungs

The delivery of biological macromolecules by the pulmonary route is today an important area of interest. Despite this, to date, most of the approved biologicals (more than 300) are still administered by injection and require the intervention of healthcare personnel and often the conservation of these formulations requires the use of the cold

chain to keep the structure of the macromolecules stable which in some cases can represent a limit for the distribution and administration of these drugs [20]. Currently, few commercial products contain biologicals, among which there is *Colobreathe®* in the form of micronized powder to be reconstituted, whose active ingredient is methosulphonated colistin, a cyclic peptide with an antibacterial action, *Afrezza®* containing insulin and deoxyribonuclease I, contained in *Pulmozyme®* for the treatment of cystic fibrosis [4, 10, 21].

Although some challenges in the delivery of biologics are common to all other inhaled drugs, such as reaching the pulmonary periphery and reducing particle clearance by mucociliary and macrophage clearance, the delivery of biologics to the lung is complicated by other factors. For example, an inverse correlation between molecular weight and absorption has been observed, which is higher for molecules with lower molecular weight [7]. However, it has also been observed that peptides with MW lower than 10 kDa are more susceptible to the effect of enzymatic hydrolysis. We must also consider some of the elements in common with small molecules, such as lipophilicity and the presence of specific transporters. The epithelium can be crossed by diffusion by lipophilic molecules; hydrophilic molecules can instead be actively transported inside the cell or cross the epithelia by passing through the tight junctions. Furthermore, also from the point of view of formulation of inhalation powders containing biological agents, some problems must be considered, for example, the possibility of the Maillard reaction in the case of the use of reducing sugars such as lactose and amino groups, the need to have a formulation with a low of humidity to avoid hydrolysis and degradation phenomena. Added to this is that the choice of excipients approved by the FDA to date for inhalation use is short and greatly restricts the list of possible excipients approved instead for other routes of administration, such as the oral one [22]; moreover, it is always necessary to maintain the lung functionality.

1.4 Dry Powder Inhalers

To date, inhalation therapy makes use of three main tools, nebulizers, pressurized metered dose inhalers (pMDI) and dry powder inhalers (DPI).

While nebulizers use solutions or suspensions in an aqueous medium or propellants in the case of pMDIs, DPIs contain the active ingredient and any excipients in the form of dry powder.

As far as the administration of biologicals by pulmonary route is concerned, pMDIs and nebulizers require the overcoming of some problems, which are more easily overcome with the use of DPIs, for example in pMDIs, the high pressure inside the canister could denature the active principle, and the delivered volume could represent a limit for the required dosage. Moreover, these devices also require the peculiar coordination between activation and inhalation, while as regards the nebulizers would require a long period for the administration of the dose (5-15 min); furthermore, macromolecules in the aqueous environment, proteins or peptides, could easily be hydrolysed, the heat and shear stress that can occur in some aerosolization processes could also, in this case, lead to denaturation of the biological active ingredient [20]. The formulation of a biological in the form of an inhaled powder would instead offer the possibility of stabilizing the macromolecule and of being able to administer it even at high doses, in a short time, and without the necessary coordination between activation of the device and the inspiratory act [20].

The main features of DPIs, therefore, reside in the characteristics of the powder and the design of the device [4].

The devices on the market today, although numerous, have some fundamental elements in common: a mouthpiece, a portion in which the powder is deagglomerated, the compartment in which the powder is contained, an air inlet [20, 23]. In DPIs defined as unit doses such as *Rotahaler®*, *Spinhaler®*, *RS01®*, *turbospin®*, and *Ultibro®* that can contain a single dose at a time which is manually loaded by the patient, multiple unit-dose devices can contain a series of capsules or a blister, such as *Diskus®* or *Genuair®* while other devices contain a reservoir such as *Turbohaler®* (Figure 2) [24].

In general, an ideal device should facilitate patient compliance and maximize treatment efficacy. This objective requires that the device possess some specific characteristics such as the possibility of emitting a sufficient respirable fraction of drug for each actuation, the protection of the dose from humidity and degradation, and the

simplicity of its use [24]. Although, as described in the literature, this type of device has many of the characteristics of an ideal device, the flow of air generated by the patient and the relative turbulence generated inside the device can influence the effectiveness of using this system. In fact, the disaggregation of the powder, its aerosolization and the variability of the dose emitted and the inhaled respirable fraction depend on this [24]. Much also depends on the intrinsic resistance of the device, broadly categorized as low to medium or high resistance. Low resistance devices (0.017 KPa $^{0.5}$ L/min) require a higher flow rate. From this, it follows that the deagglomeration and dispersion of the powder depend more on the patient's inspiratory act than devices with medium resistance (around 0.027 KPa$^{0.5}$ L/min) and above all to high resistance devices (0.035-0.058 KPa $^{0.5}$ L/min) which require a lower flow rate [24].

Although the large surface area and their vascularity make the alveoli suitable for the absorption of small molecules as well as macromolecules, the ability to generate an aerosol that reaches the pulmonary periphery represents a challenge and is hampered precisely by the complicated structural organization of this organ.

The dose needed depends on the drug potency used. These differences can be significant. While bronchodilators or corticosteroids require a dosage in the microgram range, antibiotics require a dose in the milligram range [14]. The dose of umeclidinium bromide, a muscarinic antagonist, in *Incruse® Ellipta®* is, for example, 65 µg in *Onbrez®* containing indacaterol in the *Breezhaler®* device is 300 µg, while colistimethate sodium in *Colobreathe® Turbospin®* device is 125 mg [14]. This makes the choice of the device and the formulation approach one of the critical parameters to be carefully evaluated in the development of these inhaler products.

1.4.1 Powders for inhalation

The formulation contained within the device consists of a powder made up of particles with an aerodynamic diameter of less than 5 μm in the form of weak agglomerates of micronized drug (spheronized particles), in combination with a carrier, typically lactose, or as spray dried particles (engineered particles) [23, 25]. The morphology of the powder itself contributes to successful redispersion and repeatability of the delivered dose since this factor affects the packing and flowability of the powder, as well as the van der Waals forces between the particles [14].

Figure 2. Different types of dry powder inhaler devices: single dose (*Ultibro*®); multiple single-dose (*Ellipta*®) and multi-dose with reservoir (*NEXThaler*®). (Source:Photograph from the web: https://www.rightbreathe.com, www.consumermedsafety.org and https://www.omnia-health.com/).

In the case of a formulation containing a potent active ingredient, which therefore requires a low dosage, the formulation approach is typically to use a micronized active ingredient mixed with a carrier, typically lactose, which is required to improve the flowability of the powder. In this case, the morphological characteristics of the carrier, in particular the surface will influence the interaction capacity between API and carrier, the rough particles in fact, have a large contact surface which favours these interactions [14]. Cavities in the micrometre size range favour this process and also influence the flowability of the powder [26]. These formulations can then contain other excipients with a lubricant function, such as magnesium stearate or fine lactose [14]. However, this approach is sometimes not compatible with the final dosage of the drug and with the possibility of being adequately administered with a DPI due to the

limited internal space of capsules and blisters. Moreover, this methodology cannot be used as it would not guarantee the stability of the macromolecule.

The formulation of inhalation powders with a high dosage, or whose function includes the stabilization of the active ingredient, requires the application of other technologies. For this purpose, the spray drying process is one of the most used methodologies in the formation of inhalable particles, as well as in other industrial branches such as the food one, and it is a continuous, rapid and scalable process [10]. As previously mentioned, the excipients used do not have the sole function of acting as a bulk agent to improve drug dosage but actively take part in the formation of the particle, determining its morphology and drug stability [27].

The resulting particle type will be the result of a "bottom-up" process and can also be controlled through the spray parameters used. The resulting characteristics of these particles can be described in terms of size, morphology, internal structure and surface properties as well as in the case of inhalant powders by the aerodynamic diameter [26]. The process leads to the formation of particles and at the same time removes the solvents, in a process consisting of a single step, and is currently used in the production of inhalation powders already on the market such as tobramycin formulated as *Pulmosphere®* in *TOBI® Podhaler®*. Engineered particles of tobramycin or amikacin have also recently been developed by the pharmaceutical technology research group of the University of Parma (Figure 3).

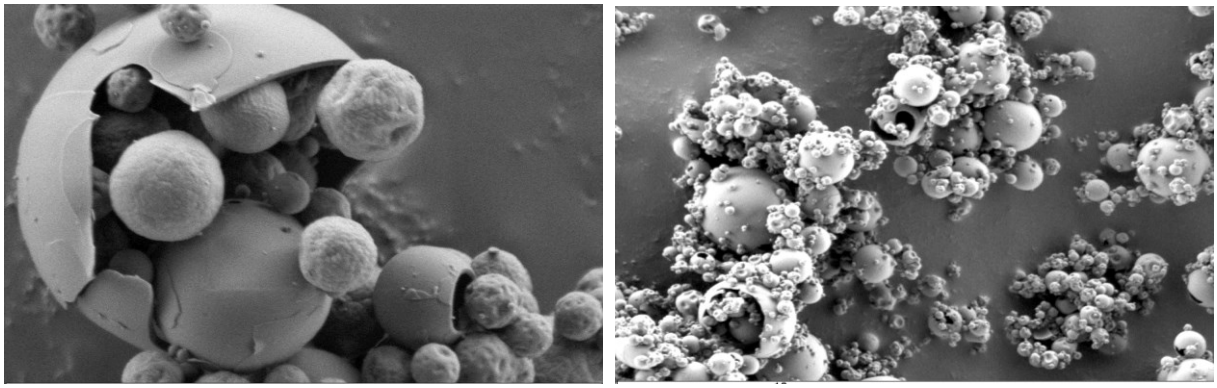

Figure 3. Images obtained by scanning electron microscopy showing spray-dried particles of aminoglycosides obtained in the laboratories of the University of Parma.

An interesting example is the inhaled powder formulation of insulin, marketed for the first time under the trade name *Exubera®* (Pfizer) in 2006 but withdrawn from the market the following year due to the lack of success of this product, subsequently replaced by *Afrezza®* (MannKind, Sanofi) with improved and more successful design [28], however numerous examples of dry powder formulations containing biologics are found in the literature [20, 29].

The re-dispersion and aerosolization of particles from a DPI are critical parameters which will also depend on the device used. However, particle characteristics play a crucial role. One of the strategies useful for reducing the aggregation and agglomeration phenomena, which are typical of micronized particles, is to formulate engineered particles by spray drying [26]. It has been demonstrated that solid and corrugated particles that can be obtained with this technique had better aerodynamic characteristics than particles with a smooth surface due to the reduction of the contact surface area between the particles with subsequent reduction of the Van Der Waals forces [30].

In general, in the development of a powder intended for inhalation administration, one of the critical parameters is the aerodynamic diameter, defined as the diameter of a unit-density sphere (1 g/cm^3) that has the same settling velocity as the measured particle and described by equation 1:

$$d_a = \sqrt{\frac{\rho_p}{\rho_0 \chi}}\, d_g$$

Equation 1. Aerodynamic diameter.

Where ρ is the density of the particle, ρ_0 is equal to 1 g/cm^3, d_g is the geometric diameter of the particle, and χ is the shape factor that is 1 for spheres and becomes less than 1 for particles other than spheres [10]. The equation, therefore, shows that in addition to the morphology, the other critical parameters for aerodynamic performance are the geometric diameter and the density of the particle, parameters that can be controlled using spray drying technology as described by Vehring [27], which make this technique highly successful in the formulation of inhalation powders.

1.5 Nanosystem to the Lungs

Another innovative sector in the field of inhalation therapy concerns the delivery of nanosystems to the lung.

There are different types of nanosystems that can be differentiated into three macro categories, which are polymeric, inorganic and lipid-based nanoparticles which include micelles, solid lipid nanoparticles and liposomes. The latter represents one of the most successful and most approved nanosystems by the FDA. Liposomes offer numerous advantages, such as the possibility of loading both lipophilic and hydrophilic drugs, considered biocompatible and biodegradable; this technology also offers the possibility of modifying the surface in order to obtain a direct target to the affected tissue, or to escape macrophage clearance [31]. The delivery of liposomes to the lung would allow a slow release of the drug, reducing the systemic concentration and side effects. Furthermore, through this system, it is possible to target specific cells, as in the case of macrophages in the treatment of tuberculosis and the penetration of bacterial biofilms [32, 33]. In addition to the commercial products *Arykace*® and *Ambisome*®, containing respectively amikacin and amphotericin B, loaded in liposomes and administered by nebulization, other formulations have been studied in clinical trials: The gene delivery of the plasmid for the expression of the cystic fibrosis transmembrane conductance regulator (CFTR) gene, whose mutation leads to incorrect mucus secretion that causes cystic fibrosis, was delivered by nebulization of liposomes [34]. Cisplatin for the treatment of lung cancer was inserted into liposomes of dipalmytoylphosphatidylcholine (DPPC) and cholesterol and administered by mesh nebulizer [35]. Liposomal amikacin has been administered in patients with Mycobacterium avium complex or *Mycobacterium abscessus* infections demonstrating reduced systemic toxicity due to the drug [36].

Another formulation was studied by Tagami *et al.*, containing doxorubicin loaded in liposomes composed of DPPC and P188, a PEGylated block-copolymer, to obtain a controlled release of the drug to the lung [37].

Alongside the liposomal liquid formulations, some formulation studies have been carried out on the production of spray-dried liposomes and therefore in the form of dry inhalation powder, combining the advantages of this type of formulation with the use of a DPI. The ciprofloxacin nanocrystals contained in liposomes were effectively dried using sucrose as a lyoprotectant, to obtain a prolonged release compared to the liquid formulation [38]. Another study concerned the formulation of an inhalation powder containing tacrolimus in the liposomal form to prolong drug retention in the lung in the prevention of lung transplant rejection [39].

2. AIM

The aim of this work was the design and characterization of inhalation powders containing therapeutic peptides characterized by low oral bioavailability and therefore requiring high doses, such as cyclosporine or, as in the case of pramlintide, whose administration today requires the use of the parenteral route. For this reason, the administration of these peptides by inhalation would offer the possibility of improving the therapies currently used.

The third chapter of this thesis describes the optimization of a cyclosporine inhalation micronized powder through the use of a design of experiment. The fourth chapter concerns the design of a dry powder formulation using a more innovative approach. Cyclosporine was loaded in calcium phosphate coated liposomes and embedded in mannitol spray-dried powder.

The fifth chapter of this study is a careful evaluation of the excipients used in the stabilization of pramlintide during the spray drying process.

3. An Enhanced Dissolving Cyclosporin-A Inhalable Powder Efficiently Reduces SARS-COV-2 Infection *In Vitro*

3.1 Introduction

CsA is a cyclic peptide with immunosuppressive action, administered for the treatment of various pathologies that share uncontrolled activation of the immune system *e.g.*, atopic dermatitis and psoriasis.

Since entering the market in 1983, cyclosporine A (CsA), a calcineurin inhibitor peptide, has been widely used in the treatment of various autoimmune conditions characterized by the strong activation of the immune system [1]. The success of this molecule is related to its selective and reversible inhibition of the production of pro-inflammatory cytokines by T-lymphocytes [2]. CsA is intravenously and orally (as soft capsules) administered and is currently used for the prevention of allograft rejection in various organ transplantations. Indeed, continuous activation of T-cells in the transplanted lung is the key factor bringing to bronchiolitis obliterans syndrome (BOS) characterized by extensive fibroproliferation and loss of lung functionality [3]. BOS is considered a marker of chronic rejection and causes 30% of deaths after lung transplantation [4,5].

Despite the efficacy of CsA, severe adverse side effects, including nephrotoxicity, hepatotoxicity, hypertension, and neurotoxicity, usually arise during chronic treatment with CsA [6,7]. Moreover, the delivery of a sufficient and reproducible amount of CsA can hardly be achieved by oral administration because of its poor aqueous solubility, its pre-systemic metabolism at the gut level [8,9] and its erratic absorption, related to interindividual variability, food intake and by comorbidities such as diabetes [10,11]. Overall, the oral bioavailability of CsA is around 30%, which entails a dosage range between 5 and 15 mg/kg/day, and the need to carefully monitor the patient's drug plasma concentration over time [12].

For this reason, pulmonary administration would be a promising strategy for the treatment of lung transplant patients, given the possibility of avoiding pre-systemic metabolism and obtaining high drug local concentrations (i), having a rapid onset of action (ii), keeping lower, than the oral route, the doses administered with limited systemic exposure to the drug (iii). In this regard, the administration of a 100 μg intratracheal dose of CsA to rats, in addition to being effective in reducing lung inflammation, led to a distribution of CsA in the side effect-related organs that were one hundred times lower than that of an oral dose of 10 mg/kg [13]. The pulmonary administration of a dose of just 5 mg of CsA by nebulization of a propylene glycol solution was able to produce an improvement in lung transplanted patients' conditions, expressed as forced expiratory volume in one second (FEV1) [14]. This study demonstrated a strong relationship between the administration of CsA directly to the lungs and an increased anti-rejection effect. Further clinical trials have confirmed the benefits of direct pulmonary administration of CsA by nebulization in patients who underwent single or double lung transplantation [15] or in BOS patients [16].

Besides the effect on the prevention of allograft rejection, CsA has been widely studied also as a potential anti-viral drug [17–19]. In 2011 de Wilde and colleagues first demonstrated in vitro inhibitory activity of CsA at micromolar concentrations on the replication of different coronavirus genera [20]. The effective inhibition of replication towards SARS-CoV-2 has also recently been demonstrated by Fenizia *et al*., on the human lung epithelium Calu3 cell line [19]. In addition, CsA anti-inflammatory and immunomodulatory activities would be beneficial in containing the cytokine storm experienced by many COVID-19 patients, leading to airway damage and respiratory loss of function [19,21].

At the moment, COVID-19 has been treated using antiviral drugs as *molnupiravir* [22], *nirmatrelvir* [23], *ritonavir* [24] and *remdesivir* [25], anti-inflammatory drugs (*dexamethasone* [26]), immunomodulatory agents as *baricitinib*, *tocilizumab*, an anti-IL-6 antibody [27], and monoclonal antibodies against the receptor binding domain as *sotrovimab* [28].

The aim of this work was the development of a highly respirable formulation of CsA obtained by spray drying with excipients already approved for inhalation. A critical parameter for the evaluation of the quality of the powders produced was the Weibull dissolution time obtained from the in vitro release rate profile. The most promising powder was then further analysed in vitro in terms of tolerability, reduction of inflammation and antiviral activity in terms of SARS-CoV-2 reduction of infection in Vero E6 cells.

3.2 Materials

Cyclosporine A (CAS Number 59865-13-3, Metapharmaceutical, Barcellona, Spain) was purchased from ACEF (Fiorenzuola d'Arda, Italy). HPMC extra-dry capsules for use in dry powder inhalers, Quali-V®-I size #3, were provided by Qualicaps (Madrid, Spain), while the high resistance dry powder inhaler RS01 was a kind gift of Plastiape (Lecco, Italy). Mannitol was purchased from Roquette (Lestrem, France) and glycine was purchased from Sigma Aldrich (Merck, Milano, Italy). All other chemicals used were obtained from commercial suppliers and were at least of analytical grade. The human lung adenocarcinoma cell line A549 (CRM-CCL-185), monocytic cell line THP-1 (TIB-202) and Vero E6 (CRL-1586) were purchased from American Type Culture Collection (ATCC, Manassas, VA, USA).

3.3 Methods

3.3.1 Preparation of CsA spray-dried powders

The spray-dried (SD) CsA powders were obtained starting from a solution of water and ethanol 96% with a variable ratio, according to the design of experiment (DoE), containing 1% (*w/v)* solids. The effect of different amounts of excipients on yield of production, respirability, residual solvent and dissolution rate was assessed. The DoE was employed in order to limit the number of experiments aimed at characterizing the effect of individual excipients on the critical quality attributes of the powder. The experiments were designed by means of the Design-Expert 12 software (Stat-Ease, Inc., Minneapolis, MN, USA). A half-fractional factorial design with 3 factors at 2 levels and 3 additional centre points for curvature check was applied,

requiring a total of 11 experiments detailed in Table 1. Mannitol (10-20% *w*/*w*), glycine (0-5% *w*/*w*) content in the dry formulation and ethanol (45-60% *v*/*v*) concentration in the feed solution were the three factors investigated, fixed at two levels equally distant from the central point.

CsA raw material (CsA_rm) was solubilized in ethanol where the solubility of CsA is more than 100 mg/g [40], while mannitol and glycine were solubilized in water at room temperature. The aqueous solution was added to the CsA solution under magnetic stirring (160 rpm). The CsA remained in solution in all the ranges of water added (from 40 to 55 % *v*/*v*) in the hydroalcoholic solution.

Table 1. Composition of powders studied according to the DoE with three factors and two levels and three center points (*). M= Mannitol; G= Glycine. Each experimental point was replicated to calculate the experimental error.

Powder (#, code)	**Factor A: Mannitol** %(*w*/*w*)	**Factor B: Glycine** %(*w*/*w*)	**Factor C: Ethanol** %(*v*/*v*)
1 (CsA_M15)*	15	2.5	52.5
2 (CsA_M10G)	10	5	45
3 (CsA_M20G)	20	5	60
4 (CsA_M10)	10	0	60
5 (CsA_M20)	20	0	45
6 (CsA_M20G)	20	5	60
7 (CsA_M15)*	15	2.5	52.5
8 (CsA_M15)*	15	2.5	52.5
9 (CsA_M20)	20	0	45
10 (CsA_M10G)	10	5	45
11 (CsA_M10)	10	0	60

To produce the powders, 50 mL solution was spray dried (Mini Spray Dryer B-290, Büchi, Flawill, Switzerland) using the following parameters: inlet temperature 140 °C, drying air flow rate 742 L/h, aspiration 35 m^3/h, solution feed rate of 3.5 mL/min and a nozzle diameter 0.7 mm. Under these conditions, an outlet temperature of 80-87 °C was measured.

Analysis of variance (ANOVA) was performed to investigate the effect of factors on the critical quality attributes (CQAs). In detail, the CQAs selected were the production yield, the percentage of residual solvent, and the Weibull dissolution time obtained from the dissolution profile. The probability value of the model was considered significant when lower than 0.05.

3.3.2 CsA quantification by High Performance Liquid Chromatography

The quantification of CsA in spray-dried powders was done by dissolving 20 mg of powder in 25 mL of water:acetonitrile 40:60. Six samples were prepared and analysed by HPLC. The drug content analysis was done after powder preparation and during the stability study.

CsA A was quantified using HPLC (LC-10, Shimadzu, Kyoto, Japan) equipped with an UV-vis detector, set at a wavelength of 230 nm and using the column Nova-Pak C18 (3.9x150 mm, 4 μm; Waters, Italy). The mobile phase was constituted by a mixture of 65% acetonitrile and 35% ultrapure water, acidified with 0.1% of trifluoroacetic acid. The column temperature was set at 65°C and the flow rate was fixed at 1.6 mL/min. The injection volume of the sample in the column was 10 μl. The run time of every analysis was 10 minutes and the retention time for the CsA was about 5 minutes. The method linearity over the range 0.1 - 2 mg/mL.

3.3.3 Aerodynamic Performance characterization

Screening of aerodynamic performance of all batches produced was assessed through Fast Screening Impactor (FSI; Copley Scientific, Nottingham, UK), with a 65 L/min insert to provide a 5 μm cut-off size. The FSI was connected to an SCP5 vacuum pump (Copley Scientific, Nottingham, UK) through a critical flow controller (TPK Copley

Scientific, Nottingham, UK). A flow rate of 65 L/min, measured with DFM 2000 Flow Meter (Copley Scientific, UK), was required to activate RS01 (Plastiape, Lecco, Italy) device at (DPI) with a 4 kPa pressure drop. TPK actuation time was adjusted so that a volume of 4 L of air was drawn through the inhaler. The content of one capsule filled with 20 mg of powder was discharged and each experiment was repeated three times. The amount of CsA present in the formulation was in the range between 16.5-18 mg according to the formulation drug content. CsA was quantified by HPLC according to the method reported in section 3.3.2. The Emitted Fraction (EF) was calculated as the percentage ratio between the total CsA mass recovered in FSI and the CsA loaded in the capsule. The Respirable Fraction (RF) was calculated as the percentage ratio between the mass of particles with an aerodynamic diameter less than 5 μm and the emitted dose.

The same analysis setup was maintained to further investigate the aerodynamic performance using the Next Generation Impactor (NGI; Copley Scientific, Nottingham, UK). To obtain a more accurate analysis and avoid eventual particles bouncing on the collection cups, the cups of the impactor were coated using a solution of 2% (*w*/*v*) Tween 20 in ethanol. As above, the content of one capsule was aerosolized and the CsA in the NGI was collected and quantified by HPLC.

The metered dose (MD) is the mass of the drug quantified by HPLC, calculated by adding the drug amount recovered in the inhaler and the impactor (induction port, stages 1 to 7 and Micro Orifice Collector (MOC)). The Emitted Dose (ED) is the amount of drug leaving the device and entering the impactor (induction port, stages 1 to 7 and MOC). The Mass Median Aerodynamic Diameter (MMAD) was determined by plotting the cumulative percentage of mass less than the stated aerodynamic diameter for each NGI stage from 1 to 7, on a probability scale versus the aerodynamic diameter of the stage on a logarithmic scale. The Fine Particle Dose (FPD) is defined as the mass of drug with an aerodynamic diameter less than 5 μm (calculated from the log-probability plot equation) and the Extra Fine Particle Dose (EFPD) is the mass of the drug with an aerodynamic diameter less than 2 μm. The Fine particle fraction (FPF)

and the Extra Fine Particle Fraction (EFPF) were calculated as the percentage ratio between the FPD or EFPD, respectively and the ED.

3.3.4 Thermogravimetric analysis

The analysis was carried out using TGA 1 STARe System (Mettler Toledo, Columbus, OH, USA) to determine the loss on drying (LOD) *i.e.,* the percentage of residual humidity and solvents present in the powder at the end of the manufacturing process. For this purpose, approximately 4 mg of powder was placed in a pan of aluminium oxide, the analysis was carried out in nitrogen flow at 80 mL/min and increasing the temperature from 25°C to 150°C with a rate of 10°C/min. The LOD was measured in the range between 25-125°C where the weight change was observed.

3.3.5 Dissolution profile of respirable particle fraction

In vitro dissolution tests to compare the dissolution performance of CsA powders were conducted using RespiCell™ [41], an innovative vertical diffusion cell apparatus.

The apparatus comprises a 170 cm^3 receiving cell, that was filled with the dissolution media and the sampling was performed through the sidearm. The apparatus is constituted of two portions: the upper part acts as a donor chamber and the lower part is a receptor chamber maintained under magnetic stirring at 180 rpm.

The receptor was filled with 170 mL of medium consisting of phosphate-buffer saline (PBS) containing 0.2% of sodium dodecyl sulphate and the cell was connected to a heating thermostat (Lauda eco silver E4, DE) set at 37 ± 0.5 °C. The dissolution was carried out on the RF of the powder, following separation by FSI. In the case of spray-dried CsA, four capsules of 20 mg were aerosolised for each experiment and the analysis was performed in triplicate. In the case of the raw material, the content of ten capsules was aerosolised due to the low respirability of the material. The filter (Type A/E glass filter 7.6 cm diameter, Pall Corp.) containing the mass of powder < 5 μm was then placed on the diffusion area of the RespiCell™ and 2 mL of PBS containing 0.2%

of SDS was added before starting the dissolution to create a thin liquid layer on the powder bed. At fixed intervals, 1 mL of the receiving solution was removed and replaced with 1 mL of fresh buffer to maintain a constant volume inside the receptor chamber.

Finally, at the end of the experiment, the residual undissolved powder was recovered by washing out the filter with 10 mL of ethanol:water (50:50 *v/v*). The samples were quantified by HPLC according to the method described. The drug dissolved was expressed as a percentage of CsA dissolved relative to the total CsA recovered at the end of the test both on the filter and receptor compartment.

The dissolution profiles were analysed by means of the Weibull equation [42] in order to determine the time parameter, recognised as the time at which the 63.2 per cent of the drug was dissolved.

3.3.6 Morphological Analysis by SEM

Particle morphology was determined by Scanning Electron Microscopy (SEM, Zeiss AURIGA, Zeiss, Oberkochen, Germany) and was operated under high vacuum conditions with an accelerating 1.0 kV voltage, at a 5k times magnification. Powders were deposited on adhesive black carbon tabs pre-mounted on aluminium stubs and imaged without undergoing any metallization process.

3.3.7 Viability study on A549 and THP-1

A549 cells (seeding 10^4 cells/well), following overnight culture, and THP-1 cells (seeding 5×10^4 cells/well), immediately after seeding in a 96-well plate at 37°C, were exposed to the following treatments: vehicle (DMSO 0.5% in PBS), CsA_rm (1, 10 μg/mL of CsA), spray-dried powder CsA_M20 (containing 20% *w/w* of mannitol) (1, 10 μg/mL), and mannitol 2 μg/mL. Cell viability was quantified using the MTS assay. Briefly, 20 μl of 3-(tributylammonium)-propyl methanethiosulfonate bromide solution (MTS, 1 mg/mL) was added to each well and, following 4h incubation at 37°C, the supernatants were collected. The absorbance of each well was measured at 490 nm on a microplate reader (Sunrise™ powered by Magellan™ data analysis software,

TECAN, Mannedorf, Switzerland). The impact of the various treatments on cell viability was expressed as the percentage of viability with respect to vehicle-treated cells.

3.3.8 Co-culture assays and cytokines determination

For the co-cultures, A549 cells (10^5 cells/well) were seeded at the bottom and THP-1 cells (10^5 cells/well) were plated on the insert (0.4 μm pore polyester filter) of Transwell culture plates (#3470, Corning Inc., Corning, NY, USA), the two cell cultures being physically separated to avoid their direct contact, according to the method described by Li *et al*., [43]. After 24h co-culture, cells were exposed to the following treatments: vehicle (DMSO 0.5% in PBS), CsA_rm 10 μg/mL, CsA_M20 at 10 μg/mL, in respect to CsA, mannitol 2 μg/mL in DMSO 0.5% in PBS. After 1h, LPS 1 μg/mL (*Escherichia coli* O55:B5; cat# L6529; Sigma Aldrich, Merck, Milano, Italy) was added to the culture and maintained for 24h. Cells incubated with the vehicle and not exposed to LPS were used as control. The concentration of IL-6 in the conditioned media was subsequently determined using ELISA kit (Boster Biological Technology, Milano, Italy; cat. no. IL-6, EK0410), according to the manufacturer's protocol and expressed as pg/mL.

3.3.9 Cell treatment and viral replication inhibition assay

The inhibitory effect of CsA_M20, CsA_rm and mannitol on viral replication on Vero E6 cell cultures was tested against Omicron subvariant BA.1 (lineage B.1.1.529.BA.1).

The viral strain was isolated from a residual clinical specimen conferred to the Unit of Microbiology, Greater Romagna Area Hub Laboratory (Cesena, Italy). The sample underwent an anonymization procedure, in order to adhere to the regulations issued by the local Ethical Board (AVR-PPC P09, rev.2; based on Burnett *et al*., 2007 [44]). Detailed description of Vero E6 cell culture and propagation, as well as titration and isolation of the virus from biological samples are reported in Annex A.

The day before treatment and infection, Vero E6 cells were seeded at a density of 2×10^6 cells per plate in 96-well plates and allowed to attach for 16 to 24 hours at 37 °C, 5% CO_2. On the day of infection, each tested compound stock suspension in PBS was

freshly diluted in cell culture medium containing 2% FBS. CsA_rm was tested at concentrations of 8, 16, 32 and 64 μM, corresponding to 9.6, 19.2, 38.4, and 76.9 μg/mL; CsA_M20 was diluted to obtain the same CsA concentrations considering the CsA content in the spray-dried powder of about 80% *(w/w),* determined by HPLC. The selected CsA concentrations, in the case of powder CsA_M20, involved the presence of dissolved mannitol at concentrations of 2.4, 4.8, 9.6, 19.2 μg/mL since mannitol represents a 20% *(w/w)* of the formulation. These values were then adopted when mannitol was applied to the cells and tested as vehicle alone.

To better determine at which level the viral replication cycle was inhibited, cells were subjected to different treatment regimens: treatment before infection(pre-treatment), treatment 2 hours after infection (post-infection) treatment during infection (simultaneous). In any case, each treatment lasted one hour. Antiviral efficacy was tested against the viral concentration of 0.0005 m.o.i. Infected cultures were incubated for one hour at 37 °C to allow viral adsorption. Treated and infected cultures were incubated at 37°C, 5% CO_2 for 72 hours. For each treatment protocol, cell culture was infected directly with the virus suspension to assess viral replication in the absence of any potential inhibition.

3.3.10 SARS-CoV-2 nucleic acid quantification

Viral replication in treated and untreated cell cultures was evaluated by qRT-PCR by comparing the cycle threshold (Ct) values of each treated sample (Ct treated) and its corresponding untreated control (Ct control) obtained after 72 hours of incubation. For this purpose, the Allplex SARS-CoV-2 Extraction-Free system (Seegene Inc., Seoul, South Korea) was used. It consists of a real-time qRT-PCR multiplex assay based on the use of TaqMan probes. Sample preparation, reaction setup and analysis were performed accordingly to the manufacturer's instructions and the details are described in the Annex A. Positive and negative controls were included in each run. Fluorescent signals were acquired after every amplification cycle. By comparing the Ct values referred to the N-gene of each treated sample and its corresponding untreated control

reached at the end of the test the percentage of infectivity reduction was calculated as follows:

$$\%\ viral\ infectivity\ reduction = \frac{Ct\ treated - Ct\ control}{Ct_0 - Ct\ control} * 100$$

where Ct_0 represents the cycle threshold at the time of treatment application.

Cells treated with the same treatment protocols but not infected were used to assess the effects on cell viability. To quantify cell viability, after the incubation period, the cell monolayers were fixed and stained using 4% formaldehyde solution in crystal violet; absorbance was read at 595 nm. For each tested compound concentration, the percentage of viable cells for each tested concentration was calculated, setting the mean absorbance value of the cell control wells (neither treated nor infected cells) as 100% viability. None of the CsA_M20, CsA and mannitol concentrations significantly compromised cell viability.

3.3.11 Stability studies

Stability studies were conducted on CsA_M20 spray-dried powder by storing the capsules containing 20 mg of powder in closed glass vials at 25°C and 60% of relative humidity (RH) and 40°C and 75% of RH. The CsA content and *in vitro* aerodynamic performance by NGI were studied after 1 and 3 months of storage.

3.3.12 Statistical analysis

Statistical analysis was conducted using the Analysis of Variance (ANOVA test) with a post hoc test using Prism 9 (GraphPad Software, v.9.4.0). Data were considered to be statistically significant when the p-value was < 0.05 (*= $p < 0.05$; **= $p < 0.01$).

3.4 Results and Discussion

3.4.1 CsA dry powder development by DoE

CsA is a lipophilic molecule with a logP of 3 and a poor water solubility (3.69 mg/L at 37°C), falling into class II of the Biopharmaceutics Classification System (BCS) among molecules with low water-solubility and high permeability [45]. These physico-chemical properties limit the bioavailability of CsA and many studies have been performed to improve the dissolution profile of CsA including the use of nanoparticles incorporated in microparticles by spray drying or spray-freeze drying and ultrasonic spray-freeze-drying [46–48].

Moreover, the direct deposition of CsA to the lung could be an effective strategy in preventing lung rejection due to the high local drug availability also enhanced by the avoidance of intestinal pre-systemic metabolism.

The low water solubility of CsA represents an issue for the development of an inhalation product both from the point of view of the formulation and the release of the drug on-site. In the case of a nebulisation product, a CsA solution using propylene glycol as a solvent, or a liposomal formulation has been proposed to increase the pulmonary exposure of the drug. Despite the good performance in clinical trials, the CsA solution for nebulization did not reach the market, perhaps because of the possible irritant effect of the solvent used [49–51]. Other clinical trials conducted using inhaled liposomal CsA, demonstrated the capability of the drug to increase BOS-free survival [52, 53].

Compared to a CsA liquid nebulization, the use of a CsA inhalation powder offers numerous advantages: the powder can be administered by a quick inhalation act and, as a solid-state formulation, the stability of the product is increased. On the other hand, the development of a powder containing CsA requires particular attention to the choice of excipients and the production technique capable to improve the release of the drug from the solid particles. In this context, some strategies have been proposed to enhance pulmonary release and absorption such as the construction of CsA particles

with pulmonary surfactants or with hydroxypropyl-beta-cyclodextrin and hydrosoluble chitosan [54–56].

In this work, the spray-drying process and water-soluble excipients were chosen to develop physically stable CsA respirable particles with improved dissolution. Mannitol was selected as it is currently approved for pulmonary administration [57] and is widely used in particle engineering. The addition of glycine was investigated to promote powder deaggregation and aerosolization.

A preliminary study was carried out to identify which was the most suitable amount of mannitol to add to the formulation and subsequently to keep it as a starting point for a more in-depth investigation by DoE. Figure 1A illustrates the EF and RF of powders containing CsA and mannitol in the two ratios of 80:20 (CsA_M20) and 50:50 (CsA_M50) spray-dried starting from a solution containing 45% (*v*/*v*) ethanol in water. Similar EF and RF values were shown by the two CsA-mannitol powders: the EF was around 85% and RF was about 68-70%. On the contrary, CsA_rm, which had a volume median diameter of 7.67 μm, had a large deposition in the induction port of the impactor which led to a very low RF of 6%.

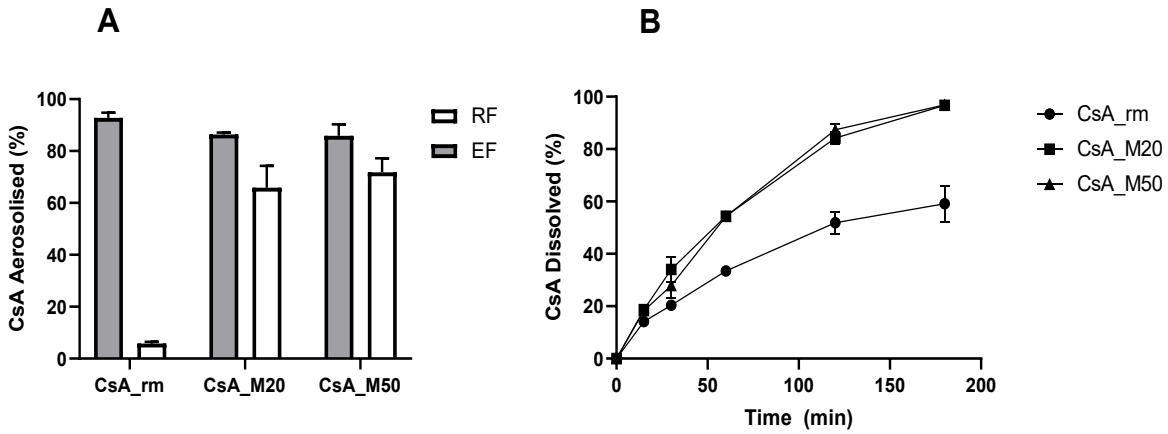

Figure 1. Aerosolisation performance (RF = respirable fraction, EF = emitted fraction) (**A**) and dissolution profiles (**B**) of CsA raw material (CsA_rm), CsA_M20, and CsA_M50. Data presented as n = 3, mean value ± SD.

Both the CsA spray-dried powders exhibited a faster dissolution rate than the CsA_rm: about 87% of the spray-dried powder was dissolved after 3 hours of the experiment while only 50% for the raw material (Figure 1B). However, the addition of mannitol in different quantities did not lead to a difference in the release profiles of CsA_M20 and

CsA_M50. This preliminary test shows that, when mannitol exceeded 20% (*w*/*w*) in the powder composition, it no longer had any positive effect on the formulation for both qualitative parameters studied. Hence, with the purpose to limit the amount of powder to inhale, it was decided to keep the amount of mannitol in the formulation fixed at 20%.

A screening DoE was setup to investigate the influence of excipients on the quality of the powders. The effect of the ethanol content in the feedstock solution and the addition of glycine along with mannitol on the CQAs of the powders were investigated and are illustrated in Table 2. The yield of the process and the loss on drying (LOD) describe the quality of the spray-drying process, whereas the powder aerodynamic behaviour (*i.e.* RF) and the dissolution time are related to the quality of the formulation. The residual solvent in the dried powder could affect not only its chemical stability but also its respirability over time as it could modify the powder's properties.

Table 2. Values of the CQAs investigated for the eleven CsA spray-dried powders: yield of the production process, respirable fraction (RF) <5 μm, loss on drying (LOD), and time parameter of Weibull equation (time for 63.2% of CsA dissolved from composite powders) indicated as WDT. Data presented as n = 3, mean value ± SD.

Batch	Yield	RF (%)	LOD (%)	WDT (min)
1 (CsA_M15)*	55.7 ± 2.6	64.5 ± 6.3	2.85 ± 0.20	89.7 ± 7.4
2 (CsA_M10G)	55.4 ± 4.1	71.6 ± 1.6	3.41 ± 0.31	99.9 ± 4.8
3 (CsA_M20G)	59.1 ± 7.9	72.0 ± 4.1	1.96 ± 0.12	116.2 ± 8.3
4 (CsA_M10)	61.1 ± 3.9	64.5 ± 1.6	1.75 ± 0.33	109.6 ± 5.7
5 (CsA_M20)	59.5 ± 6.5	70.9 ± 0.4	2.04 ± 0.24	61.76 ± 0.2
6 (CsA_M20G)	56.9 ± 3.2	61.7 ± 0.3	1.98 ± 0.14	138.5 ± 6.7
7 (CsA_M15)*	62.6 ± 6.0	65.4 ± 2.4	2.52 ± 0.55	90.8 ± 14.1
8 (CsA_M15)*	65.0 ± 3.2	70.5 ± 8.7	2.45 ± 0.14	89.7 ± 13.7
9 (CsA_M20)	61.6 ± 4.1	59.9 ± 3.1	2.12 ± 0.31	57.7 ± 0.2
10 (CsA_M10G)	61.1 ± 5.1	61.3 ± 4.4	3.06 ± 0.42	110.6 ± 1.5
11 (CsA_M10)	65.3 ± 2.9	56.6 ± 2.9	1.75 ± 0.25	119.3 ± 10.1

*= central points of the DoE.

Table 3. Probability values for the model terms relating to selected CQAs. RF = respirable fraction; LOD = loss on drying; WDT = Weibull dissolution time. The model was significant at $p < 0.05$ and highlighted in bold.

Term	Yield	RF	LOD	WDT
Model	0.425	0.748	**0.033**	**0.006**
R^2	0.312	0.187	0.944	0.934
Mannitol	0.643	0.580	**0.006**	0.107
Glycine	0.152	0.443	**0.006**	**0.015**
Ethanol	0.568	0.636	**0.0004**	**0.004**

ANOVA analysis of the responses for the selected factorial model was performed. The generated model was not significant for the yield of production and for the respirable fraction. Actually, the yield value was similar for all powders, regardless of the composition of the stock solution. In general, the results indicate that the process was efficient in terms of the amount of powder produced and robust. The yield of the manufacturing process was for all powders in the range of 55-65%. This result indicates that micronized CsA powders can be successfully prepared by spray-drying, since the average yield of the lab scale process is usually not optimal and is typically reported to be between 20 and 70% [58]. In all cases, the microparticles did not give rise to visible aggregates and the powders were not electrostatic. Not only the process was considered robust, with acceptable values, but also regarding the respirable fraction, the composition of the feed solution did not have a significant impact within the investigated ranges.

Conversely, ANOVA revealed that the model was significant for the LOD and WDT with a probability value of 0.033 and 0.006, respectively (Table 3). Furthermore, the robustness of the relationship between the model and the variables analysed was high as indicated by the R^2 values. Figure 2 illustrates the perturbation graph of WDT versus the critical factors and contour plot of LOD and WDT as a function of ethanol and glycine proportion.

Ethanol is the main factor influencing the different degrees of residual solvents in the particles. As the percentage of ethanol increases, the LOD value approaches zero per cent. On the contrary, glycine had a negative effect on the powder LOD: the presence of this excipient increased the amount of residual solvent in the powder; hence it was not beneficial for the formulation quality aspects. According to this model, the percentage of mannitol also positively influences the LOD, however, this would seem to be a parameter deriving from the combined effect of ethanol and glycine. A low LOD value is important because it usually correlates with improved peptide stability in a solid-state formulation and decreases the possibility of mannitol recrystallization. The graph in Figure 2b illustrates the trend of the LOD as ethanol and glycine vary.

The main contribution to the variation of the dissolution time is due to glycine and ethanol, while the effect of mannitol was not significant. Therefore, as the percentage of ethanol and glycine increases, the time to dissolve the 63.2% of the API rises (See Figure 2c). Mannitol did not have a statistically significant effect, although indicated as a factor reducing WDT, *i.e.* leading to a faster dissolution rate (see Figure 2a).

In general, the spray-drying process was always able to produce particles with an enhanced dissolution rate as compared to the non-formulated API (WDT of 169.0 min). Among all the formulations, the powder CsA_M20, which was prepared starting from a feed solution containing 45% of ethanol and without glycine, had the lowest WDT of about 59 min. The drug release profile of CsA_M20 was similar to that obtained by Yamasaki *et al*., (WDT of about 62 min) when CsA was precipitated in nanoparticles and spray-dried into nano-matrix structures with lactose mannitol and lecithin [46]. However, although the dissolution profile of engineered powders was improved compared to the raw material, it is still a rather slow dissolution rate which places undissolved particles at risk of removal by mucociliary clearance or phagocytosis. Therefore, *in vivo* studies will be useful to fully prove the beneficial effect of such formulation.

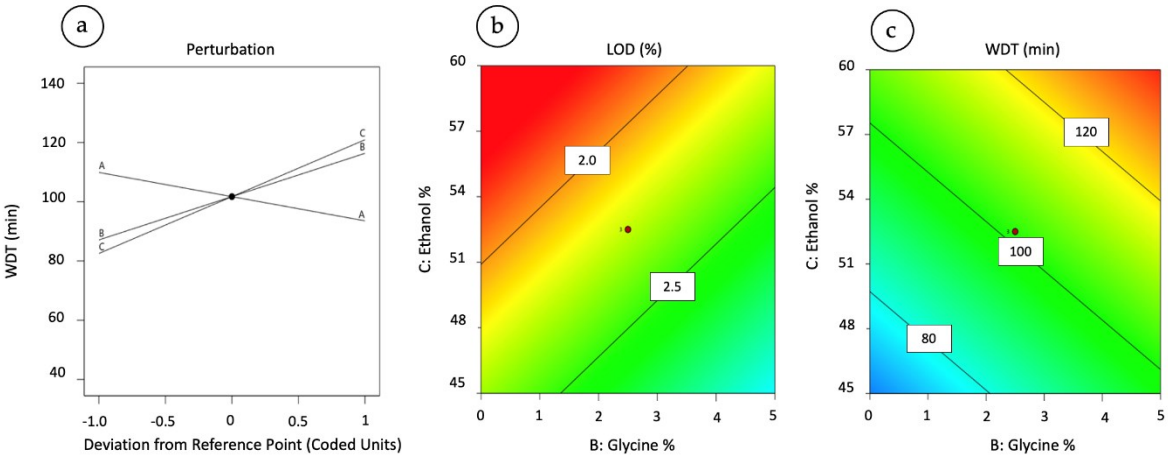

Figure 2. Figure 2. Perturbation graph of Weibull Dissolution Time (WDT) versus the critical factors plotted as deviation from the reference point (A=Mannitol; B=Glycine; C=Ethanol) (**a**). Contour plot of LOD (**b**) and WDT (**c**) as function of ethanol and glycine proportion in feed solution at the mannitol concentration of 15% (*w*/*w*).

The observed behaviour indicated that when the particle composition consisted only of mannitol and CsA this was more favourable for dissolution and in terms of residual solvent content. The reason why the composite CsA particles have a higher dissolution rate than the raw material is that during particle formation the mannitol precipitates together with the CsA forming a solid structure where the two materials are intimately dispersed. In contact with an aqueous medium, the mannitol dissolves immediately leaving the CsA, with a high surface area, free for dissolution. Interestingly, the presence of glycine, although it is a hydrophilic excipient but less hygroscopic than mannitol, lowered the release of CsA.

Given the significance of the data, it will be worthwhile to further investigate by a full factorial DoE the effect of the interactions between the factors and the CQAs.

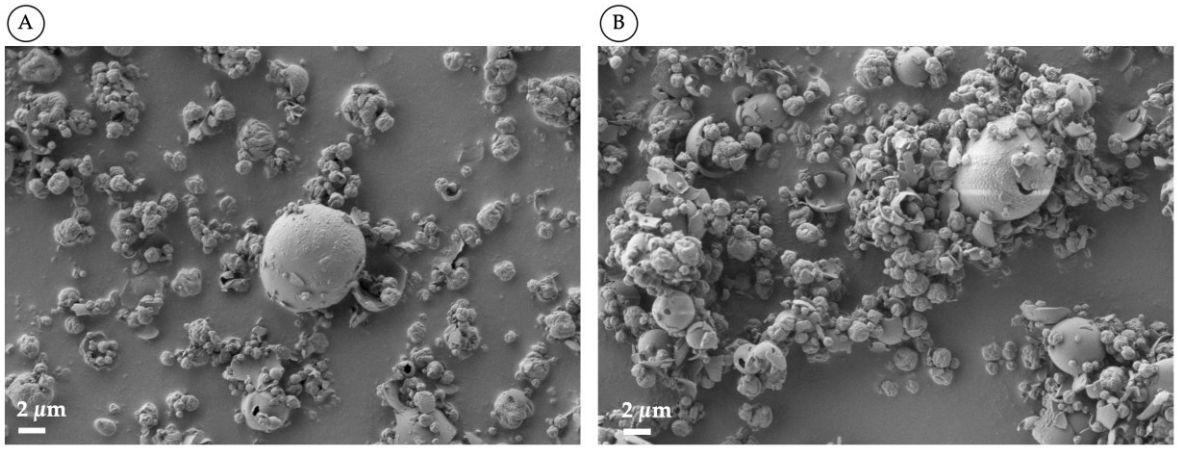

Figure 3. SEM images of CsA spray-dried powders produced with 45% (*v/v)* (A), and 60% (*v/v)* of ethanol in the feedstock solution.

The ethanol content of the feed solution also influenced the morphology of the microparticles obtained. When the ethanol was 45% (Figure 3A), particles appear to be less inflated and more corrugated as compared with particles produced starting from a solution containing 60% of ethanol (Figure 3B) where a greater number of large, fractured particles were observed. This behaviour is in agreement with what was reported for the production of amikacin spray-drying powders [59]: the particles are much larger or exploded when the evaporation rate is rapid and therefore the precipitation of the solute occurs early. The evaporation rate increases as the percentage (*v*/*v*) of ethanol in the feed solution rises.

As regards the solid state of the produced, CsA powders all were amorphous as evidenced by the typical halo of the X-ray pattern (see Annex B). The structure of the CsA raw material was also amorphous before spray drying and no crystallinity peaks were observed in the powders after the production.

From this first part of the work, CsA_M20 was selected as the best-performing powder and was then further characterized and tested for tolerability, anti-inflammatory and antiviral activity.

Full characterization of the CsA_M20 spray-dried powder

The CsA drug loading in the CsA_M20 powder after its production was 76.3 ± 1.4%. This value agreed with the theoretical one (80%) considering that the powder had a solvent content, determined by TGA, of about 2%.

The aerodynamic particle size distribution of the powder CsA_M20, assessed by NGI, showed that the formulation had a very high respirability. The emitted amount of powder from the RS01 device was 16 mg (corresponding to 90% of the metered dose) containing 13.2 mg of CsA. The FPD was 8.8 mg of CsA which corresponds to an FPF of 66.5 % (Table 4). The favourable aerodynamic behaviour can be attributed both to the poor cohesiveness of the particles and their good flowability and the efficient deaggregation mechanism of the RS01 device.

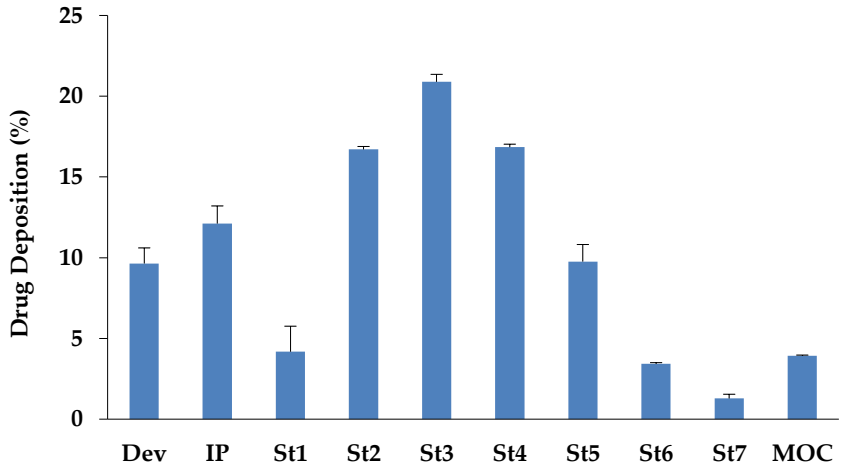

Figure 4. Distribution of CsA_M20 powder on Next Generation Impactor. The loaded amount of powder in the capsule was 20 mg containing 16 mg of CsA, (n = 3, mean value ± SD). Dev = device; IP = induction port; St = stage; MOC = micro-orifice collector

Table 4. Aerodynamic characterisation of the CsA_M20 powder at time zero and during the stability investigation in standard and accelerated conditions (n = 3, mean value ± SD).

	Metered Dose (mg)	Emitted Dose (mg)	MMAD (μg)	FPM (mg)	FPF (%)	Extra-fine dose <2 μm (mg)	Extra-fine fraction <2 μm (%)
CsA_M20 0 time	14.8 ± 0.1	13.2± 0.3	2.97 ± 0.12	8.80 ± 0.18	66.5 ± 2.6	3.61 ± 0.08	27.3 ± 1.2
CsA_M20 1 month 25°C 60%RH	14.7 ± 0.3	13.0 ± 0.5	2.58 ± 0.03	9.35 ± 0.46	71.4 ± 0.95	4.24 ± 0.13	32.4 ± 0.2
CsA_M20 1 month 40°C 75%RH	15.3 ± 0.3	12.6 ± 0.2	2.38 ± 0.12	8.82 ± 0.41	69.7 ± 4.4	4.38 ± 0.29	34.6 ± 2.8
CsA_M20 3 months 25°C 60%RH	14.6 ± 0.3	12.6 ± 0.3	2.61 ± 0.10	9.47 ± 0.22	74.7 ± 0.1	4.11 ± 0.09	32.4 ± 1.5
CsA_M20 3 months 40°C 75%RH	15.0 ± 0.3	12.5 ± 0.9	2.58 ± 0.15	8.55 ± 0.85	68.3 ± 2.0	3.75 ± 0.04	30.1 ± 1.8

From Figure 4, illustrating the deposition of the CsA in the NGI, it is possible to observe that most of the particles were collected on Stages 2, 3 and 4 and about 4% was collected in the MOC capturing particles with a size lower than 0.5 μm. This led to obtaining an MMAD value of 2.97 ± 0.1 μm.

A clinical trial, evaluating the CsA anti-inflammatory efficacy in BOS by the nebulization of 300 mg, demonstrated that a deposition of CsA greater than 5 mg in the lung correlates with an improvement of lung functionality, and 12 mg was indicated as an anti-rejection protective dose [49]. In light of these results, it can be considered that the FPD of 8.8 mg, generated by the aerosolization of 20 mg of CsA_M20, is in the correct therapeutic range for the prevention of BOS.

Regarding the management of the COVID-19 infection, there are no efficacy or pharmacokinetic data upon the delivery of CsA by inhalation. However, COVID-19 patients who received 300 mg of CsA orally showed positive results on survival [60]. Of this dose, the amount of CsA available to the lung will have been very low but still sufficient to dampen the inflammatory reaction of the respiratory tract. Inhalation

administration would make it possible to obtain equal or higher efficacy in the face of a reduction in the administered dosage and reduced systemic exposure.

Stability analyses on the CsA_M20 powder stored in HPMC capsules, conducted at 1 and 3 months in standard and accelerated conditions, provided drug content values in a range between 78-82% without being significantly different from the initial value ($p<0.05$). In the aerodynamic assessment, the CsA ED was around 13 mg and the FPD was in the range of 8-9 mg, independently of the storage condition and check time of the analysis (Table 4). These data, albeit preliminary, show that the use of mannitol as a bulking excipient was able to protect the physicochemical stability of the formulation preserving its initial characteristics. The use in this work of Quali_V®_I capsules specifically produced for DPI, with optimised puncturing properties and internal lubricant features certainly contributed to this positive achievement [61]. Finally, the CsA_M20 showed a differential scanning calorimetry profile at three months equal to that at time zero, supporting that the powder did not undergo solid-state transformations during the observation time (see Annex B).

3.4.2 CsA_M20 cytotoxicity and anti-inflammatory efficiency

The viability of human lung adenocarcinoma cell line A549 and monocytic cell line THP-1 was not affected by the various CsA tested treatments, which were well tolerated by cells as reported in Figure 5. Indeed, under these conditions, neither CsA_rm nor the spray-dried powder of CsA containing mannitol did display any cytotoxic effect on the two cell cultures compared to the vehicle (0.5% DMSO in PBS).

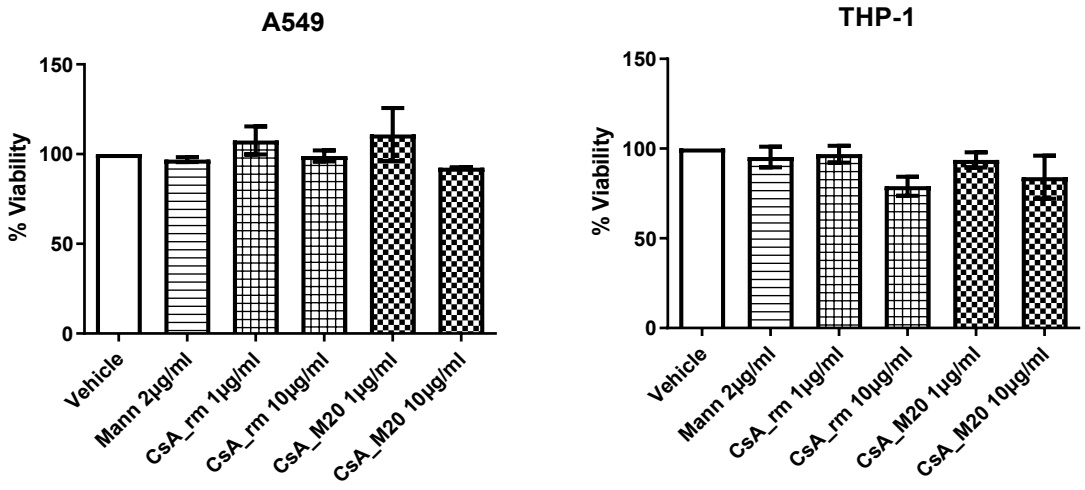

Figure 5. Viability of A549 and THP-1 cell cultures exposed to the vehicle, mannitol (Mann) 2 μg/mL, CsA_rm at 1 and 10 μg/mL, CsA_M20 spray-dried powder at 1 and 10 μg/mL, expressed as a percentage with respect to the vehicle.

IL-6 is a pro-inflammatory cytokine involved in numerous cellular processes such as proliferation and survival. Furthermore, the high serum levels of IL-6 in patients who have undergone a lung transplant were a marker for the development of chronic lung allograft dysfunction [62, 63]. In parallel, it was observed that COVID-19 infection is accompanied by an aggressive inflammatory response with the release of a large amount of pro-inflammatory serum cytokines in an event known as "cytokine storm" [64]. In particular, IL-6 was reported to be a potential predictor for the development of severe COVID-19 since elevated levels of this cytokine were associated with critical patient conditions such as acute respiratory distress syndrome, and the need for mechanical ventilation [64]. As IL-6 is the most frequently reported cytokine to be increased in COVID-19 patients and as IL-6 elevated levels have been associated with higher mortalities, this cytokine was selected in this work to test the CsA anti-inflammatory effect.

The levels of IL-6 were determined by ELISA test 24 hours after the treatment of cell co-cultures exposed to LPS. The levels of the cytokine were significantly reduced either by CsA_rm or by formulated CsA compared to the vehicle (Figure 6). Mannitol used as an excipient in the formulation, showed as well a slight anti-inflammatory effect, albeit not statistically significant, as already reported *in vivo* [65]. The results confirm

that by the spray-drying process was possible to construct highly respirable particles with improved dissolution rate preserving the CsA anti-inflammatory effect. An inhaled powder of CsA, therefore, represents a favourable therapeutic strategy to avoid the triggering of a vigorous immune reaction in the lungs. Consequently, this action would limit the production of cytokines and their consequent spillover into the circulatory system preventing the systemic cytokine storm.

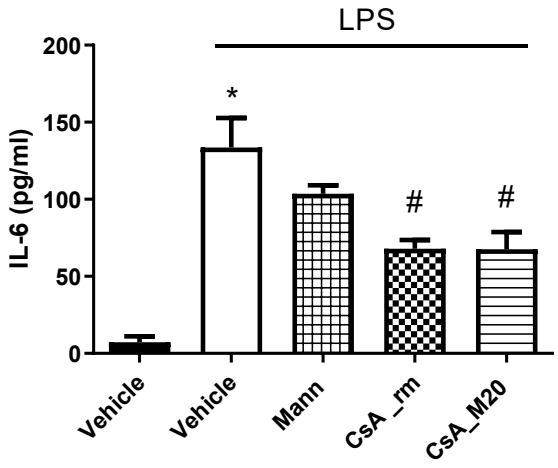

Figure 6. *In vitro* inhibition of IL-6 production by THP-1/A549 co-culture exposed to LPS in the presence of the vehicle, CsA_rm at 10 μg/mL, CsA_M20 at 10 μg/mL of CsA, or mannitol (Mann) at 2 μg/mL; * $p < 0.05$ vs. vehicle; # $p < 0.05$ vs. vehicle + LPS, ANOVA test followed by Bonferroni's post-test.

3.4.3 In vitro anti-viral efficacy against SARS-CoV-2

As mentioned before, CsA has been shown to have a direct inhibitory effect on the replication of different types of coronaviruses including SARS-CoV-2. For this purpose, orally administrated CsA has also been the subject of clinical trials, reporting positive results on the survival of patients affected by COVID-19 [60, 66]. Moreover, to date, other ten clinical trials are ongoing, although the results have not yet been available, indicating the high interest in CsA for the treatment of this disease.

In light of these considerations, the last part of the study explored the inhibition activity of CsA_M20 powder on viral replication in Vero E6 cells, in comparison to the CsA_rm. Furthermore, different types of treatment (pre-treatment, post-treatment, or

simultaneous regimen) were adopted to assess the more effective one to contain the virus.

The infected cells were treated with CsA_rm, CsA_M20, or mannitol powders applied according to the different treatments. Figure 7 illustrates the virus infectivity reduction in relation to the CsA concentrations applied. The effect of mannitol alone was as well assessed since it is a component of the engineered CsA powder. The range of CsA concentrations investigated was selected according to the one proposed by de Wilde *et al.* [67]. A 100% viral infectivity reduction corresponds to the maximal reduction in the viral load.

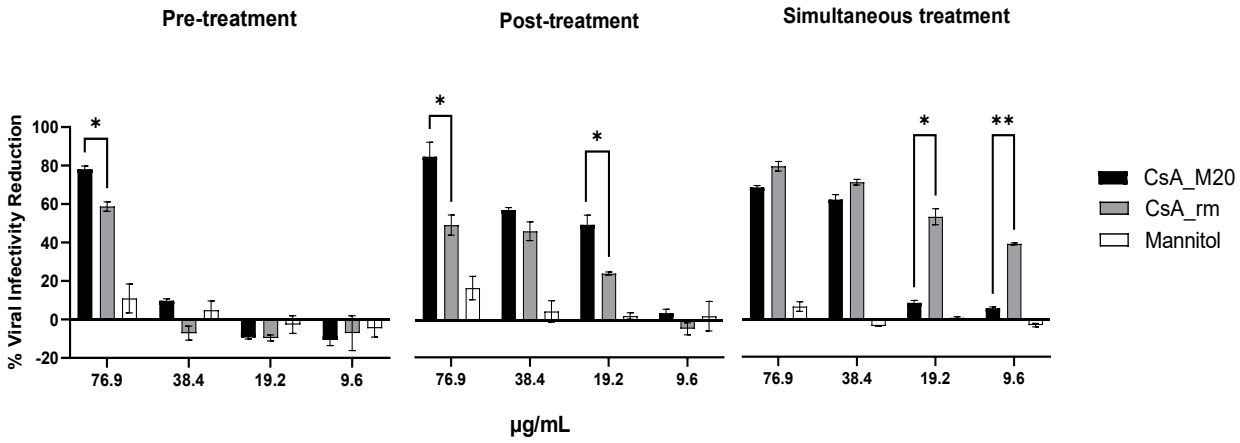

Figure 7. *In vitro* SARS-CoV-2 omicron BA.1 infectivity reduction produced by CsA_rm, CsA_M20 or mannitol. Pre-treatment: one hour before infection. Post-treatment: two hours after infection. Simultaneous treatment: cells were infected and treated with the powders at the same time. The mannitol concentrations corresponding to CsA formulation at 76.9, 38.4, 19.2, and 9.6 µg/mL were respectively 15.4, 7.7, 3.8, and 1.9 µg/mL. Data were analysed with two-way analysis of variance (ANOVA) (* $p < 0.05$; ** $p < 0.01$; CsA_M20 vs. CsA_rm).

During the pre-treatment, only the highest CsA concentration applied (76.9 µg/mL) showed an antiviral effect. The reduction of viral infectivity was 78% when the drug was formulated as a spray-dried powder and was statistically superior to the raw material, which reduced the infection of 58%. At lower concentrations, CsA did not have any relevant antiviral effect. Similarly, mannitol did not produce inhibitory effects at any of the tested concentrations. At the lowest concentrations (19.2 and 9.6

μg/mL) of all the treatments even greater viral growth was observed in the treated samples compared to the control, this is identified by the negative value of the infectivity percentage. To interpret the data, it should be mentioned that the cell culture medium containing CsA was replaced with fresh medium before applying the virus, therefore, the drug that interacted with the pathogen replication was only the fraction that was internalized by the cell. **The fact that CsA_M20 has superior efficacy than CsA_rm could be due to the higher dissolution of these composite particles, possibly increasing the host intracellular concentration of the drug where the virus was replicating**. These positive inhibition results show that CsA is active not only against SARS-CoV as shown in 2011 by de Wilde *et al.,* [67], but also on the SARS type CoV_2 responsible for the current sanitary emergency. It was demonstrated that CsA treatment rendered the virus RNA and protein synthesis almost undetectable [67]. In parallel, the reduction of cyclophilins did not interfere with the SARS-CoV replication. Finally, has been demonstrated *in silico* a further blocking mechanism: CsA was able to bind and block through molecular docking two membrane proteins (TMPRSS2 and CTSL) necessary for SARS-CoV-2 to penetrate the host cell [68].

Differently from the pre-treatment condition, in the post-treatment regimen, the viral inhibitory activity was present for all CsA concentrations tested except for the lowest one. Furthermore, the CsA_M20 powder was always more effective than the CsA_rm although statistically superior only at the concentration of 19.2 and 76.9 μg/mL. Mannitol, as in the previous case, showed a slight activity of reducing infectivity. As regards the adopted protocol, in this case, the treatment was applied after the virus had been allowed to absorb and then removed from the culture. Therefore, as in the case of the pre-treatment, the block of the virus infection presumably took place inside the host cell, where the viruses remained after washing resided. The engineered CsA powder had, in these conditions, superior efficacy likely due to its enhanced dissolution leading to a higher amount of drug entering the host cell where the virus was replicating.

In the simultaneous treatment, the CsA_M20 and CsA_rm powders performed similarly at the two highest concentrations tested where the inhibition reached 75-80%. This trend changed at 19.2 and 9.6 μg/mL, at which only raw CsA showed an antiviral effect of 30% significantly higher than that of CsA_M20 (5%). This was the only experimental protocol in which the cells were exposed to the virus simultaneously with the treatment, therefore the only situation in which the drug-virus interaction took place both in the extracellular compartment and subsequently intracellularly. The inhibition data of the CsA_rm highlight that an interaction may occur between drug suspension and the virus which does not happen in the case of the more soluble CsA_M20 powder. In fact, the members of the *Coronaviridae* family possess a phospholipid envelope, therefore an interaction between the pure CsA_rm and the viral membrane would be possible. It is known that CsA binds lipid membranes following the classic hydrophobic effect and that CsA affects the membranes in a concentration-dependent manner by perturbation of the organization of fatty chains [69]. Hence, it can be hypothesized that in the case of the CsA_rm, the solid particles create a concentration at the particle-virus interface close to saturation, higher than that generated by the CsA_M20 solubilized in the medium. This difference could explain the high ability to interact with the cell membrane of the virus. Furthermore, the presence of solid particles could represent a further obstacle to infection as they act as a physical barrier and reduce the surface area available for virus adsorption. In contrast, CsA_M20, which was successfully dissolved in the medium, could little hinder the interaction between the virus and the host cell membrane. In this regard, the creation of a polymeric barrier is exploited as a system to inhibit virus-cell interaction by numerous commercially available nasal sprays to antagonize the infection.

In summary, the most effective treatment regimens were post-infection or simultaneous infection treatment. In both cases, the infectivity of SARS-COV-2 was reduced and in the case of post-treatment more efficiently by the CsA_M20 powder than the raw material. This post-infection approach is also the most plausible

considering that commonly the pharmacological treatment follows and does not simultaneously accompany the entry of the virus. Moreover, the raw material, although effective, cannot be administered as such due to its low respirability. At variance, the prophylactic treatment, although *in vitro* data, has not proved to be effective except at the highest concentration tested, probably because in cases of treatment with a lower dosage, an effective drug concentration is not internalized and retained by the cells.

3.5 Conclusions

The work demonstrated that, through the modulation of mannitol and ethanol, it was possible to achieve an inhalation powder with high respirability (FPF of 66.5%) and improved CsA release (WDT of 59.5 min). This aspect is of crucial importance considering CsA has a very low oral bioavailability and therefore a rapid lung release would be extremely advantageous to obtain high pulmonary exposure.

Besides, the fact that the inhalation powder developed could represent an advantageous strategy in the prevention of lung transplant rejection, the collected findings provide strong *in vitro* evidence that this therapeutic approach could be efficient in the reduction of SARS-CoV-2 infectivity, especially as post-infection treatment. CsA_M20 powder, applied to cells one hour after contact with the virus, was able to inhibit its replication by 93%. Finally, the CsA-engineered powder showed an anti-inflammatory effect in terms of IL-6 reduction that could also be useful in containing the COVID-19 cytokine lung storm.

This chapter, as research article, has been published in Pharmaceutics Journal.

ANNEX A Chapter 3

Details of the *in vitro* analysis on viral infectivity reduction on VERO E6

In vitro cell culture setup

Vero E6 cell cultures (American Type Culture Collection [ATCC] CRL-1586) were grown in Minimum Essential Medium (MEM) supplemented with 2 mM L-glutamine, 100 U/mL penicillin, 100 μg/mL streptomycin (complete culture medium) and 10% heat-inactivated fetal bovine serum (FBS), as recommended [70]. Cells were incubated at 37°C in a humidified, 5% CO_2 atmosphere-enriched chamber until use. For compound treatment studies, cells were seeded in 96-well plates and cultured in MEM containing 2% FBS. Cell culture medium and supplements were purchased from EuroClone (Milan, Italy).

Virus propagation and titration

The viral strain was isolated from a residual clinical specimen conferred to the Unit of Microbiology, Greater Romagna Area Hub Laboratory, Cesena, Italy, for routine diagnostic purposes and sequenced as part of the project for monitoring the prevalence and distribution of SARS-CoV-2 variants in Italy, promoted by the Italian Institute of Public Health (ISS). Before being used for this study, the sample underwent an anonymization procedure in order to adhere to the regulations issued by the local Ethical Board (AVR-PPC P09, rev.2; based on Burnett *et al*., 2007 [44]). In brief, 500 μL of clinical specimens were used to infect the Vero E6 cell monolayer at confluency. After one-hour adsorption, the culture was maintained in 2% FBS MEM and incubated for 72 hours. The viral strain was titrated using the endpoint dilution method [71]. In brief, serial 10-fold dilutions (from 10-1 to 10-10) in 2% FBS MEM were used to infect confluent monolayers of cells in a 96-well plate. After 72 hours, cells were fixed and stained using a 4% formaldehyde solution in crystal violet. The absence or presence of cytopathic effect at each dilution was assessed by comparison of each well with virus

control and cell control wells. Viral titres, expressed as TCID (Median Tissue Culture Infectious Dose) 50/mL, were calculated with the Reed and Muench formula based on eight replicated for dilution [72].

Preparation of the sample for the PCR analysis and details of amplification

For the PCR quantification, 15 μL of the sample was diluted 1:4 in 45 μL of RNase-free water in a 96-well PCR plate, and hence 5 μL of the dilution was transferred to another plate with 16 μL of PCR master mix, containing 5 μL of MOM (MuDT Oligo Mixture, with dNTPs, oligos, primers and TaqMan 5′ fluorophore/3′ Black Hole Quencher probes), 5 μL of enzymes, 5 μL of RNase-free water and 1 μL of exogenous internal control for every reaction.

The assay was run on a CFX96 real-time thermal cycler (Bio-Rad, Feldkirchen, Germany). The amplification process includes cDNA denaturation at 95 °C for 10 seconds, primers annealing at 60 °C for 15 seconds and elongation at 72 °C for 10 seconds (44 cycles). Results analysis and target quantification were performed with 2019-nCoV Viewer from Seegene Inc.

ANNEX B Chapter 3

Solid State Analysis of CsA_M20 Powder and Stability

Methods

Differential scanning calorimetry

A differential scanning calorimeter DSC 821e (Mettler Toledo, Switzerland) was employed to investigate the thermal behaviour of powders in the temperature range from 25 °C to 200 °C at a heating rate of 10 °C/min. Data were acquired and analysed using a STARe software (Mettler Toledo). About 4 mg of powders were placed in 40 μL aluminium pans, sealed and double pierced. Analysis was performed under a flux of nitrogen of 100 mL/min.

X-Ray Powder Diffraction

This analysis was assessed using a MiniFlex diffractometer (Rigaku, Tokyo, Japan) with a 30 kV Cu Kα radiation (λ = 1.5418 Å). The powder was placed in the aluminium sample holder and subsequently flattened to obtain a smooth surface. The goniometer was set at a scanning rate of 1.5° min^{-1} (step size = 0.05°) over the 2 θ range 5–35°.

Results

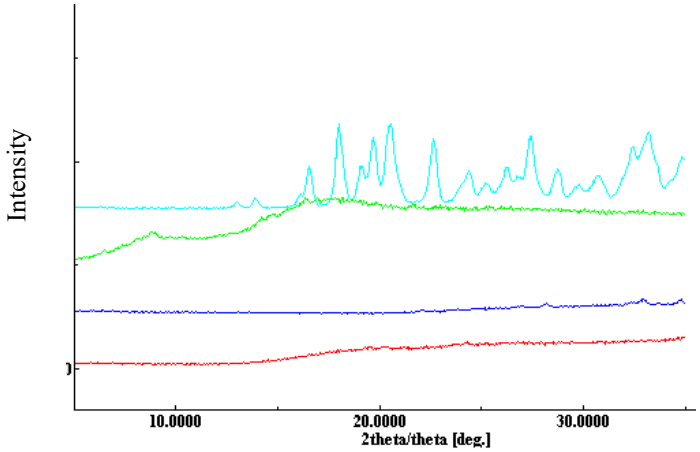

Figure 1B. XRPD scan of mannitol raw material (light blue), CsA raw material (green), CsA_M20 powder at time 0 (blue) and after 6 months (red).

The XRPD patterns in figure 1B indicate that CsA_rm was amorphous, while mannitol raw material was crystalline. Moreover, the CsA_M20 powders were amorphous both at time 0 and 6 months after production, and no characteristic peaks of the crystalline state were observed.

DSC scan was performed with the aim of characterizing the spray-dried powders and of the single excipients before the drying process. It is known that it is extremely important to assess that the solid state of the material does not change over time to prevent changes in the aerodynamic profile and other fundamental characteristics of the powder. Initially, a DSC analysis of CsA_rm and pure CsA SD was performed (Figure. 2B). Raw cyclosporine, before and after spray drying, appears to have a similar DSC profile characterized by an initial broad endotherm, between 35 and 100 °C, that was ascribed to the evaporation of the moisture in the samples. This endothermic event was followed by a further endothermic event at 130°C attributable to glassy-rubbery

transition as previously reported by Jiang *et al.,* [73].

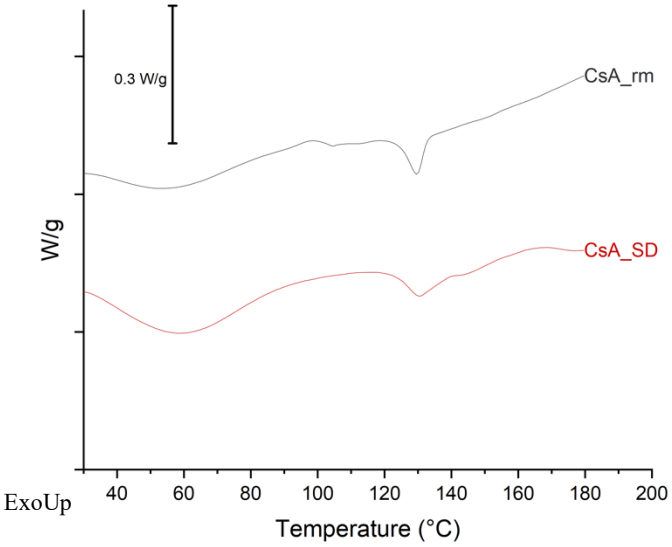

Figure 2B. DSC scan of: CsA raw material (CsA_rm) (black); CsA spray dried: (CsA_SD) (red).

Subsequently, the DSC traces of mannitol raw material and pure mannitol spray-dried, prepared using the same conditions of solution composition and process parameters of CsA M20, were compared (Figure 3B).

Both raw mannitol and spray-dried mannitol showed a single endothermic event at 166.78°C and 167.32°C for spray-dried and raw mannitol respectively, in strong agreement with what is reported in the literature in analyses concerning the beta form of mannitol, moreover as previously reported in the literature, spray dried mannitol alone recrystallize in the beta form [74, 75].

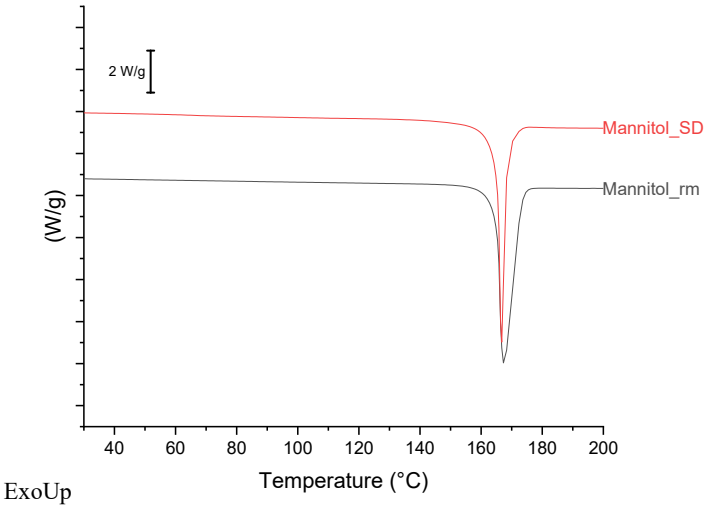

Figure 3B. DSC scan of mannitol spray dried (red) and mannitol raw material (black).

Finally, Figure 4B shows the analysis of the CsA_M20 powder at time zero and after 6 months of storage at room temperature. This powder contains 20% mannitol; it is known that this material can exist in various polymorphic forms (α, β, δ) and that as a pure amorphous material, it tends quickly to convert into the most stable β crystalline form.

The DSC analysis of CsA_M20 showed a similar profile at time zero and after storage of 6 months at room temperature. At time zero, the thermogram showed an initial endothermic peak at 60°C likely due to the glass transition of the material (composite mixture of amorphous drug and mannitol). At 143°C an exothermic peak was observed, interpreted as the recrystallization of the amorphous mannitol followed by an endo-exo event starting at 156°C attributable to the melting of mannitol delta form immediately followed by the recrystallization of the beta form that eventually melted at 168°C [73, 75].

As regard the behaviour of the CsA_M20 after 6 months of storage, two slight differences were observed: the initial endothermic peak was anticipated at 45°C and the mannitol exothermic recrystallization event (at 142°C) was more evident. Despite these thermal behaviour modifications, the aerodynamic behaviour and chemical stability of the peptide was not different form time zero, indicating that these events

do not affect the critical characteristics of the product.

This analysis shows how the spray drying process of mannitol with cyclosporine leads to the formation of an amorphous solid, in which mannitol under heating recrystallised in the delta polymorph different to the one of mannitol alone (the beta-crystalline phase)

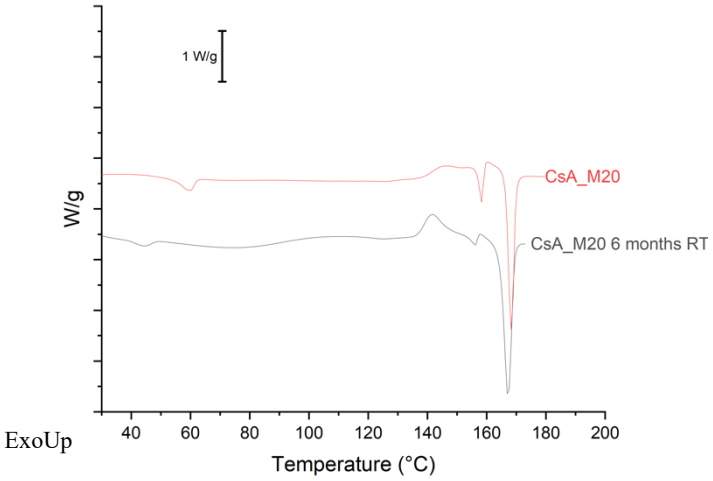

Figure 4B. M20 powder at time 0 after production (CsA_M20) and CsA_M20 after 6 months at room temperature (CsA_M20_6RT).

4. Calcium Phosphate Coated Liposome loaded with Cyclosporin-A as Inhalable Powder Improved the Anti-inflammatory Effect

4.1 Introduction

In this second part of the thesis, **CsA was loaded into calcium phosphate-coated liposomes** to build a formulation with CsA promptly available in the liposome membrane and with improved release/internalization properties compared to the CsA raw material.

As previously mentioned in Chapter 3, cyclosporine A is a drug with low oral bioavailability mainly due to its poor water solubility, the use of which in the prevention of transplant rejection and the onset of BOS is accompanied by a high dosage and side effects affecting the kidney and liver. In 2009 Bher and colleagues carried out a clinical trial employing a liquid liposomal CsA formulation administered by aerosolization in patients who had undergone a lung transplant [53]. The formulation was designed with the aim of developing a colloidal safe-stable suspension and avoiding the administration of propylene glycol used as co-solvents in previous clinical trials that require the use of bronchodilators and local anaesthetics [52, 53, 76].

The results were positive in terms of local tolerability of the formulation, however, the study did not proceed, probably due to problems relating to the financing of the clinical trial which subsequently led to premature termination of the study [51]. In detail, a dose between 5 and 20 mg of CsA was delivered in form of liposomal liquid formulation. Among the positive results, it was reported a BOS free survival improved by 58% compared to placebo, in patients with a single lung transplant accompanied by a reduced occurrence of side effects such as nephrotoxicity.

Liposomes are one the most approved type of nanoparticle by FDA [31]. This structure was first discovered by Professor Bangham in 1964 [77]. They are spherical structures composed of phospholipids, often in combination with sterols such as cholesterol, surrounding an aqueous core [31].

Phospholipids are amphiphilic molecules containing a hydrophilic headgroup and two hydrophobic chains. In an aqueous environment, phospholipids organize themselves to form membranes. The polar heads will therefore have the tendency to interact with the aqueous environment, while the hydrophobic tails will be found inside the membrane. Due to their nature, this nanosystem can be used for the encapsulation of both lipophilic drugs that will be dissolved between the fatty acids chains of the phospholipid, and hydrophilic drugs, which will be encapsulated in the aqueous core [78].

It is then possible to classify the liposomes according to their size and internal structures or the number of bilayers. Unilamellar liposomes can be distinguished according to the size in small unilamellar vesicles (SUVs; 20–100 nm) or large unilamellar vesicles (LUVs; 100 nm −1000 nm) and giant unilamellar vesicles (GUVs;>1000 nm). Phospholipids can be assembled to form multilamellar liposomes with concentric bilayers called multilamellar vesicles (MLV; >500nm) or multi-vesicular vesicles (MVV) Figure 1 [78, 79].

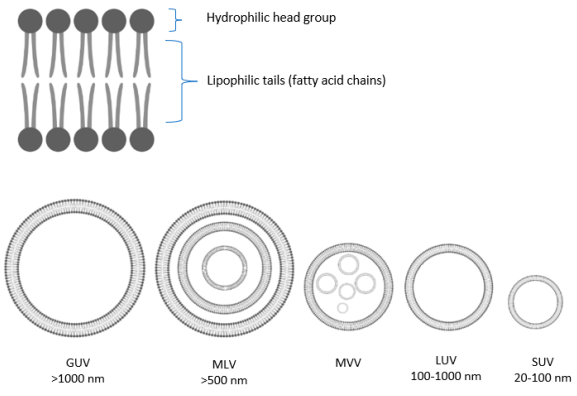

Figure 1. Details on the phospholipid composition of the liposomal membrane and types of liposomes. Created with BioRender.com

This type of nanoparticle has some advantages that make it an interesting drug delivery system. Given its composition, this system can be considered biodegradable and biocompatible. It also allows passive cellular targeting and improves transport across cell membranes. It is also possible to carry out active receptor-ligand targeting on tumour cells by functionalizing the surface of the liposome with antibodies, peptides, proteins and aptamers [79, 80]. Due to these advantages, one of the main applications of liposomes is in anticancer therapy. This is due to the possibility of reducing the systemic toxicity of the treatment and, at the same time targeting the tumour tissue. An important passive targeting mechanism is the so-called EPR effect (Enhancer Permeation and Retention), which takes advantage of the peculiar vascular system of the tumour. One of the historical examples is *Doxil®*, the first liposomal system approved by the FDA, containing doxorubicin encapsulated in pegylated liposomes.

Another important application of liposomes is in the treatment of systemic fungal infections. *Amphotericin B*, for example, is a drug characterized by high systemic toxicity such as hypertension, nausea, hypoxia, fever, whose encapsulation in liposomes represents an excellent drug delivery strategy, as in the case of the commercial product *AmBisome®* [79, 81, 82]. Encapsulation of amphotericin B in liposomes would favour the interaction with fungal cell membranes containing ergosterol, and the release of the drug within fungal cell, meanwhile reducing the interaction with human cell membranes [83]. Additionally, *Ambisome®* has been used off-label in patients with cystic fibrosis, for the treatment of aspergillosis [84].

Another interesting application of liposomes is the treatment of lung pathologies through inhalation therapy. Amikacin is a broad-spectrum antibiotic with low oral bioavailability. The use of this molecule has been limited due to systemic side effects (nephrotoxicity and ototoxicity). However, this drug has found use in the treatment of pulmonary infections Mycobacterium avium complex and *Mycobacterium abscessus*, in patients with cystic fibrosis and immunocompromised as in the case of *Arikayce®*,

containing amikacin encapsulated in liposomes, administered to the lung by nebulization [4].

Calcium phosphate (CaP) is a naturally occurring material also as a normal constituent of teeth and bones in the form of hydroxyapatite. Although it is an insoluble material at pH 7.4, it is rapidly degraded into calcium and phosphate ions at pH values below 5 [85, 86]. These characteristics have also made synthetic CaP interesting as a drug delivery system. If formulated as nanoparticles, the drug can be adsorbed on the surface or encapsulated within the nanoparticle[85]. CaP has also been used in the coating of vincristine-loaded liposomes. The authors observed an approximately 4-fold increase in the uptake of CaP-coated liposomes on A549 compared to uncoated liposomes[86]. Therefore, the possibility of increasing cellular uptake and having a pH-dependent release makes CaP-coated liposomes potentially useful also in the delivery of cyclosporine through the lungs in the prevention of rejection. With this system, it would potentially be possible to reduce the clearance operated by the alveolar macrophages, increase the uptake by the cells of inflamed tissues and obtain a release of the drug inside the cell after fusion with the lysosome at pH 5.

One of the main problems of liposomal formulations is the relative chemical instability of the phospholipids mainly due to oxidation and hydrolysis phenomena, to which is added the instability of the nanosystem, which can go against phenomena such as membrane fusion, aggregation, drug release encapsulated [87]. Once the liposomal formulation has been optimized, delivery to the lung can be accomplished by nebulization or by constructing an engineered dry powder. In this case, it is necessary to add a bulk excipient that acts as a matrix former during the construction of the microparticle. Once in contact with an aqueous medium, the excipient must dissolve and the liposomes with their original size should be restored.

These degradation phenomena take place in an aqueous environment whereby the stabilization of the liposomes can be carried out through the inclusion of the liposomes in an amorphous matrix. The elimination of water can be done with several well-

known drying techniques such as freeze-drying, spray freeze-drying, and supercritical fluid technology [87]. The basic principles of stabilization during the drying phase also apply to the stabilization of macromolecules such as peptides and proteins and are mainly explained by the water replacement theory and the vitrification theory [27, 29, 87–89]. The first theory explains how during the drying process, the water molecules which form the bonds with the liposome in the formulation would be replaced by the other hydrogen bonds which are formed with the bulk or stabilizing agent. The second theory would explain how the stabilizing excipients would form a glassy matrix around the liposome which would reduce its molecular movements and degradation. However, the two theories are not mutually exclusive but participate in the explanation of the process [10]. Furthermore, powder production by spray drying would make it possible to formulate a powder with aerodynamic characteristics favourable for inhalation therapy, *i.e.* obtaining inhalable particles with an aerodynamic diameter of less than 5 μm.

The aim of the work was the development of an innovative inhalable powder of CsA for the prevention of BO development after lung transplantation. The powder consists of microparticles embedding calcium phosphate-coated liposomes. This formulation was designed for local administration to the lung and with the purpose to reduce the dose. This would let to obtaining a high local concentration in the lung and consequent long-term CsA side effects reduction. The use of an inhaled powder would give the possibility of obtaining a higher concentration of the drug at the site of action (the lung) compared to the oral or injectable formulation. The powder described below contains liposomes loaded with CsA and coated with calcium phosphate. The size of the liposomes would favour cellular internalization. The calcium phosphate coating also participates in this process, which would also offer the possibility of reducing the clearance operated by the alveolar macrophages, and of obtaining a controlled release inside the cell, limiting the dispersion of the drug to the systemic circulation. Overall, the formulation would make it possible to reduce the dosage currently used orally or by injection, in the prevention of pulmonary rejection following transplantation and

to reduce undesirable effects. The ability to decrease IL-6 expression in THP-1/A549 cells co-culture was used to verify the improved anti-inflammatory effect of the coated liposomal formulation compared to the uncoated liposomes or raw material.

4.2 Materials

CsA (CAS Number 59865-13-3) was purchased from Metapharmaceutical (Barcellona, Spain). HPMC extra-dry capsules for use in dry powder inhalers, Quali-V®-I size #3, were provided by Qualicaps (Madrid, ES) and a single dose dry powder inhaler RS01 high resistant was gifted by Plastiape (Lecco, IT). Glycine (Sigma-ALDRICH lot. SLCC7952), lecithin from soybean containing 75% phosphatidylcholine (Lipoid S80) was purchased from Lipoid GmbH (Germany). L-leucine USP (A.C.E.F. SPA, lot number 7096004, Pearlitol 100SD-Mannitol (Roquette, batch number: E 172D), Zinc sulphate monohydrate (AnalytiCals CARLO ERBA, batch number: I289MI00), Ethylenediaminetetraacetic acid disodium salt dihydrate (Sigma-ALDRICH, batch number: 61930); Eriochrome black T (AnalytiCals CARLO ERBA, batch number: 464221) Sodium stearate (Sigma-ALDRICH, lot number: SZBC0170V).

All other chemicals used were obtained from commercial suppliers and were of analytical grade.

4.3 Methods

4.3.1 Preparation of CsA-loaded coated liposomes

Liposomes were prepared by solubilizing lecithin (Lipoid S80) and, cholesterol, if present, in ethanol (17.5% *w*/*v*). Cholesterol was added with a molar ratio of 30% or 20% on the number of moles of Lipoid S80. The composition of Lipoid S80 is 78% phosphatidylcholine (MW= 760 g/mol), 4% phosphatidylethanolamine (MW= 299.21 g/mol) and 2% lysophosphatidylcholine (MW=299.26 g/mol), the molecular weight of the LipoidS80 was calculated as a weighted average, obtaining 727.09 g/mol. CsA was dissolved in 60 mL of water: ethanol 66:33 solution under stirring at 500 RPM. The amount of CsA dissolved was 100, 150 and 200 mg representing Batch A, B and C

respectively. Both solutions were heated up to 70°C above the glass transition temperature of the lipidic components [90]. The lecithin solution was added drop by drop to the hydroalcoholic solution containing CsA. After reaching room temperature, the size of the particles was reduced by means High-Pressure Homogenizers (HAP) (Panda Plus 2000, GEA Niro Soavi SpA, Parma, Italy) for 5 min at a pressure of 800 bar corresponding to 20 cycles of homogenization. The size and Z-potential of the sample were then analysed by dynamic light scattering (DLS) using Malvern Zetasizer (Malvern Instruments, Worcestershire, UK).

After this process, the liposomes were coated with calcium phosphate. Calcium phosphate coating was produced using a sequential step addition approach in which 1.5 mL 50 mM calcium chloride dihydrate solution and disodium hydrogen phosphate dihydrate 50 mM were added to a 1:10 diluted with ultrapure water liposome dispersion. At room temperature, 10 mL of the liposome dispersion was added to 87 mL of ultrapure water under magnetic stirring at 350 rpm for 5 minutes.

Under magnetic stirring (500rpm) 1.5 mL of 50 mM $CaCl_2$ $2H_2O$ solution was added to the formulation, and after 60 minutes, 1.5 mL of 50 mM Na_2HPO_4 $2H_2O$ solution was added and left under magnetic stirring for 60 minutes. Finally, the 100 mL volume dispersion of liposomes was dialyzed for 24 h using a Spectra/Por® 3 dialysis membrane with 3.5 kDa MW cut-off (Spectrum Laboratories) in a hydroalcoholic (4.28% EtOH) medium volume of 9 L. under constant magnetic stirring (160 rpm).

Table 1. Summary of the quali-quantitative composition of CsA liposomes coated with CaP before the dialysis. Three different batches of lecithin liposomes (Lipoid S80®) containing three concentrations of CsA (4.8, 7.0 or 9.0% w/w concerning the solid content) were produced. Two batches of liposomes were prepared by replacing 20 or 30% (calculated relative to the number of moles) of the lecithin.

	Liposomes Composition (Concentration of components pre-dialysis)				
Batch (CsA initial conc.)	CsA (mg/mL)	Lipoid S80 (mg/mL)	Cholesterol (mg/mL)	$Na_2HPO_4 \cdot 2H_2O$ (mg/mL)	$CaCl_2 \cdot 2H_2O$ (mg/mL)
A (4.8% w/w)	0.14	2.54	-	0.13	0.11
B (7.0% w/w)	0.21	2.54	-	0.13	0.11
C (9.0% w/w)	0.29	2.54	-	0.13	0.11
B_Chol30	0.21	1.77	0.40	0.13	0.11
B_Chol20	0.21	2.01	0.27	0.13	0.11

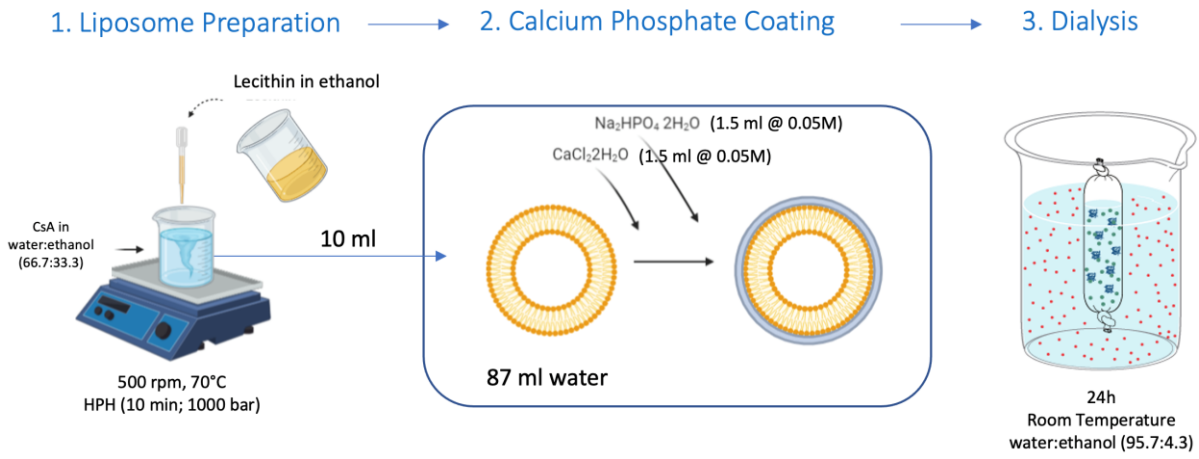

Figure 2. Scheme of liposomes preparation process. Created with BioRender.com

4.3.2 HPLC drug content quantification and solid quantification

Quantification of cyclosporine was performed by HPLC, according to the method described in section 3.3.2. Briefly: A Nova-Pak C18 column, 4 μm was used; 3.9x150 mm, maintained at 65°C. the wavelength of the UV detector was set at 230 nm. the mobile phase consisted of a solution of acetonitrile and water in a 63:35 ratio. However, in this case, an injection volume of 100 μL was selected and the liposomal sample required solubilization in acetonitrile: water solution with a ratio of 80:20 and subsequent sonication for 5 minutes in order to ensure the complete solubilization of the liposomal structure. The solid content present in the liquid formulation following coating and dialysis was obtained by drying 2 mL of dispersion for 24 hours in an oven with a controlled temperature of 40°C. The data were then expressed as mg/mL.

4.3.3 Calcium titration in coated liposomes

The presence of the calcium phosphate salt present in the formulation, after the dialysis process, was carried out by calcium back-titration as described in USP 40 mL of CaP coated liposomes was dissolved adding 1.2 mL of HCl 0.1M solution. An excess of EDTA was added to the sample solution. The solution was buffered using NH_4Cl/NH_3 to pH 10. EBT (Eriochrome Black T) was used as indicator. A solution of $ZnSO_4$ (0.02 M) was used as titrant to determine moles of unbounded EDTA. The volume EDTA needed to bind the Ca+ in the sample was obtained from the difference between the volume of $ZnSO_4$ and EDTA used. Knowing that EDTA binds calcium with a stoichiometric ratio 1:1 it was possible to calculate the moles of calcium present in the solution[91]. Before the sample was coated with CaP, this process was applied to the same formulation used as a blank to validate the titration method.

4.3.4 Dynamic light scattering (DLS)

This analysis was conducted using Nano Zetasizer (Malvern Panalytical, Malvern, UK) in order to achieve the size of the liposomes and their distribution in the dispersion, considering the value of the PDI, the polydispersity index.

Liposomes' size was evaluated after their preparation, after their homogenization and after their CaP coating and dialysis. In the first two cases, the samples were analysed after a 1:100 dilution to reduce the concentration of the dispersion, avoiding multiple scattering or viscosity effect. For this reason, 100 μl of the dispersion of liposomes was added in a 10 mL volumetric flask and made up to the mark with Ultrapure water. In the third case, instead, because a 1:10 dilution occurs during the coating procedure, the liposomes are analysed without any other handling. The ζ-potential of the liposomal dispersion was studied using the same equipment. The analysis was performed before and after the coating process, to verify the presence of the CaP on the liposome surface. The restoration study was assessed through DLS analysis by dissolving 10 mg of powder in 100 mL of Phosphate buffer saline (pH=7.4) or sodium acetate buffer (pH=5).

4.3.5 Cryo-transmission electron microscopy (cryo-TEM)

Cryo-TEM images of unfixed frozen hydrated liposomal samples were obtained in the laboratories of the Department of Life Sciences of the University of Siena. This technique allows the sample to be displayed in its natural state. The preparation of the sample provides for rapid freezing of the liquid sample in hexane cooled with liquid nitrogen. This avoids the formation of crystals in the sample that could damage the fragile structure of the liposome [92].

Before the analysis 2.3 mL of sample were placed on Quantifoil® copper grid and frozen using the Vitrobot Mark IV (FEI) instrument with blot force -2, blotting time 3 seconds at 20°C and 100% of humidity.

The sample was then observed by means of TEM CM200 FEG (FEI) Low, 200kV equipped with Tem Cam F224HD (TVIPS) and cryotransfer specimen holder 626 DH (Gatan).

Cryo-EM is a type of electron microscopy in which the samples are frozen, the electron beams are gentler, and the image processing is sophisticated. With the technique

employed, the water contained in the samples is so rapidly frozen that it is not allowed to form ice that could diffract the electron beam.

The sample was analyzed at "The Department of Life Sciences" at the University of Siena. The transmission electron microscope (TEM) employed was the CM200-FEG (Philips, Eindhoven, Netherlands) characterized by an acceleration voltage of 200 kV, a cryo stage, a point of resolution of 0.19 nm and a tungsten filament. It is equipped with TVIPS CCD Camera (TemCam-F22HD) and TVIPS software EMMENU4 and EMTool. Before the analysis, there was a long sample preparation. In particular, 2.3 µl of the sample was deposited in a Thermo Scientific Vitrobot Mark IV (FEI company, Oregon, USA) that completely automates the vitrification process. With this instrument, the sample is transferred on a Quantifoil® copper grid and the excess material is removed to form a thin film across the holes. Then, the grid with the sample is shot into ethane at about -170°C; this vitrifies the water around the sample without ruining the sample. The grid is maintained cooled by liquid nitrogen at -121°C. Because the supporting surface is often hydrophobic, it can prevent the efficient spreading of the aqueous solution onto grids. In order to remove these charges, they are treated before their use with an instrument that can make a "glow discharge". The instrument employed to uniform the surface charge of the grid before depositing the sample is the Balzer's Med 010 Mini Deposition System (Balzers, Bal Tec AG, Furstentum, Lichtenstein). Multiple image acquisitions were obtained in order to assess the general distribution of the sample. For this reason, several images were acquired with varying features of the acquisition such as sharpness, contrast, magnification, and position in the grid.

For the analysis, three samples were prepared: Batch B without the coating, Batch B with the calcium-phosphate coating and Batch B with cholesterol (20:80 – cholesterol: lipid). The sample was analyzed without any further dilution or modification.

4.3.6 Spray-dried Microparticles Embedding CsA Liposomes

Spray-dried microparticles for inhalation embedding CsA coated liposome were manufactured using a Büchi Mini Spray Dryer B-290 (Büchi Laboratory Equipment, Flawil, Switzerland). The aqueous dispersions to be dried were prepared starting from the prepared CsA liposome batches previously described. Mannitol was dissolved in the liposome dispersion in a ratio from 1:1 to 1:4. The dispersions were kept under magnetic stirring throughout the drying process. The other spray drying operating parameters were fixed as follows: inlet temperature 140 ◦C, air flow rate 742 L/h, aspiration 35 m^3/h, nozzle 0.7 mm and feed rate 3.5 mL/min. The yield of the process was calculated using Equation (1):

$$\text{Yield}=\frac{W_a}{W_t}\cdot 100 \qquad (1)$$

where Wa is the weight of the powder recovered from the collection vessel and the cyclone, while Wt is the weight of total solids in the dispersion to dry. Finally, the dry powders recovered were stored in a sealed glass vial at 25 °C. Microparticles were then observed using SEM as reported in section 3.3.6.

4.3.7 Aerodynamic characterization

For the analysis, an NGI Copley S/N NGI-0497 (Copley Scientific Limited, Nottingham, UK) was used. The air flow was set at 65 L/min and the duration at 3.69 seconds, in order to obtain an air passing volume of 4 L. For the analysis an RS01® (Plastiape, Italy) high-resistance device was employed to aerosolize about 20 mg of spray-dried powders used to fill capsules type 3 of HMPC (Qualicaps). After the deposition of the powder in the induction port, stages and MOC (Micro Orifice Collector), the API was collected using a ACN:H_2O solution (65:35) acidified with HCl (1% *w*/*v*) to pH 4. The powder in the capsule was collected in the same solvent, while the device was washed with a solution of H_2O:EtOH (50:50) to avoid the use of acetonitrile on a plastic device that can be corrosive. To quantify the API in each stage,

an analysis was performed using HPLC at the same conditions as the ones described in (section 3.3.2) using an injection volume of 100 μl. The aerodynamic parameter was calculated as reported in (section 3.3.3).

4.3.8 In vitro anti-inflammatory activity of CsA loaded liposomes.

4.3.8.1 Viability study on A549 and THP-1 treated with liposomal formulations.

Cell viability was assessed on two types of cells in a 96-well plate at 37°C. A549 cells were seeded at a concentration of 10^4/well, after the overnight culture expression. THP-1 cells were seeded at a concentration of $5x10^4$/well. Both cell cultures were exposed to the following treatments: vehicle (PBS); SD powder containing mannitol, leucine and CsA coated liposomes providing a CsA concentration of 0.015, 0.15 and 1.5 μg/mL); SD powder containing mannitol, leucine and CsA uncoated liposomes providing a CsA concentration of 0.015, 0.15 and 1.5 μg/mL; SD powder were dissolved in PBS and diluted. Cell viability was quantified as previously described in section 3.3.8 "*Co-culture assays and cytokines determination*".

The impact of the various treatments on cell viability was expressed as the percentage of viability with respect to vehicle-treated cells.

4.3.8.2 Co-culture assays and cytokines determination

In Transwell® culture plates (Corning 3470), A549 cells (10^5 cells/well) were seeded at the bottom and THP-1 cells (10^5 cells/well) were plated on the insert (0.4 μm pore polyester filter). The two cell cultures were physically separated to avoid their direct contact, according to the method described by Li *et al*., 2020 [93]. After 24h co-culture, cells were exposed to the following treatments:

- Vehicle (PBS);
- Mannitol at a concentration of 0.25 μg/mL;
- CsA_rm 1 μg/mL suspended in PBS;
- SD powder containing mannitol, leucine and CsA-coated liposomes providing a CsA concentration of 1.5 μg/ml;

- SD powder containing mannitol, leucine and CsA uncoated liposomes providing a CsA concentration of 1.5 μg/mL; 56
- Lecithin (Lipoid) at a concentration of 100 g/mL;
- Physical mixture of Lecithin 100 g/mL and CsA_rm 1.5 g/mL.

After 1 hour from the treatment application, LPS (Escherichia coli O55:B5; cat. no. L6529; Sigma-Aldrich, Merck) at a concentration of 1μg/mL in the well was added to the culture and maintained for 24h. Cells incubated with the vehicle and not exposed to LPS were used as control. The concentration of IL-6 in the conditioned media was subsequently analysed using ELISA kit (Boster Biological Technology; cat. no. IL-6, EK0410), according to the manufacturer's protocol and expressed as pg/mL.

4.4 Results and Discussion

Liposomal formulation development

In this chapter, a more innovative strategy in the delivery of CsA to the lung for the prevention of rejection after lung transplantation was applied. CsA was encapsulated in calcium phosphate-coated lecithin liposomes and subsequently transformed into a dry inhalation powder by spray drying and using mannitol as bulking agent.

Calcium phosphate is a biocompatible material that would allow the reduction clearance operated by macrophages in the pulmonary periphery. In addition to this effect, the calcium phosphate coating would allow a pH-dependent release as it is soluble at pH values below 5. This would permit the drug to be released into the phagolysosome and into the acid environment of the inflamed tissue [85]. Moreover, in two batches of liposomes, the 20% or 30% of the phospholipids (calculated relative to the number of moles) were replaced by cholesterol to study the effect of this excipient in liposomal physical stability and drug encapsulation.

In the first part, the CsA liposomes were characterized after each step of the process production. Table 2 reports the values of the liposome dimension and of the Z potential related to the liposomes before and after the homogenization process and after coating with CaP. Liposome size is a critical parameter that especially affects cellular uptake and internalization and other liposome characteristics such as mucoadhesion, drug encapsulation efficiency, and drug release profile. Furthermore, nanoparticles with a diameter between 100 and 150 nm can be phagocytosed by macrophages, limiting their uptake by the target tissue [94, 95].

The particle size average value was therefore the first critical parameter that was assessed. The PDI (polydispersity index) was also carefully evaluated as it is considered another important quality parameter for a liposomal formulation. It is a dimensionless parameter, indicative of the heterogeneity of the particle size distribution. This value ranges from 0 to 1, where 0 represents a monodisperse particle

population and 1 a polydisperse population. Although FDA industry guidance does not indicate a reference range, it is customary to indicate a PDI of less than 0.3 for liposomal systems as indicative of a homogenous monodisperse system [94, 96–98].

Table 2. Value of the size as median hydrodynamic particle diameter (A), PDI (B) and surface charge as zeta potential (C) of CsA liposomes before and after the coating process with CaP and dialysis. The initial measurement was conducted after the CsA liposome formation upon High-Pressure Homogenization. The after-measurement was conducted after CaP coating process and upon 24 h of dialysis.

	Initial_after assembly		**After HPH**			**After Coating and After Dialysis**		
Batch	Size (d.nm)	PDI	Size (d.nm)	PDI	ζ-potential (mV)	Size (d.nm)	PDI	ζ-potential (mV)
A	291.3±35.12	0.422±0.01	40.00±13.24	0.275±0.09	-51.90±11.81	44.68±12.16	0.168±0.04	-18.63±6.22
B	330.5±27.44	0.472±0.10	67.37±11.88	0.275±0.08	-58.12±8.62	43.32±5.77	0.290±0.22	-27.92±10.32
C	299.35±17.32	0.306±0.02	67.12±39.39	0.191±0.07	-55.51±0.13	47.91±4.31	0.431±0.30	-29.41±0.51
B_Chol_30	454.23±34.29	0.256±0.01	45.91±3.63	0.188±0.04	-43.52±7.12	114.52±4.77	0.431±0.06	-15.13±0.73
B_Chol_20	405.10±55.64	0.420±0.06	46.56±6.11	0.190±0.02	-51.34±3.01	91.71±13.53	0.43±0.04	-18.41±0.72

Immediately after the liposome formation, the size between 300 and 400 nm and with a PDI that only in the case of batch B_Chol_30 can be considered within the acceptability range. After high-pressure homogenization, it was possible to obtain smaller liposomes with a lower polydispersity index and in every case below the value of 0.3. After the coating process, a reduction in the diameter of liposomes B and C was

further observed. Probably the material that did not take part in the formation of the liposome, and which interacted with the liposomal structures through weak interactions may have been eliminated during the process of dialysis. On the other hand, for the last two batches containing cholesterol, the increased size of the nanostructures after dialysis was due to the formation of cholesterol crystals. As previously mentioned, the addition of cholesterol led to formulations with low physical stability, which tended to aggregate and precipitate. For this reason, these two preparations were excluded from subsequent investigations.

For all the batches the final zeta potential values for the liposomes were higher (*i.e.* less negative) compared to the initial one, suggesting a change in the surface of the nanostructures due to the positively charged CaP presence. The zeta potential values range from about -68 to -43 mV, before the coating, to about -29 to -15 mV in every batch. A reduction of the Z-potential value was also obtained by Thakkar and colleagues using the same 50 mM $CaCl_2$ solution for the coating of vincristine liposome with CaP. Also in this case a reduction in the value of the Z potential was observed after coating [86]. Moreover, the value of the potential Z is an index of the stability of a colloidal system. Colloidal systems with a Zeta potential in the range of -30 to – 40 are referred to as stable [99, 100]. In this phase of the study, however, the parameter was mainly interpreted as an effect of the successful coating rather than a quality criterion.

Tracking the amount of material dispersed during liposome production is critical to understand the final concentration of the dispersion. During the dialysis process, the material which has not taken part in the formation of liposomes permeates the dialysis membrane according to a concentration gradient. After the removal of the not reacted materials, the solid concentration assessment and the CsA analytical quantification allowed to obtain the encapsulation efficiency.

Table 3. Summary of the quali-quantitative composition of CsA liposomes coated with CaP after the dialysis. Three different batches of lecithin liposomes (Lipoid S80®) containing three concentrations of CsA (4.8, 7.0 or 9.0% *w*/*w* with respect to the solid content) were produced. Two batches of liposomes were prepared by replacing 20 or 30% (calculated relative to the number of moles) of the lecithin; EE%=Encapsulation Efficiency was calculated as the ratio expressed in percentage between the total amount of CsA recovered in liposomes and the initial amount added at the beginning of the preparation; conc.= concentration.

	Composition of CsA liposome after dialysis				
Batch **(CsA initial conc.)**	Solid content (mg/mL)	CsA (mg/mL)	Ca^{2+} (mg/mL)	EE %	CsA conc. (*w*/*w* %)
A **(4.8% *w*/*w*)**	2.37±0.08	0.14±0.01	0.03±0.01	100	5.4±0.01
B **(7.0% *w*/*w*)**	2.34±0.12	0.20±0.03	0.03±0.02	95.2	8.6±0.7
C* **(9.0% *w*/*w*)**	1.57±0.10	0.08±0.05	N/A	27.6	5.01±0.3
B_Chol30	1.99±0.14	0.20±0.02	0.02±0.01	95.2	9.9±0.2
B_Chol20	1.97±0.04	0.18±0.01	0.03±0.01	85.7	9.3±0.2

**Precipitation of cyclosporine*

Table 3 reports the composition of liposomes after dialysis. After dialysis, the concentration of the total solid determined after evaporation of the solvent was about 2-2.3 mg/mL. **As regards the batches without cholesterol, the maximum percentage of CsA that was encapsulated in the liposomes was 0.20 mg/mL corresponding to 8.6 % (*w*/*w*) (Batch B).** When a larger amount of CsA for the preparation of Batch C (corresponding to an initial 9 % w/w) was used, a drug crystal precipitation was observed immediately after the lecithin solution addition. After the dialysis, the components that have not taken part in the formation of the structures were removed from the formulation by passing through the dialysis membrane. For this reason, in Batch C, the total solid concentration was drastically reduced (1.57 %). Moreover, in this batch, the concentration of CsA also fell below the expected value of 0.29 mg/mL and only 0.08 mg/mL was found in the final formulation.

As regards the formulations in which part of the phospholipids had been replaced with cholesterol, the results did not show advantages. In fact, the EE% was already maximum when only lecithin was used for the construction of the lipid membrane, demonstrating that CsA interacted perfectly with phospholipids' aliphatic chains. All the amount of drug that was used for the formulation preparation was encapsulated and detected in the final product after dialysis. As specified above, it was not possible to go beyond a final loading of 8.6 % (*w*/*w*), as an initial CsA concentration exceeding 7% (*w*/*w*) CsA caused drug precipitation without increasing drug encapsulation. In parallel, cholesterol did not even improve the particle size and PDI values as shown in Table 2.

The successful quantification of calcium after dialysis ensured that even after this process, this component was part of the formulation, and presumably precipitated as a coating. For this reason, the morphological analysis by Cryo-TEM was conducted to confirm the correct deposition of CaP on the liposome surface. Cryo-TEM, also known as Cryo-EM, was used to visualize in detail the structure of the liposomes produced. This technique allows obtaining images by limiting the distortion of the observed nanometric structures and the formation of artefacts in the sample which usually occurs when the sample is a dried form [92]. Morphological analysis was done just after the sample production. The preparation of the sample provides for rapid freezing of the liquid sample in ethane cooled with liquid nitrogen this technique allows the sample to be displayed in its natural state.

Figure 3 illustrates Cryo-TEM images of CsA loaded liposomes, without a CaP coating (A), coated liposomes, or coated liposomes containing also cholesterol with a molar ratio of 20% with respect to lecithin.

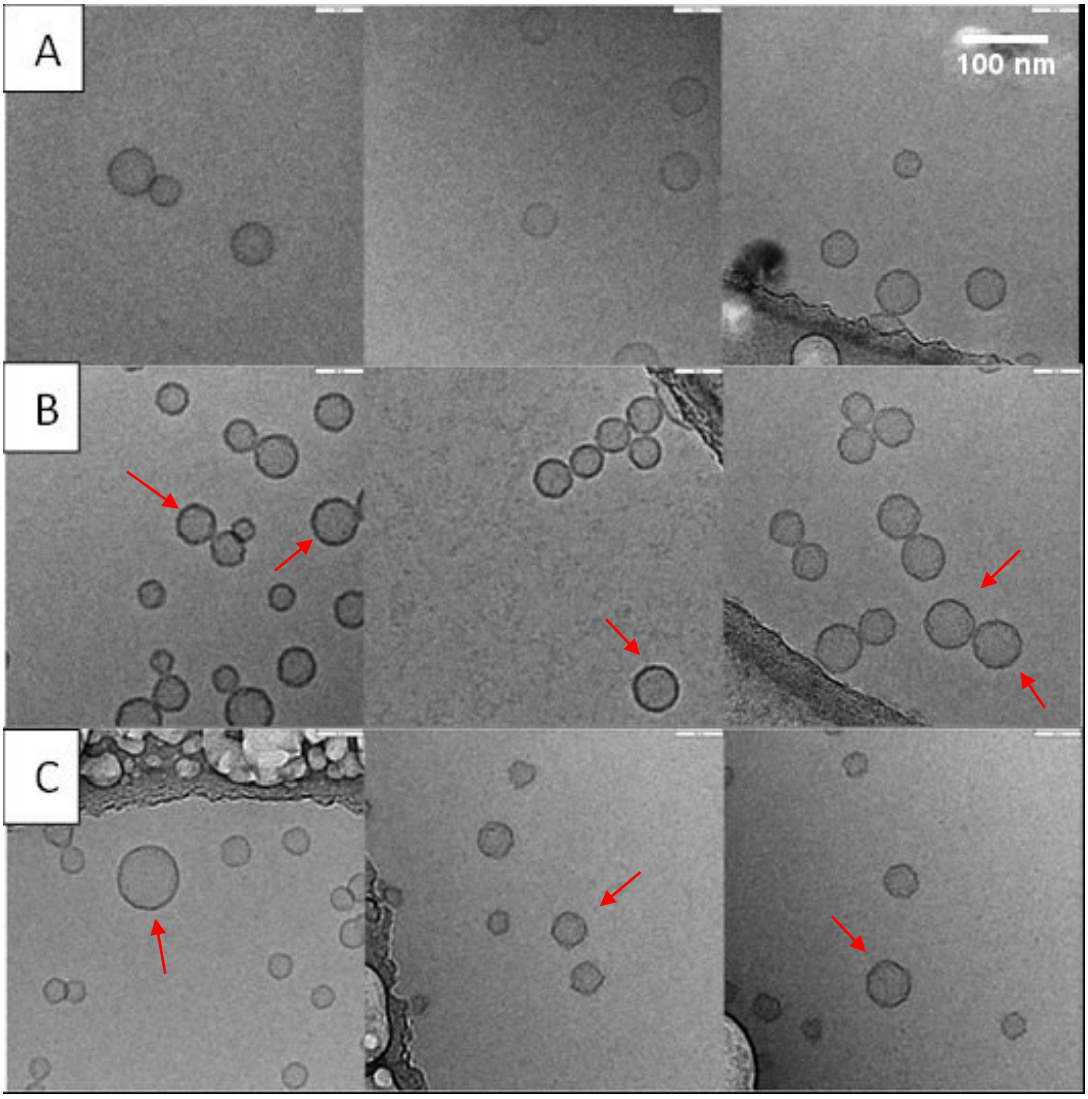

Figure 3. Cryo-TEM images of uncoated liposomes (A), CaP coated liposomes (B) and Cholesterol CaP coated liposomes (C). Arrows indicates the CaP coating on liposomes surface.

The presence of the CaP liposome coating was confirmed by the images obtained. Regarding the structure, all the observed liposomes are unilamellar spherical structures. Liposomes that do not have the coating (Fig 3_A), were less visible but with a more regular surface than coated liposomes. Moreover, coated liposomes (Figure 3_B), had a more markedly visible margin due to the presence of calcium phosphate salt on its surface. Furthermore, these appear as small aggregates of two or more liposomes although this behaviour does not affect the measured PSD value. Cholesterol-containing liposomes (Figure 3C) had a greater heterogeneity size: many small liposomes and some large ones. Confirming data obtained from DLS analysis,

this batch was characterized by a higher polydispersity index. In the images obtained, these liposomes seem to have often irregular margins and a less markedly visible coating than liposomes without cholesterol of Figure 4B. Another difference that can be pointed out is the fact that the CaP-coated liposomes had a different behaviour if compared to the ones uncoated: they are not isolated from one to each other, but they keep together in groups or pairs. A suitable explanation for this is the fact that the coating leads to a change in the surface charge, as confirmed by the change in zeta potential, resulting in stronger attractive forces.

Embedding Coated Liposome in Microparticles

Following the characterization of the liposomes, the goal was the formation of an inhalable powder containing the liposomes. Mannitol was considered an ideal excipient as approved for inhalation. It is a non-reducing sugar and capable of stabilizing the liposome during drying by replacing the hydrogen bonds and forming an amorphous matrix around the nanostructures. Moreover, the previous chapter led to the formation of a respirable powder regardless of the percentage used. The possibility of forming respirable particles, in this case, is more challenging by the presence of liposome structure to be preserved during the spray process. Although exposed for a period in the order of milliseconds to high temperatures, lecithin could melt, leading to the coalescence of the microparticles. The bulk excipient was always added to the liposomal nanosuspension without proceeding with dilution since in all cases, the concentration of the solid in the medium was < or around 1 % (*w*/*v*), a value known to be suitable for the process (Table 1).

The result of this process will therefore depend on the correct weight ratio between the mass of liposomes and the bulking agent. Different mass ratios between liposomes and mannitol were tested to obtain a well-dried and no-aggregated powder. It is known from the literature that the amount of mannitol plays a fundamental role in the construction of the particle. In fact, although they were not liposomes, it has been

shown that at least a ratio of 1:4 (nanoparticle: mannitol) was required to produce respirable microparticles containing CaP nanoparticles [101]. Increasing the mannitol concentration *vs* the CaPs amount increased the microparticle respirability and, more evidently, preserved the size of released nanoparticles. These quality attributes are crucial for the use of microparticle embedding nanoparticles for targeting the lung.

Table 4 illustrates the concentration of the components used for the construction of the spray-dried powders, the yield of the process and the CsA content in the powder quantified by HPLC.

Table 4. concentration of the components used for the construction of the spray-dried powders, solid content concentration, yield of the process and the CsA content in the powder quantified by HPLC.

Powder	**Liposome Concentration (mg/mL)**	**Mannitol (mg/mL)**	**Lubricant (mg/mL)**	**Solid conc. (% *w*/*v*)**	**Yield (%)**	**CsA *(% w/w)***
Lipo_Mann 1:1	2.34±0.12	2.34	-	0.5	3%	NA
Lipo_Mann 1:2	2.34±0.12	4.68	-	0.7	7%	NA
Lipo_Mann 1:3*	2.34±0.12	7.02	-	0.9	63%	1.59±0.01
Lipo_Mann 1:4	2.34±0.12	9.36	-	1.1	68%	1.19±0.01
Lipo_Mann_Leu*	2.34±0.12	5.96	1.05	0.9	65%	1.73±0.08
Lipo_Mann_NaST*	2.34±0.12	6.98	0.03	0.9	70%	1.68±0.01
Uncoated_Lipo_Mann_Leu*	2.34±0.12	5.96	1.05	0.9	65%	1.66±0.01

**Powder batches then further characterised*

The attempt to use a 1:1 and 1:2 ratio between liposomes and mannitol confirmed that it was not suitable for the construction of the microparticles that deposited in the chamber and cyclone of the spray drier (yield <10%). On the contrary, when the amount of mannitol was increased, both in the ratio 1:3 and 1:4, a non-adhesive micronized powder was obtained with a process yield > 60%. With the purpose to limit the amount of excipient to be inhaled, the 1:3 ratio appeared to be a good compromise

between the success of the powder production process and the maximised drug content in the powder (1.59% *w/w*).

For the improvement of the respirability/flowability of this powder, two common excipients (leucine od sodium stearate) used as lubricants have been considered. The ratio between excipients and liposomes unchanged, leucine was used at 15% *w/w*, while sodium stearate was at 0.5% *w/w* of the total mass of mannitol. Even with the addition of these lubricant excipients, the production process was successful (Table 4).

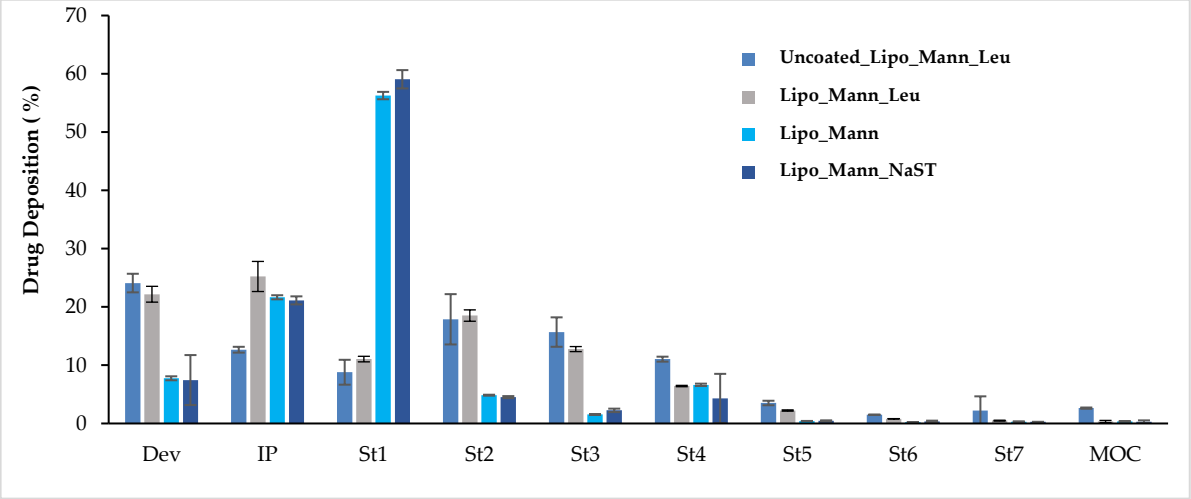

Figure 4. Distribution of embedded coated liposomes in mannitol (Lipo_Mann), mannitol and leucine (Lipo_Mann_Leu), mannitol, leucine and sodium stearate (Lipo_Mann_NaST) and mannitol and leucine embedding uncoated liposomes (Uncoated_Lipo_Mann_Leu) on Next Generation Impactor. The loaded amount of powder in the capsule was 20 mg containing 0.32 mg of CsA (n=3 ± st.dev.) Dev= Device; IP= Induction Port; St = stage; MOC= Micro Orifice Collector.

The CsA-coated liposomes embedded in a mannitol-only powder (Lipo_Mann) gave a low aerodynamic performance. Although the ED was high, the FPF was very low due to the poor deaggregation of the microparticles, which mainly deposited in stage 1 of NGI (see Figure 4). This behaviour leads to an MMAD of 9 μm.

The addition of sodium stearate did not improve the characteristics of the powder, which showed a performance almost unchanged compared to the powder without lubricants, with a very low fraction of fine particles and the MMAD was around 10 μm.

Leucine, on the other hand, brought a significant improvement to the powder. **The emitted dose of the coated liposome powder (Lipo_Mann_Leu) was around 80% and the FPF reached 36%.** The fact that the powder was deaggregated better than the previous two is shown by the higher deposition on Stages 2 and 3. The MMAD, however, remained around 4 μm (Table 5).

Table 5. Aerodynamic characteristics of spray-dried powders produced with a 1:3 weight ratio between liposomes and excipients: coated liposomes in mannitol (Lipo_Mann), mannitol and leucine (Lipo_Mann_Leu), mannitol, leucine and sodium stearate (Lipo_Mann_NaST) and mannitol and leucine embedding uncoated liposomes (Uncoated_Lipo_Mann_Leu). MMAD=Mass Median Aerodinamic diameter; FPM=Fine Particle Mass; FPF=Fine Particle Fraction.

Powder	Emitted Dose (%)	MMAD (μm)	FPM (mg)	FPF (%)
Lipo_Mann	92.2±0.3	9.88±0.00	0.01±0.01	3.3±0.1
Lipo_Mann_NaST	92.5±4.2	10.09±0.02	2.12±0.01	2.5±2.5
Lipo_Mann_Leu	77.8±1.3	4.88±0.03	0.08±0.01	33.6±1.6
Uncoated_Lipo_Mann_Leu	75.9±1.6	4.03±0.16	0.12±0.01	50.5±0.6

The coating leads to a slight reduction in the respirability of the powder, the reason for this phenomenon may be due to the prevalence of attractive forces between coated liposomes. Considering the Z potential value of coated liposomes, in agreement with what is reported in the literature, stability is defined as moderate (Z-potential around -30mV) compared to uncoated liposomes, which had a Z-potential value of around -60mV (Table 2) [99, 100]. However, the potential advantages of the coating still make the powder containing the coated liposomes more interesting.

The morphological analysis of the Lipo_Mann_Leu powder conducted by SEM confirms that the microparticles are fused to each other creating aggregates of 4-7 μm (Figure 5). Future optimization will be devoted to improving the drying or compounding conditions to keep the microparticles individual.

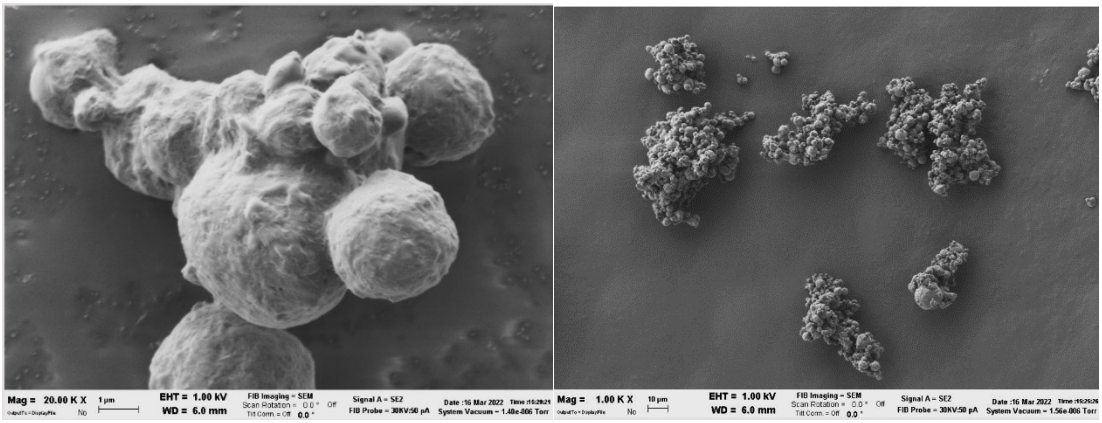

Figure 5. SEM image of the spray-dried powder Lipo_Mann_Leu, containing liposomes embedded in mannitol and leucine at different magnification.

Restoration

Although the powder containing leucine has reported acceptable respirability values, it is appropriate to investigate what is the fate of liposomes that have undergone a spray drying process. It is important to ensure the formulation releases the liposomes at the original size.

The drying process, as already mentioned above, could lead to aggregation phenomena between the liposomes, and the initial size could not be regained following reconstitution of the dispersion in an aqueous medium. Table 5 illustrates the particle size values of powder Lipo_Mann_Leu after the dissolution of mannitol carried out in two aqueous media at different pH.

Table 6. Values of size, PDI and Z-potential relating to the reconstitution of the powder spray dried in buffer BPS pH 7.4 and sodium acetate pH 5.

	Size (d.nm)	**PDI**	**ζ-potential**
Initial value	43.3 ± 5.7	0.2	-27.9 ± 10.2
PBS (pH=7.4)	176 ± 4.5	0.3	-14.4 ± 0.5
Sodium acetate (pH=5)	232.8 ± 2.5	0.3	-12.9 ± 0.9

The values shown in Table 6 indicate that following reconstitution, the original size is no longer observed, and there is an increase in both buffers and the polydispersity index. The Z-potential also experienced substantial variations from the starting value. However, under these conditions, it was possible to observe some differences depending on the presence of the CaP coating of the liposomes. A greater value is observed in the size of the liposomes resuspended in acidic conditions, while a smaller value is observed for the liposomes resuspended in a physiological pH buffer. This data is also accompanied by a difference in the Z-potential which could explain the different aggregation phenomena observed.

In vitro study

The in vitro toxicity study wanted to check that the formulation, although made up of excipients considered safe, did not affect the vitality of the cells. Indeed mannitol is approved by the FDA [102–104] and phosphatidylcholine (PC), the main component of lecithin, is a surfactant produced also by type II alveolar cells in the pulmonary alveoli [16, 105]. A549 alveolar basal epithelial cells and macrophages (THP-1) were used to study the activation of the inflammatory process *in vitro.*

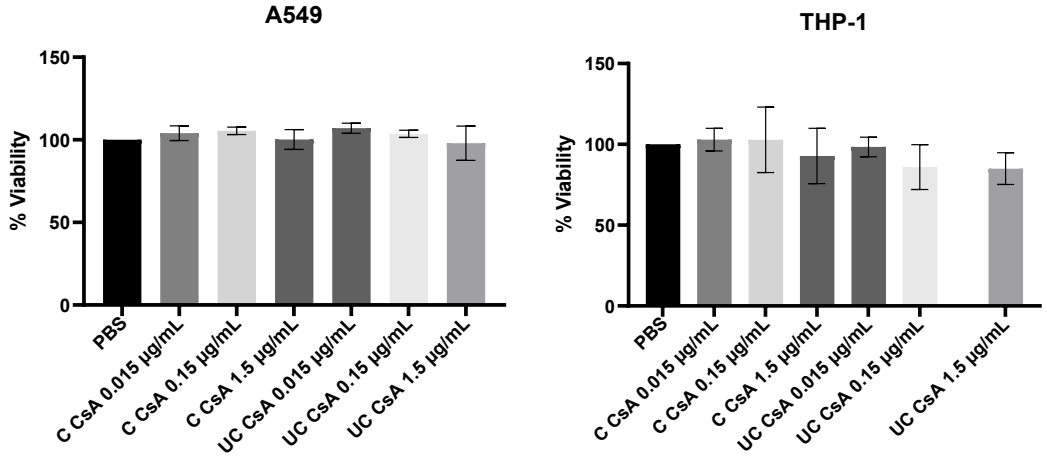

Figure 6. Viability of A549 and THP-1 cell cultures exposed to PBS and to two types of Lipo_Mann_Leu spray-dried powders containing CsA coated or uncoated liposomes. C=Coated liposomes; UC= Uncoated liposomes. Concentrations reported refers to CsA (0.015 , 0.15 and 1.5 μg/mL were obtained dissolving dry powder at 1, 10 and 100 μg/mL respectively).

It was previously demonstrated in the third chapter that CsA_rm and mannitol had no impact on the viability of the test cells up to 2 μg/mL for mannitol and up to 10 μg/mL for CsA_rm. Similarly, the MTT test on A549 and THP-1 cell monocultures did not show any changes in the viability of the cells when treated with the dissolved Lipo_Mann_Leu spray-dried powders, regardless of the chosen concentrations (Figure 6). The two powders contained coated and uncoated liposomes which were released to the cell after the mannitol-leucine dissolution in the medium.

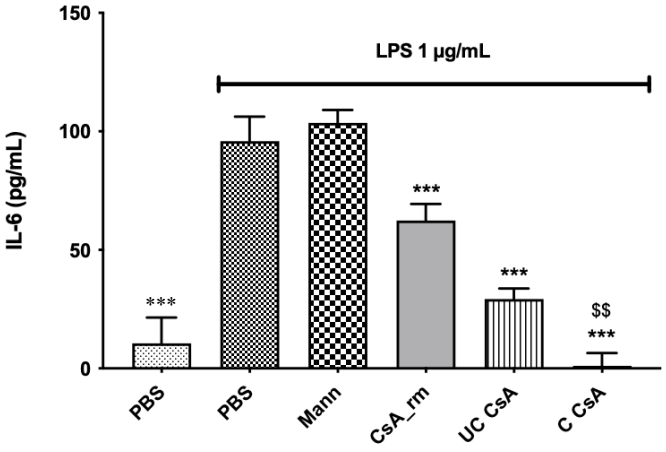

Figure 7 Il-6 production in A549/THP-1 co-culture, stimulated with LPS 1 μg/mL. Mann=Mannitol 0.25 μg/mL; CsA_rm (raw material) 1.5 μg/mL. UC CsA= Coated liposomes containing 1.5 μg/mL of CsA; C CsA= Coated liposomes containing 1.5 μg/mL of CsA; ***=P<0.001 vs PBS +LPS 1 μg/mL; $$=P<0.01 vs UC CsA One Way Anova, Bonferroni's post-test. Data are reported as Mean ± SEM (n=3-5).

LPS-stimulated co-culture effectively expressed IL-6. The concentration of this proinflammatory cytokine was not reduced in mannitol-treated cells.

As regards the treatments conducted with CsA, all reduced inflammation but the extent of the reduction depended significantly on the type of formulation applied (Figure 7). In particular, the CsA_rm reduced the value of IL-6 to about 60 pg/mL. The uncoated liposomes containing CsA were more efficient than the CsA raw material and statistically ($p<0.05$) decreased the IL-6 to a concentration of 40 pg/mg. This data supports the knowledge that these lipidic structures increase the uptake of lipophilic

drugs thanks to the fusion of their membrane with the cellular one and hence favouring its internalization. **Surprisingly, when liposomes were coated with CaP, the reduction in IL-6 was total indicating the maximal efficacy of this formulation**. As previously reported [86], the calcium phosphate coating would lead to an increase in cellular uptake and therefore potentially a higher drug concentration within the cultured cells. **Although drug uptake was not directly investigated in this study, it could be hypothesized that the observed difference between uncoated and coated cyclosporine-containing liposomes is due to the different degrees of internalization of the nanoparticles.**

This finding was demonstrated in a study by Thakkar and colleagues in which vincristine loaded in CaP-coated liposomes was more efficiently internalized by the A549 cell line. In that case, the uptake was up to 4 times greater for coated liposomes than when loaded in uncoated liposomes [86].

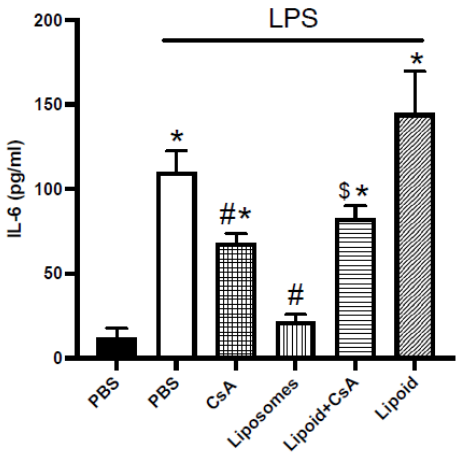

Figure 8 *In vitro* inhibition of IL-6 production by THP-1/A549 co-culture exposed to LPS 1 μg/mL, in the presence of the vehicle; CsA 1 μg/mL, Liposomes: 100 μg/mL; Liposomes + CsA: 100μg/mL containing 1.5 μg/mL of CsA; Lipoid+CsA: Physical mixture of LipoidS80 (100 μg/mL) and CsA (1.5 μg/mL) Lipoid: LipoidS80; *P<0.05 vs. vehicle; #P<0.05 vs. vehicle + LPS, ANOVA test followed by Bonferroni's post-test.

A further investigation was conducted in order to ascertain that the more effective reduction of inflammation of liposomal CsA compared to CsA_rm was to be attributed to its organized lipid structure rather than to a possible summed contribution of the

two individual components (Figure 8). Indeed, it is known that phospholipids can show anti-inflammatory properties on the modulation of interleukins. Data in the literature report a potential interaction between phospholipids and cytokine expression under LPS stimulation [106, 107]. The mechanism underlying the anti-inflammatory action of phospholipids is not clarified, but only antagonism of the TNF-α receptor or inhibition of the NF-κB and MAPK pathways are hypothesized [108].

However, when phospholipids were applied alone to the cells they did not lead to any reduction in inflammation (see Lipoid column in Figure 8). If they were mixed with CsA they lead to a reduction in inflammation, but this effect was due to the presence of the drug, in fact, the amount of IL-6 was similar to that detected by applying CsA_rm alone. In summary, the graph, therefore, demonstrates that the reduction in inflammation was maximum (20 pg/mL) only when the phospholipids were organized in liposomal structures and loaded with CsA, demonstrating that the effect was exerted by the drug and that the liposomal structure improved its internalization.

4.5 Conclusions

This study led to the production and characterization of an inhalation powder containing cyclosporine loaded in calcium phosphate-coated liposomes. This formulation was designed to reduce the dosage necessary for the prevention of lung transplant rejection. The liposomal formulation was, therefore, initially optimized by selecting the maximum percentage of drug in the formulation, which would not compromise the formation of liposomes. **Subsequently, the presence of the coating was confirmed, by various methods, including the variation of the Z-potential, the effect of reconstitution in buffers at different pH, direct observation by cryo-TEM, and calcium titration.** It was also possible to obtain an inhalable powder by spray drying using L-leucine as a lubricant and mannitol as a bulk agent for liposome stabilization and microparticle formation. **Furthermore, the *in vitro* data were encouraging, demonstrating an increased anti-inflammatory effect of this formulation compared to the raw material cyclosporine, demonstrating the increased efficacy not only thanks to the liposomal system but also due to the coating**. This would therefore prove to be an interesting strategy in the prevention of transplant rejection and would offer lower systemic exposure to cyclosporine with a consequent reduction in adverse effects.

5. Selection of Promising Bulking Agent for Pramlintide Respirability and Stability

5.1 Introduction

Amylin is an endogenous neuroendocrine hormone peptide of 37-amino acid produced together with insulin in the β-cells of the pancreas and involved in glucose homeostasis. In particular, this effect is carried out through an inhibitory effect on the release of glucagon after the meal (Figure 1) [109]. Furthermore, an effect of amylin has been observed on the slowing of gastric emptying that leads to a prolonged sense of satiety with a consequent reduction of food intake [110]. Despite its interesting activity, formulation of amylin is not possible due to the tendency of amylin in forming amyloid formations in humans. Amylin has a disulphide bridge in the region between amino acids 2 and 7, which is responsible of this phenomenon [111].

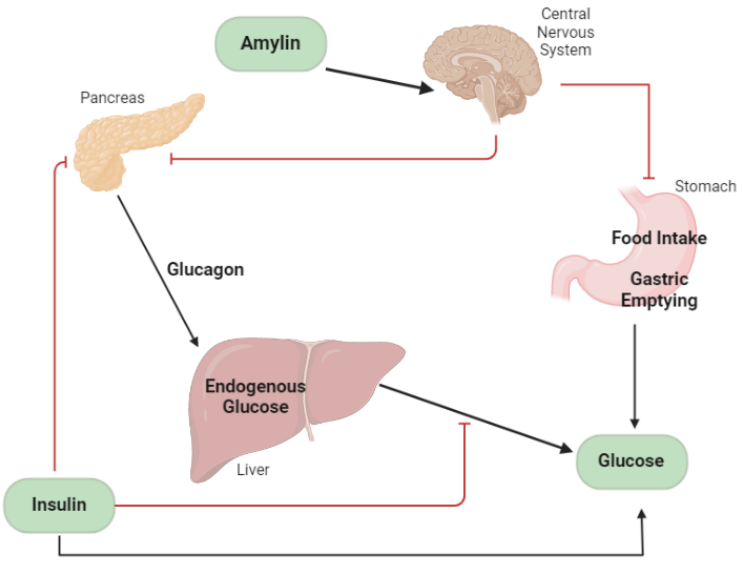

Figure 1. Scheme of the mechanism of action of pramlintide. Created with BioRender.com

Pramlintide is the synthetic analogue of amylin that differs in the replacement of the amino acids Ala-25, Ser-28 and Ser-29 of amylin with proline residues and a molecular weight of 3.9 kDa. As well as amylin, pramlintide, affects glucose homeostasis, reducing postprandial hyperglucagonemia and has an effect on the reduction of gastric motility and the consequent increase in the sense of satiety [112].

For this reason, pramlintide is currently approved by the FDA to help control glucose levels in patients with type 1 and type 2 diabetes who do not respond adequately to insulin alone therapy [113]. Pramlintide is currently commercially available as subcutaneous injectable formulations under the trade name of SymlinPen® (at a dose of between 30 and 120 μg). The inhaled formulation of this peptide, in dry powder form, would offer a less invasive route of administration, requiring no needles and potentially a more suitable route of administration for chronic treatment.

Clinical trials on obese type 2 diabetic patients treated with pramlintide have shown not only to increase glycaemic control but also a reduction in body weight [114]. Other clinical studies in non-diabetic normal-weight subjects treated with pramlintide have shown a reduction of food and caloric intake and meal duration after a single injection of 30 μg before meal [115].

The stabilization of macromolecules in a solid-state formulation poses a challenge to the shelf life of the product and the method of conservation. Water replacement effect [116, 117] and vitrification stabilization have been proposed to explain the effect of the bulking agent on the stability of the biologic macromolecule [29, 118]. Stabilizing agents are usually sugars, polyols, amino acids, polymers and organic or inorganic salts [119]. The stabilization of the protein or peptides in a glassy state could also depend on the molecular weight of the stabilizing agent, attributable to the greater ability of the smaller molecules to interact with the macromolecule and form hydrogen bonds [29, 120].

In particular, sugars are commonly used for this purpose. Trehalose and raffinose are respectively, a non-reducing disaccharide and a non-reducing trisaccharide, and, therefore not susceptible to the chemical degradation of the Maillard reaction [121]. Trehalose has been widely used with the function of stabilizing macromolecules during spray drying or freeze drying. Raffinose and trehalose have been suggested as good protein stabilizers, having a high glass transition temperature in the amorphous state [121].

Sodium hyaluronate is a linear endogenous glycosaminoglycan widely used as an excipient in pharmaceutical preparations and approved in inhalation delivery [122].

This excipient has also been used for the formulation of engineered highly respirable particles by spray drying [123]. Furthermore, the literature reports the use of this excipient in direct spray powders, to obtain a controlled release. This polymer has also been used in the formulation of spray-dried particles containing biological macromolecules such as Bovine serum albumin [124] and insulin [125].

L-leucine is an excipient known to be used to increase the flowability of powders and promote their redispersion, according to literature, due to its capacity to settle on the surface of the particles during spray drying [126]. This effect, at a percentage of leucine between 10 and 20% (*w* / *w*), would also seem to favour the stability of the formulation, protecting the API from moisture-induced degradation [127]. For this reason, this excipient was also included and taken into consideration during this study. Despite these two sugars, along with hyaluronic acid [123] have already been used in the past for the formulation of inhalation powders by spray drying, their ability to stabilize pramlintide has not yet been studied. Moreover, the formulation of this molecule in the form of inhaled powder has not yet been reported in the literature.

The aim of this part of the thesis was the formulation of a DPI produced by spray drying, containing pramlintide as an adjunctive treatment in patients with diabetes for glucose level control and as an alternative strategy in weight reduction in patients with obesity.

In detail, **a systematic study of the solid-state was performed on pramlintide spray-dried powders produced using trehalose-dihydrate, raffinose-pentahydrate or sodium hyaluronate as bulking agent.** Their role in particle formation and peptide stabilization was studied. The results illustrated in this part of the work were collected at the laboratory of Professor Mingshi Yang at the university of Copenhagen.

5.2 Materials

Pramlintide acetate lot. P21112504 was purchased from Cabru s.a.s. (Milan,Italy), L-leucine USP (A.C.E.F. SPA, lot number 7096004), D (+) trehalose dihydrate, batch number SR03975 was obtained from MP Biomedicals (Ohio, USA), D (+) raffinose pentahydrate lot. WXBD1996V was purchased from Sigma-ALDRICH. Sodium hyaluronate 92kDa, batch n. 1000014109 and Sodium hyaluronate 804kDa batch n. 1000007837 were purchased from Altergon Italia s.r.l (Avellino, Italy), All other chemicals used were obtained from commercial suppliers and were of analytical grade.

5.3 Methods

5.3.1 Preparation of spray-dried powders

During this study, pramlintide-free powders were produced in order to study the role of individual excipients in particle formation. High molecular weight sodium hyaluronate has been shown to form viscous solutions or gels at concentrations higher than 0.3% (*w/v)*. For this reason, it was decided to maintain this concentration value for the high molecular weight hyaluronic acid formulations and for the formulations produced with the other excipients.

The composition of the powders is reported in Table 1. Bulk excipient and leucine were modulated in the composition in order to assess the role of each compound on the powder characteristics.

Pramlintide, when present, was added to the solution at a concentration of 0.3% (*w/w*) to obtain a dosage of 30 μg of pramlintide in 10 mg of powder. The feedstock solutions were prepared at the final concentration of 0.3% w/v. For all the batches, 500 mg of solid material was dissolved in 166.7 mL of water and spray-dried.

Solutions were sprayed using the Büchi Mini Spray Dryer B-290 (Büchi Labortechnik, Flawil, Switzerland) in open loop configuration. With the following process parameters: Inlet temperature has been set as 125 °C. The drying air flow rate was 742 L/h, and aspiration of 35 m^3/h. The solution was sprayed with a feed rate of 3 mL/min and using a nozzle with a diameter of 0.7 mm. Under these conditions, an outlet

temperature between 73 and 78°C was obtained. The yield of the process is reported in table 4.

Table 1. Quali-quantitative composition of spray-dried solutions.

Bulking agent	Bulk % (*w*/*w*)	Leucine % (*w*/*w*)	Pramlintide %(*w*/*w*)
Trehalose	100	-	-
	85	15	-
	84.7	15	0.3
Raffinose	100	-	-
	85	15	-
	84.7	15	0.3
HA 92kDa	100	-	-
	85	15	-
	84.7	15	0.3
HA 804kDa	100	-	-
	85	15	-
	84.7	15	0.3

5.3.2 Aerodynamic assessment of Pramlintide spray-dried powders.

The MMAD of the spray-dried powders containing leucine and pramlintide was obtained by means of an Aerodynamic Particle Sizer (APS) Spectrometer 3321 (TSI, MN, USA) connected to a small-scale powder disperser 3433 (TSI, MN, USA) for powder aerosolization. Data were acquired using Aerosol Instrument Manager® Software Version 8.1.0.0 (TSI, MN, USA). This analysis is based on the principle that particles accelerated by a flow of air throw a nozzle will pass through the detector system, consisting of two laser beams, with a certain time of flight, this will depend on the size, density and shape of the particles and correlates with their aerodynamic diameter [128, 129]. In detail for this analysis, about 5 mg of powder was placed in the disperser and analysed using an airflow of 4 L/min.

5.3.3 Thermogravimetric analysis (TGA)

Thermogravimetric analysis (TGA) was used to determine the residual water content in the spray-dried powders. The analysis was conducted using the thermogravimetric analyser Discovery thermogravimetric analyser (TA instruments Inc., New Castle, DE, USA), using a 100 µl open platinum pan. The analysis was conducted under nitrogen flow at 25 mL/min. Table 2 resumes the heating programs used for each type of powder

produced with different excipients. Data were analysed using TRIOS software (version v5.0.0.044608).

Table 2. Thermogravimetric analysis parameters for powders containing the listed bulking agents. T_i=Initial temperature; T_f= Final temperature.

	T_i (°C)	T_f (°C)	Heating rate (°C/min)
Trehalose dihydrate	35	250	5
Raffinose pentahydrate	30	250	5
Hyaluronic acid 92 kDa	30	216	5
Hyaluronic acid 804 kDa	30	216	5
L-leucine	40	300	5

Water loss was then analysed using the software, between the 35 and 180 °C for trehalose and sodium hyaluronate powders, and between 30 and 150 °C for raffinose powders.

5.3.4 Modulated differential scanning calorimetry (DSC)

The thermal properties of the powders were analysed using Q2000 differential scanning calorimetry (DSC) (TA instruments Inc., New Castle, DE, USA). Each sample, about 4 mg, was weighed into a punctured T-zero aluminium pan, and analysed under 50 mL/min nitrogen gas flow. The analysis was performed using the temperature range used is resumed in Table 3 and a modulation-amplitude of 0.32 °C over a period of 60 s. The data was analysed using TRIOS software (version v5.0.0.044608).

Table 3 Differential scanning calorimetry analysis parameters for powders containing the listed bulking agents, Ti=Initial temperature; Tf= Final temperature; Heating rate is expressed as °C/min.

	T_i (°C)	T_f (°C)	Heating rate °C/min
Trehalose dihydrate	35	220	5
Raffinose pentahydrate	27	150	5
Hyaluronic acid 92 kDa	27	216	2
Hyaluronic acid 804 kDa	27	216	2

5.3.5 Powder X-Ray Diffraction

XRPD analysis of all samples was performed using an X'Pert PRO X-ray diffractometer (PANalytical, Almelo, The Netherlands) using CuK α radiation ($\lambda = 1.541$ Å).

Measurements were taken from 5° to 35° (2θ) using a step size of 0.05° 2θ. Data were then analysed using XPert (PANalytical, Almelo, The Netherlands) software.

5.3.6 Analytical method

Pramlintide stability was assessed by HPLC quantitative analysis using the column: Aeris ™ 3.6 um WIDEPORE XB-C8 200 A Size: LC column 250 x 4.6 mm (s/n H22-036235). The wavelength was 215 nm. Under isocratic conditions, the mobile phase consisted of 28% acetonitrile: 72% buffer monopotassium phosphate 0.085 M with a pH=3. With a flow of 0.7 mL/min. Using this method, the peak of pramlintide was observed after 15 min. The injection volume was 20μL. The method was specific and linearity between 2 and 75 μg/mL was assessed.

The sample consists of an aqueous solution containing pramlintide, leucine and a bulk agent (trehalose, raffinose or hyaluronic acid). In the case of samples containing hyaluronic acid, these were filtered before injection using acetate cellulose filters with a porosity of 0.45 μm.

5.3.7 Scanning electron microscopy analysis (SEM)

The morphology of the particles produced with different bulking agents was studied by scanning electron microscopy analysis (SEM) (S-3400, Hitachi, Ltd., Japan). Samples were deposited on double-sided tape and coated with a thin layer of gold. The coated specimen was then scanned and photographed under the microscope at an acceleration voltage of 5.0 kV and 15 kV.

5.3.8 Stability study

Samples containing the API were placed into open clear glass vials. Glass vials were stored in desiccators at two conditions, at 60% RH, 25 °C and 75% RH, 40°C. XRPD TGA and DSC were performed after one month of storage to assess the solid state of the samples.

5.4 Results and Discussion

Pramlintide is a 37 amino acid peptide, analogue of amylin and involved in glucose homeostasis [111]. To date, this drug is administered exclusively by the subcutaneous route, and the administration of this peptide by inhalation could be an interesting strategy to offer an alternative to the parenteral route of administration, often characterised by low patient compliance. Despite this, the formulation of this peptide in a dry powder for inhalation has not yet been reported in the literature. Pramlintide formulation was produced using two non-reducing sugars and hyaluronic acid with two different molecular weights in order to identify a suitable bulking agent in the formation of the particles and in the stabilization of the peptide in the solid state. Leucine has been added at 15% (*w*/*w*), to improve the flowability of the powder [126, 127]. It is known that the bulk excipients constitute the structure of the particle and that during the drying process, leucine will tend to settle at the air-liquid interface, coating the particle. Placebo powders were prepared as well to assess the role of excipients in the solid state of microparticles.

Table 4. Yield of production and percentage w/w of pramlintide in spray-dried formulations at time zero after production. Tre= trehalose; Raff= raffinose; HA=sodium hyaluronate. Leu=Leucine. Numbers represent the percentage (*w*/*w*) of each component.

Powder Bulk % (*w*/*w*)	**Yield %**	**Pramlintide % (*w*/*w*)**
Tre100	16.6 ± 2.7	-
Tre85-Leu15	29.3± 1.8	-
Tre85-Leu25-P0.3	29.4± 3.2	0.29 ± 0.01
Raff100	25.0±2.1	-
Raff85-Leu15	42.02±1.5	-
Raff85-Leu25-P0.3	39.55±1.7	0.20 ± 0.01
HA-92kDa100	61.81±2.4	-
HA92kDa85-Leu15	64.11±2.3	-
HA9285-Leu25-P0.3	65.72±1.9	0.24 ± 0.01
HA804kDa100	51.74±2.2	-
HA804kDa85-Leu15	48.49±1.7	-
HA804kDa85-Leu25-P0.3	51.19±1.8	0.15 ± 0.01

The HPLC analysis was carried out with the aim of determining the fraction of the drug stable after the drying process. Although the process typically occurs in milliseconds, it can lead to the degradation of the peptide if not adequately stabilised by the bulking agent [10]. In general, small molecules are better able to stabilise macromolecules during freeze drying or spray drying. This is due to the greater number of interactions such as hydrogen bonds that can be formed during drying, up to the complete replacement of the bonds that the macromolecule formed with the starting aqueous medium [27]. As mentioned before in this chapter, this is not the only critical step as even the residual water in the formulation can lead to hydrolysis phenomena. Finally, the recrystallisation of the excipients can cause a loss of interactions between API and bulking agent and the reduction of the stabilising effect [14]. In the case of trehalose, the correlation between low molecular weight and the best stabilising capacity seems to be confirmed. Table 4 reports the drug content after the spray drying process: in the powder containing trehalose, the pramlintide content decreased from the expected value by 3%, while raffinose demonstrated less ability as a peptide stabiliser, and the titre of pramlintide was reduced by 33%. Regarding the HA 92 kDa, it was found to be an acceptable stabilising agent with a reduction of the titre of 17%. The lowest percentage of the drug was instead found in high molecular weight HA powder. In this case, the titre obtained by HPLC was reduced by 49%.

The particle morphology was visualised using SEM (Figure 2). The spray-dried trehalose alone (Figure 2A) under the spray drying conditions used, forms large particles with a surface that at 150 times magnification appears as porous or formed by the fusion of smaller particles. When leucine has been added, particles appear as predominantly spherical and with a smooth surface (Figure 2B) even when pramlintide was added to the formulation the morphology was kept as described (Figure 2C). **The presence of leucine was therefore advantageous as it allowed to obtain spherical particles.**

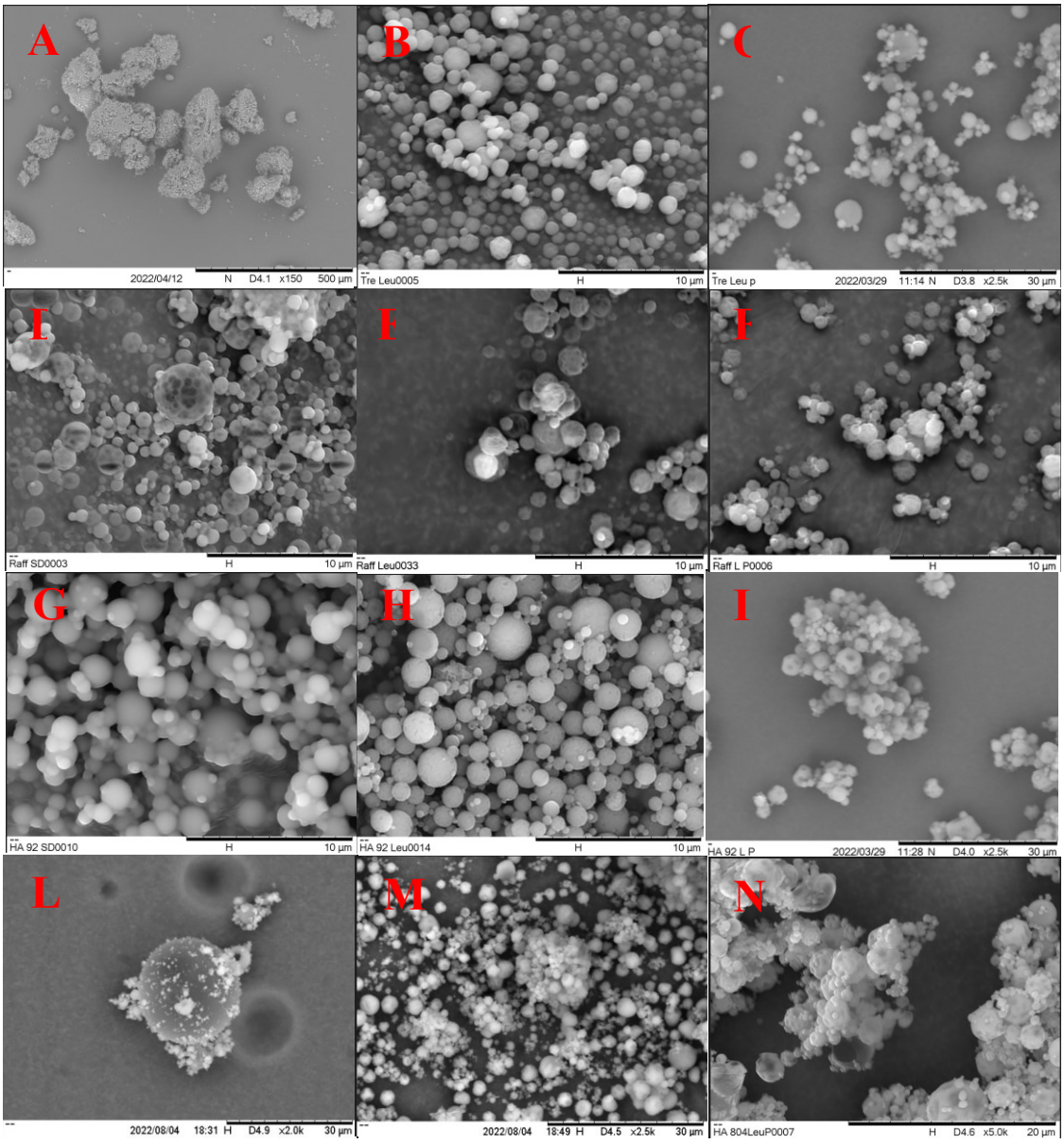

Figure 2 SEM images of spray-dried powders of Tre100 **A**), Tre85-Leu15 **B**), Tre85-Leu15-P0.3 **C**), Raff100 **D**), Raff85-Leu15 **E**), Raff85-Leu15_P0.3 **F**), HA 92kDa100 **G**), HA92kDa85-Leu15 **H**); HA 92kDa85-Leu15-P0.3 **I**), HA 804kDa100 **L**), HA 804kDa85-Leu15 **M**), HA804kDa85-Leu15-P0.3 **N**). Tre= trehalose; Raff= raffinose; HA=sodium hyaluronate. Leu=Leucine. Numbers represent the percentage (*w*/*w*) of each component.

The raffinose particles appear spherical and, in some cases, it was possible to observe ripples which make the surface of the particles rough. In this case, the effect of leucine does not appear to have contributed significantly to the modification of the particle's surface morphology (Figures 2D, E and F). It can be concluded that compared to

trehalose, raffinose is a more beneficial sugar for the formation of small spherical microparticles.

The spray-dried HA 92kDa alone particles (Figure 2G) appear like large spherical agglomerates of particles fused together (Figure 2G). When the leucine was added, particles appeared with a spherical shape, and no signs of fusion were visible. Moreover, when the peptide was included, the surface appeared partially collapsed giving rise to corrugated and "doughnut-like" particles. This feature is because the protein is a viscoelastic component which therefore decreases the stiffness of the particle surface during drying. This consideration has been widely reported in the literature for many peptides [130].

Particles produced with HA high molecular weight alone (Figure 2L) appeared as a heterogeneous particle assemblage consisting of large (>20 μm) swollen particles to which small satellite particles were adhered. The addition of leucine led to the formation of particles which appeared homogeneous in size (lower than 10 μm), although even in this case it was sometimes possible to observe the presence of small particles adhering to larger particles. As observed for the HA low molecular weight the addition of the peptide led to the formation of small dimples on the surface.

The observation of irregular surfaces could be a positive aspect since would reduce the contact area between the particles and would favour their redispersion, as previously reported for the [30]. Beside the effect on the surface characteristics, the addition of leucine appeared of extreme importance to dry the particles in individual structure and to avoid aggregates of fused particles [127]. For this reason, the 15% w/w leucine has been kept all the peptide formulation.

The characterisation of pramlintide-containing powders was then continued by screening the aerodynamic diameter and geometrical standard deviation using APS. Table 5 reports the MMAD and GSD values of the powders containing pramlintide, embedded in the microparticles produced with the different bulking agents.

Table 5. MMAD and GSD values of spray dried powders containing pramlintide, bulk excipient and leucine; Tre= Trehalose; Raff= Raffinose; HA92=Sodium hyaluronate of 92kDa; HA804= Sodium hyaluronate of 804 kDa; Leu= Leucine; Pram= Pramlintide. Data are presented as mean and st. dev of n=10.

	MMAD (μm)	GSD
Tre85_Leu15_P0.3	2.27± 0.55	1.92 ± 0.26
Raff85_Leu15_P0.3	2.08 ± 0.64	1.80 ± 0.41
HA92kDa85_Leu15_P0.3	1.85 ± 0.17	1.69 ± 0.17
HA804kDa85_Leu15_P0.3	2.47 ± 0.49	1.75 ± 0.15

The spray drying process led to the formation of particles with aerodynamic characteristics which are potentially suitable for inhalational administration to the lung. In fact, no value capable of excluding these formulations from the study emerged from this analysis. This demonstrated that the spray drying manufacturing process was robust and repeatable even using different excipients. In general, therefore, the particles were found to have a smaller diameter of less than 5 μm and the GSD values reported a narrow distribution for all the samples.

X-Ray Powder Diffraction

As previously mentioned, the solid state of the powders is a critical parameter that influences the stability of the active ingredients in the spray-dried product. For this reason, following production, the powders were analysed by XRPD. The drying process, in this case, also had the objective of forming particles consisting of material in the amorphous state which could therefore form a matrix which protected the peptide from degradation. Figure 3 illustrates the x-ray powder diffraction for the bulk excipients raw material, leucine and for the three powders produced with each excipient.

The spray drying process led to the formation of mainly amorphous particles. The characteristic peaks of the raw trehalose dihydrate, and raffinose pentahydrate raw materials, were no longer observed in the spray-dried powders (Figures 3A and B). As regards the hyaluronic acid (Figure 3 C and D) at the two molecular weights, no peaks in raw materials were observed. The analysis, therefore, reported "halos", characteristic of amorphous materials.

In all spray-dried powders containing leucine, a peak at 3.5° (2θ) could be observed. The presence of this peak is attributable to the presence of leucine in crystalline form. Leucine is typically crystalline in spray-dried formulations, as it usually reaches supersaturation earlier than other components, causing recrystallisation [27].

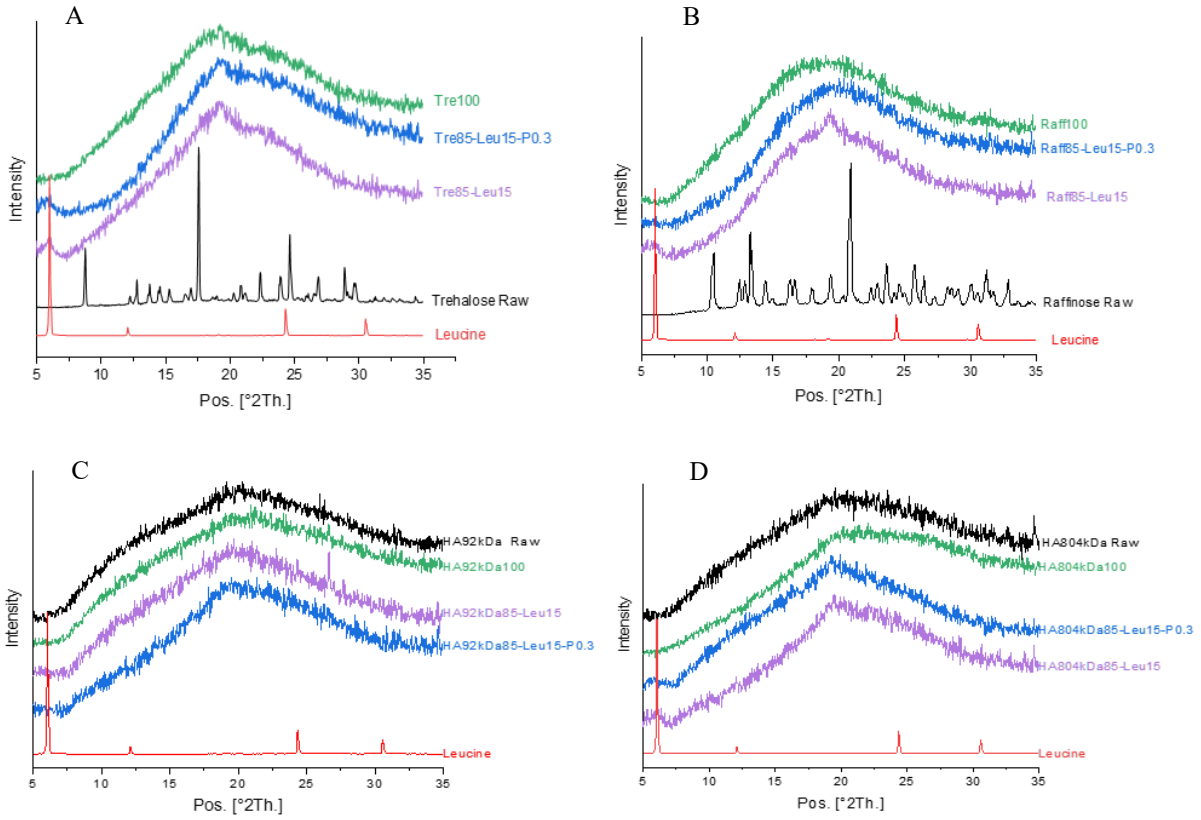

Figure 3. XRPD patterns of: Raw trehalose (black), trehalose SD (Tre100) (green), trehalose with leucine (Tre85-Leu15) (purple), trehalose with leucine and pramlintide (Tre85-Leu15-P0.3) (blue) (**A**); Raw raffinose (black), raffinose SD (Raff100) (green), raffinose with leucine (Raff85-Leu15) (purple), raffinose with leucine and pramlintide (Raff85-Leu15-P0.3) (blue), (**B**); Raw HA 92 kDa (black), HA 92 kDa SD (HA92kDa100) (green), HA 92 kDa with leucine (HA92kDa_Leu15) (purple), HA 92 kDa with leucine and pramlintide (HA92kDa_Leu15_P0.3) (blue), (**C**); raw HA 804 kDa (black), HA 804 kDa SD (HA804kDa100) (green), HA 804 kDa with leucine (HA804kDa85_Leu15) (purple), HA 804 kDa with leucine and pramlintide (HA804kDa85_Leu15_P0.3) (blue), (**D**). Raw L-leucine (red).

Subsequently, information about physical and chemical changes that involve endothermic or exothermic processes or changes in heat capacity of spray-dried powders, compared to raw materials, were obtained throw DSC analysis.

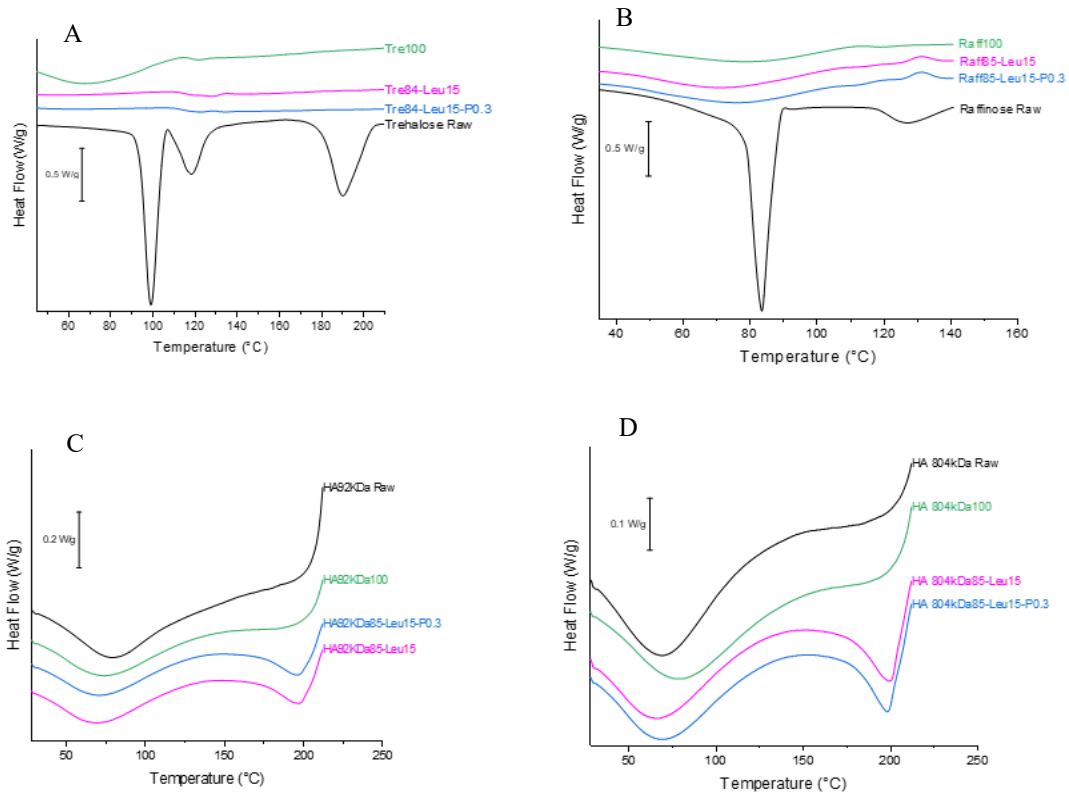

Figure 4. DSC thermograms of: Raw trehalose (black), trehalose SD (Tre100) (green), trehalose with leucine (Tre85-Leu15) (purple), trehalose with leucine and pramlintide (Tre85-Leu15-P0.3) (blue) (**A**); Raw raffinose (black), raffinose SD (Raff100) (green), raffinose with leucine (Raff85-Leu15) (purple), raffinose with leucine and pramlintide (Raff85-Leu15-P0.3) (blue), (**B**); Raw HA 92 kDa (black), HA 92 kDa SD (HA92kDa100) (green), HA 92 kDa with leucine (HA92kDa_Leu15) (purple), HA 92 kDa with leucine and pramlintide (HA92kDa_Leu15_P0.3) (blue), (**C**); raw HA 804 kDa (black), HA 804 kDa SD (HA804kDa100) (green), HA 804 kDa with leucine (HA804kDa85_Leu15) (purple), HA 804 kDa with leucine and pramlintide (HA804kDa85_Leu15_P0.3) (blue), (**D**).

Figure 4A shows the DSC scan of raw trehalose dihydrate (black) raw material. This thermogram is characterised by three endothermic peaks. The first two peaks at 99°C and 118°C, respectively, indicate the dehydration process, as previously reported in the literature [131], while the peak at 190°C could be ascribed as the melting of the anhydrous trehalose [131]. Trehalose SD, on the other hand, presents a broad endothermic event from 25 to 110°C which would correspond to the loss of water, followed by another thermal event at 119°C, corresponding to the glass transition

process in agreement with the data of Ogain *et al.* [121]. In the case of spray-dried trehalose powders containing leucine or leucine and pramlintide, the moisture loss phenomena were not observed, indicating a low water residual content. Finally, for all the three SD-trehalose powders, any recrystallisation peak was identified; hence any melting at 190°C was observed.

Figure 4B shows the thermogram of the raw raffinose pentahydrate and the spray-dried raffinose powders. In raw raffinose pentahydrate, a single endothermic peak is observed, often wrongly indicated in the literature as a melting peak [132, 133]. More properly, rather than melting, the raffinose pentahydrate collapses during dehydration with the release of the five bound water molecules, observable with the endothermic peak at 83.68°C.

No clear endothermic melting peak was observed for the trace. In literature, the same pattern was reported and the authors explained that raffinose dehydrates around 80°C and collapses into an amorphous form, and thus no melting peak was observed [133]. They also reported that no crystallization occurred on cooling raffinose in the metastable liquid form. Finally, the event observable at 122.5°C is attributable to the glass transition [121].

Being amorphous, sodium hyaluronate (HA) did not present particular thermal events, except for the loss of water observable in Figure 4 C and D between 50 and 100°C. All powders prepared using both HA 92 804kDa showed similar thermal behaviour.

Thermogravimetric analysis

The thermogravimetric analysis was carried out with the aim of studying the water content following the spray drying process in the powders. The final water content represents a parameter that is sometimes critical, as the free water molecules in the powder can lead to the fusion of the particles with loss of the initial characteristics. The residual water could also favour the recrystallisation process of the amorphous substances. Ultimately, this process would constitute the loss of the stabilising effect

of the macromolecules, explained by the theory of vitrification, which would lead the molecules of the bulking agent to interact less with the active principle and potentially lead to more rapid degradation of the API.

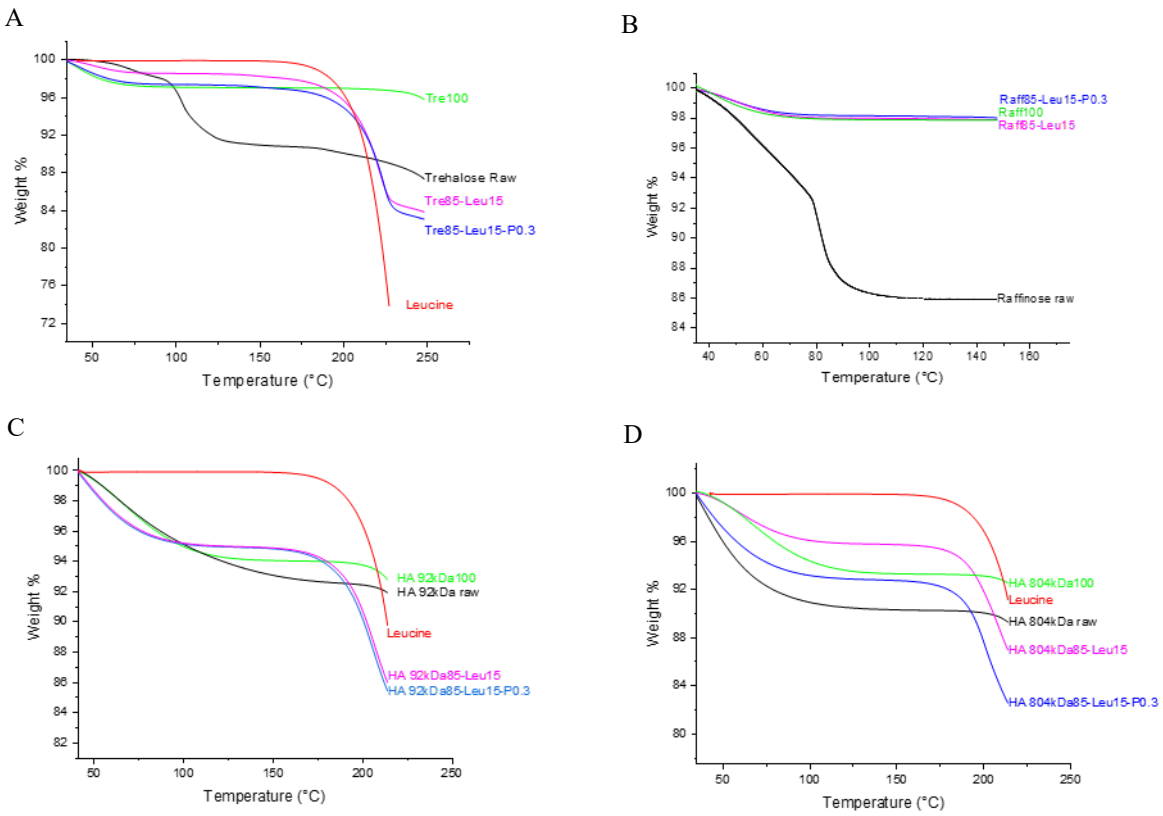

Figure 5. Thermogravimetric analysis of: Raw trehalose (black), trehalose SD (Tre100) (green), trehalose with leucine (Tre85-Leu15) (purple), trehalose with leucine and pramlintide (Tre85-Leu15-P0.3) (blue) (**A**); Raw raffinose (black), raffinose SD (Raff100) (green), raffinose with leucine (Raff85-Leu15) (purple), raffinose with leucine and pramlintide (Raff85-Leu15-P0.3) (blue), (**B**); Raw HA 92 kDa (black), HA 92 kDa SD (HA92kDa100) (green), HA 92 kDa with leucine (HA92kDa_Leu15) (purple), HA 92 kDa with leucine and pramlintide (HA92kDa_Leu15_P0.3) (blue), (**C**); raw HA 804 kDa (black), HA 804 kDa SD (HA804kDa100) (green), HA 804 kDa with leucine (HA804kDa85_Leu15) (purple), HA 804 kDa with leucine and pramlintide (HA804kDa85_Leu15_P0.3) (blue), (**D**). Raw Leucine (red).

Raw trehalose dihydrate (Figure 5A) showed in a first weight loss between 50-80°C corresponding to the evaporation of the moisture present in the powder. A second weight loss between 90-140 °C was due to the dehydration of two molecules of bounded water in the crystal corresponding to a loss of 9.45% on the initial weight.

Finally, a third weight loss was observed after 190°C, corresponding to the beginning of the degradation after the melting peak of the material observed in the DSC.

The spray-dried powders did not show a weight loss attributable to the loss of molecules of bounded water, and the weight loss observable at the beginning of the thermal process is associated with the evaporation of water on the surface of the particles. The degradation of leucine above 180°C causes a rapid loss of weight in the samples containing it.

Analogous observations can be made on the TGA analysis of the samples obtained using raffinose (Figure 5B). In raw raffinose pentahydrate, it was observed a first weight loss attributable to the evaporation of powder moisture until 80°C and a second rapid weight loss between 80°C and 120 °C, attributable to the loss of 5 molecules of water corresponding to a total weight loss of 14.28%.

The spray drying process led to the formation of particles of amorphous material, and the water loss observed in the powders produced was between 1.92 and 2.32 %, related to the residual water absorbed on particles not removed during spray drying. In the case of raffinose powders, the analysis was stopped at 150 °C (before the degradation of the material), and therefore the effect of leucine on weight loss above 200°C is not observable.

The low molecular weight HA had a water content of 13.41%, while it was 6.58% after spray drying and 6.92% in the powder containing leucine and 6.10% in the powder containing leucine and pramlintide.

The water content of high molecular weight HA was 10.37 % and 6.96%, 4.76 %, and 6.50 % for the spray-dried powders of HA only, HA and leucine and HA leucine and pramlintide, respectively (Figure 5C and D).

Stability Investigation

The stability study was carried out one month after the production of the powders and carried out under the conditions indicated in the methods. The study aimed to investigate the effect of exposure of the formulations to different humidity and temperature conditions on pramlintide stability in spray-dried powders. Different types of characterisations were performed.

Regarding the **particle morphology** (Figure 6), it was found that the trehalose, during the period of stability at 25°C 60%RH and 40°C 75%RH, had reported a significant morphological modification, the particles were in fact aggregated in microparticles of irregular shape and with dimensions of about 100 μm. The raffinose powder particles had lost the spherical shape observed at time 0 and appeared as irregularly shaped particles, often in the form of larger aggregates. Therefore, in the case of trehalose and raffinose sugars, the process of exposure to stability conditions caused significant modifications for both powders. The sodium hyaluronate particles, on the other hand, maintained a morphology congruent with what was observed immediately after production. However, the lower molecular weight of sodium hyaluronate resulted in having a surface, albeit rounded, but with ripples on the surface of the particle. Similar modifications of the surface of the high molecular weight sodium hyaluronate had been observed. Also in this case, the particles, even if they had maintained the spherical shape, resulted in having a less smooth surface and sharper edges.

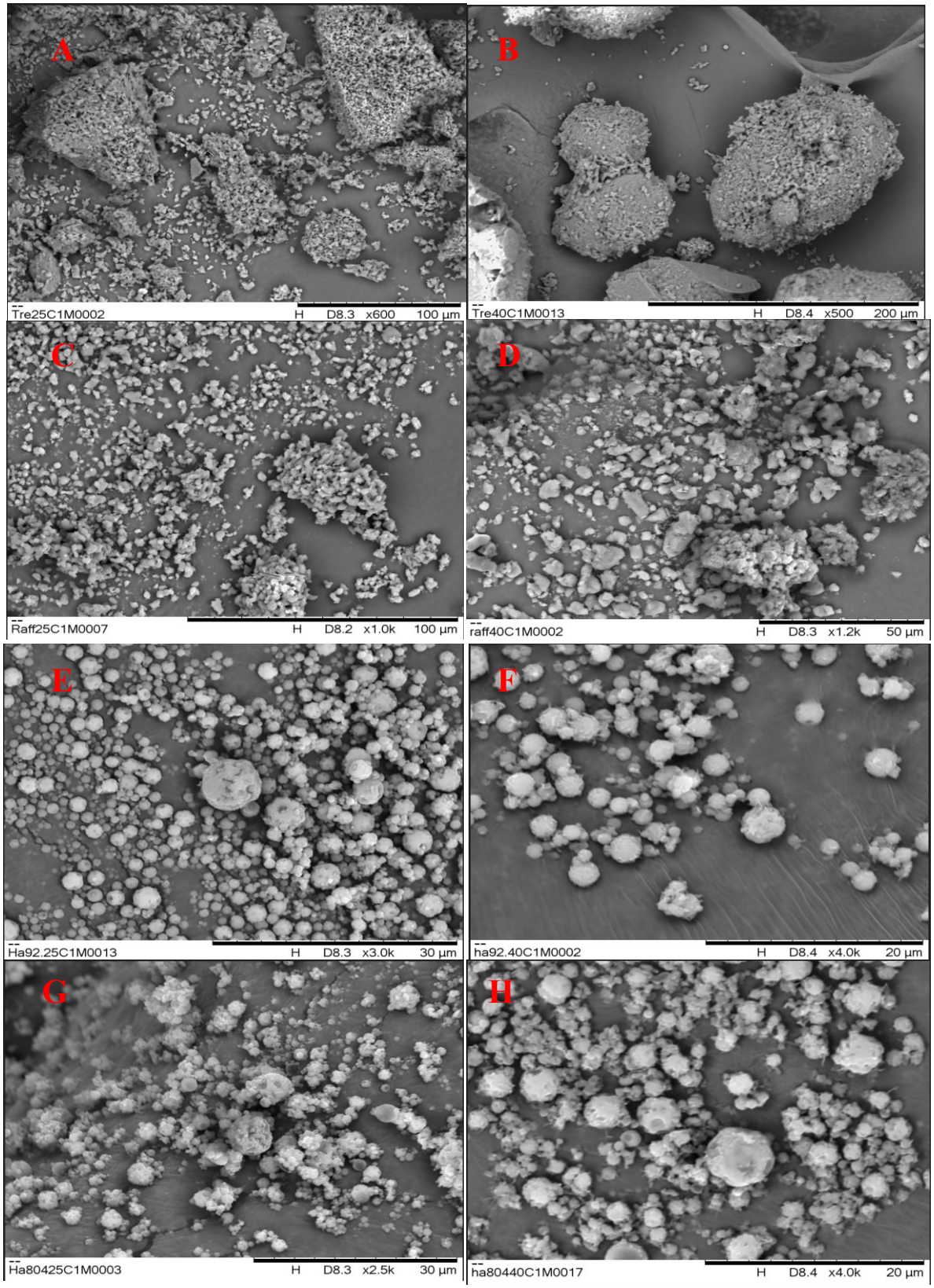

Figure 6. SEM images of spray dried powders after one month of stability at 25°C 60%RH and 40°C 75%RH : Trehalose with leucine and pramlintide (Tre85-Leu15-P0.3) **A,B**) raffinose leucine and pramlintide (Raff85-Leu15-P0.3) **C,D**), HA 92 kDa leucine and pramlintide (HA92kDa85-Leu15-P0.3) **E,F**), HA 804 kDa leucine and pramlintide (HA804kDa85-Leu15-P0.3) **G,H**).

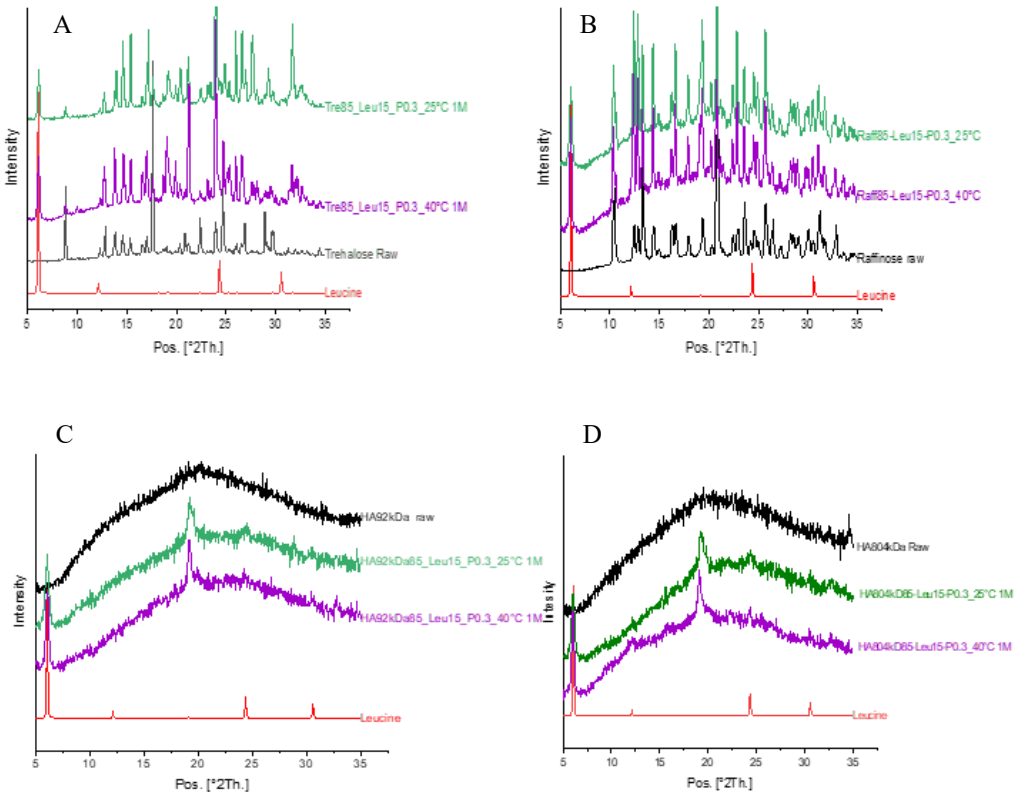

Figure 7 XRPD scans of; Trehalose raw material (black), Trehalose with leucine and pramlintide at 25°C and 60% RH (Tre85-Leu15-P0.3 25°C 1M) (green) and 40°C 75% RH (Tre85-Leu15-P0.3 40°C 1M) (purple) **A**); Raffinose raw material (black), Raffinose with leucine and pramlintide at 25°C and 60% RH (Raff85-Leu15-P0.3 25°C 1M) (green) and 40°C 75% RH (Raff85-Leu15-P0.3 40°C 1M) (purple) **B**); HA92 kDa raw material (black), HA92 kDa with leucine and pramlintide at 25°C and 60% RH (HA92kDa85-Leu15-P0.3 25°C 1M) (green) and 40°C 75% RH (HA92kDa85-Leu15-P0.3 40°C 1M) (purple) **C**); HA804 kDa with leucine and pramlintide at 25°C and 60% RH (HA804kDa85-Leu15-P0.3 25°C 1M) (green) and 40°C 75% RH (HA804kDa85-Leu15-P0.3 40°C 1M) (purple) **D**); Raw leucine: red.

XRPD data in Figure 7, demonstrates that a great change in solid-state structure occurred when sugar was used as a bulking agent for both trehalose and raffinose. The typical pattern of the amorphous solid observed after production disappeared, and for both the sugar powders stored at 25 or 40°C, many typical peaks of the crystalline solid appeared in the trace. On the contrary, the powders containing the polymer sodium hyaluronate were mainly amorphous, albeit a peak around 19°θ was detected. This could be attributable to a crystalline leucine which presented a small peak at that degree.

DSC scan of trehalose sprayed with leucine and pramlintide (Figure 8A) both stored at 25°C and 60% RH or 40°C and 75% RH, were found to have an endothermic peak at 100°C, corresponding to the first dehydration peak of raw trehalose dihydrate. Furthermore, the observed water loss was around 9.6%, corresponding to the loss of two water molecules. In this case, it was not possible to observe the second endothermic event associated with the dehydration nor the melting peak; this phenomenon can be explained by the destruction of the crystalline structure during the evaporation of water, with subsequent collapse into an amorphous state [131].

Raffinose spray dried with leucine and pramlintide, under the two conditions tested, showed the presence of the dehydration peak present in raw material raffinose, suggesting, as in the case of trehalose powders, that recrystallisation during the period of stability occurred (Figure 8B).

The powders produced with sodium hyaluronate at the two different molecular weights, leucine and pramlintide, did not undergo particular variations in the thermogram, except for the different intensity of the endothermic signal relating to the degradation of leucine which has become less evident (Figure 8 C and D).

In summary, the DSC results were complementary and in agreement with the XRPD analysis and confirmed that HA was more favourable than sugars preserving the amorphous state of the microparticles.

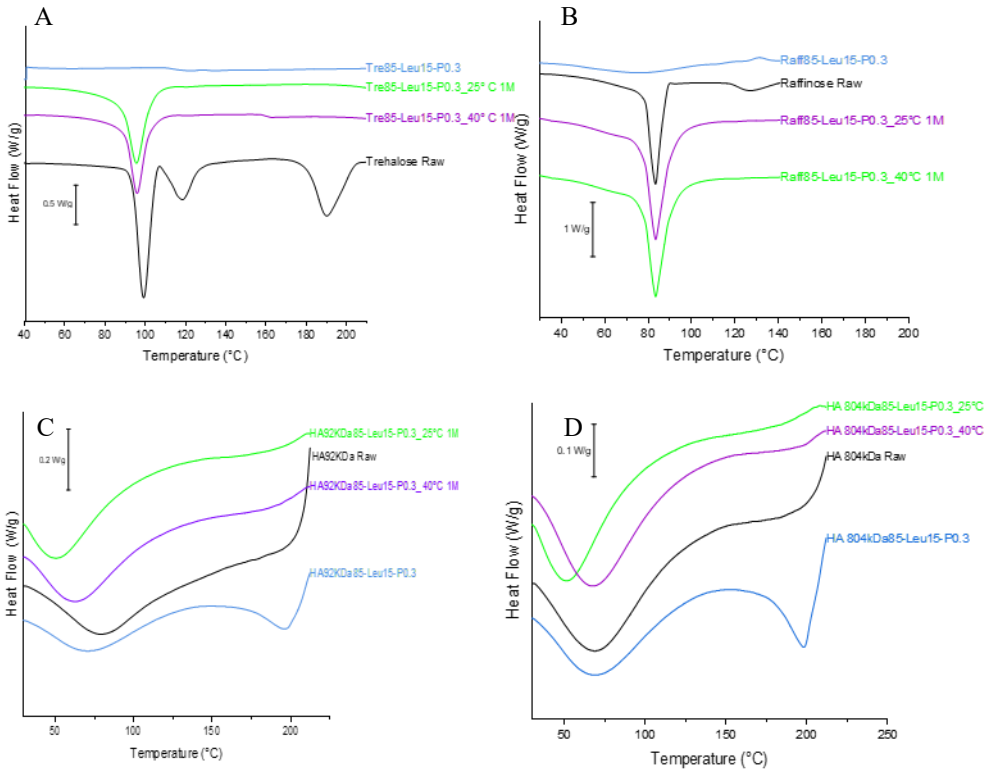

Figure 8. DSC thermograms of powders of trehalose under stability conditions. Trehalose raw material (black), Trehalose with leucine and pramlintide at 25°C and 60% RH (Tre85-Leu15-P0.3 25°C 1M) (green) and 40°C 75% RH (Tre85-Leu15-P0.3 40°C 1M) (purple), and at time 0 (blue) **A**); Raffinose raw material (black), Raffinose with leucine and pramlintide at 25°C and 60% RH (Raff85-Leu15-P0.3 25°C 1M) (green) and 40°C 75% RH (Raff85-Leu15-P0.3 40°C 1M) (purple), and at time 0 (blue) **B**); HA92 kDa raw material (black), HA92 kDa with leucine and pramlintide at 25°C and 60% RH (HA92kDa85-Leu15-P0.3 25°C 1M) (green) and 40°C 75% RH (HA92kDa85-Leu15-P0.3 40°C 1M) (purple) and at time 0 (blue) **C**); HA804 kDa with leucine and pramlintide at 25°C and 60% RH (HA804kDa85-Leu15-P0.3 25°C 1M) (green) and 40°C 75% RH (HA804kDa85-Leu15-P0.3 40°C 1M) (purple) and at time 0 (blue) **D**); Raw leucine: red.

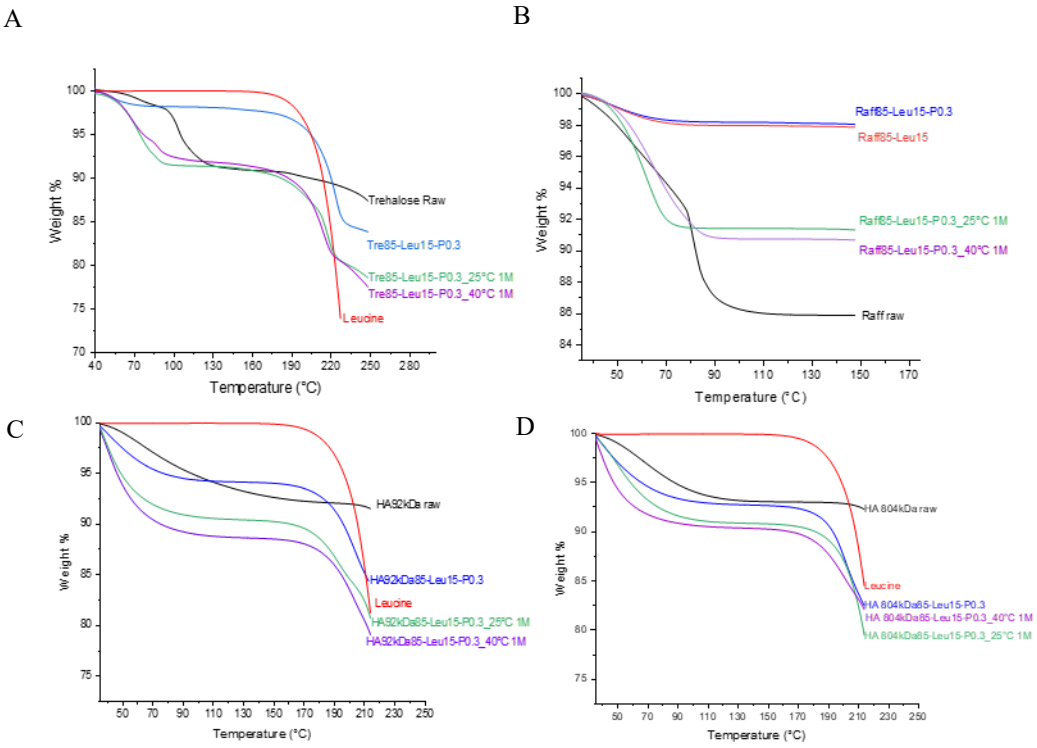

Figure 9. TGA analysis after stability study of spray-dried pramlintide and leucine-containing powders of: Trehalose raw material (black), Trehalose with leucine and pramlintide at 25°C and 60% RH (Tre85-Leu15-P0.3 25°C 1M) (green) and 40°C 75% RH (Tre85-Leu15-P0.3 40°C 1M) (purple), and at time 0 (blue) **A**); Raffinose raw material (black), Raffinose with leucine and pramlintide at 25°C and 60% RH (Raff85-Leu15-P0.3 25°C 1M) (green) and 40°C 75% RH (Raff85-Leu15-P0.3 40°C 1M) (purple), and at time 0 (blue) **B**); HA92 kDa raw material (black), HA92 kDa with leucine and pramlintide at 25°C and 60% RH (HA92kDa85-Leu15-P0.3 25°C 1M) (green) and 40°C 75% RH (HA92kDa85-Leu15-P0.3 40°C 1M) (purple) and at time 0 (blue) **C**); HA804 kDa with leucine and pramlintide at 25°C and 60% RH (HA804kDa85-Leu15-P0.3 25°C 1M) (green) and 40°C 75% RH (HA804kDa85-Leu15-P0.3 40°C 1M) (purple) and at time 0 (blue) **D**); Raw leucine: red.

The TGA analysis first made it possible to highlight that compared to the analysis at T0 (Figure 9), the powders had a significantly higher water content certainly induced by the storage conditions. In fact, it should be underlined that the powders were kept in direct contact with humidity. These applied storage conditions had the objective of accelerating potential changes that perhaps would have occurred more slowly over time. However, while the trehalose had bonded a number of water molecules equal to that of the raw material, in the case of powders with raffinose, the weight loss was lower than in the raw material. From the analysis of the TGA data it was possible to calculate that the weight loss of 9% corresponded to the loss of 3 water molecules from

the crystal. The formation of raffinose trihydrate from the amorphous form is possible and previously described by Kajiwara and Franks [132].

Sodium hyaluronate, on the other hand, had demonstrated a maintenance of its characteristics, observable from these analyses.

Pramlintide quantification in spray-dried powders after stability study

The drug content was assessed after storage. The percentage of pramlintide in the formulations was obtained by considering the quantity of drug loaded at the beginning of the production of the formulation as 100% (*i.e.* 0.3% *w/w*). Figure 10 illustrates the percentage of stable pramlintide in the formulations produced with each bulking agent, at time 0 and after one month under the conditions of the stability study.

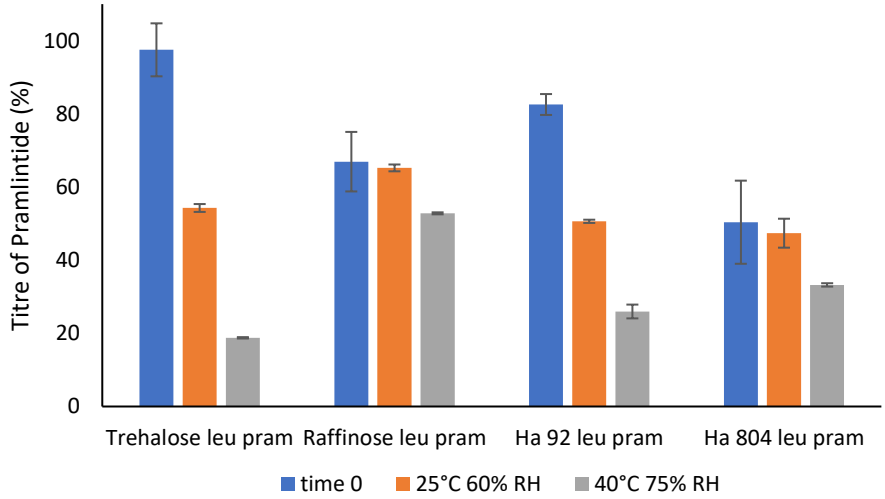

Figure 10. Percentage of pramlintide (with respect to the theoretical value of 0.3 % w/w) in the formulation after one month of stability. In powders of trehalose leucine and pramlintide (Tre85-Leu15-P0.3); Raffinose leucine and pramlintide (Raff85-Leu15-P0.3), HA92kDa leucine and pramlintide (HA92kDa85-Leu15-P0.3), HA804kDa leucine and pramlintide (HA804kDa85-Leu15-P0.3)Time 0 represents the content of pramlintide after spray drying.

Although we showed trehalose to be an effective stabilising agent for pramlintide during the spray drying process, the titre underwent a significant decrease already at 25°C, but when exposed to 40°C, the peptide was degraded more than in the other formulations. Raffinose, on the other hand, although initially, did not protect the peptide as trehalose, instead kept its content almost unchanged at 25°C, with a reduction of the titer at 40°C up to 52.8%. The low molecular weight HA, similar, to

trehalose, during stability led to a drastic reduction of the titre compared to the value at time zero, with a value of 50.6 and 25.9 % when stored at 25°and 40°C, respectively. The high molecular weight HA used instead allowed a variation of only 3% in the value of the titre at 25°C compared to the initial value, and at 40°C with a decrease was about 17%.

In general, it was observed that, while trehalose and HA 92 kDa are better-stabilising agents during drying, raffinose and higher molecular weight sodium hyaluronate, causing strong initial degradation of the peptide, albeit maintaining the titre value of pramlintide more stable than the initial value obtained after spray drying (time 0).

5.5 Conclusions

In this study, it was possible to produce by spray drying, dry powders formulations containing pramlintide, a peptide hormone used as an adjunctive treatment for the treatment of diabetes and potentially in weight reduction for patients with obesity. The powders produced were potentially suitable for inhalation administration. The production process made it possible to obtain powders in the amorphous state in the case of trehalose and raffinose, while it did not cause evident degradation of the sodium hyaluronate powders. The choice of excipients used is, therefore, a critical parameter, which in this case, significantly influenced the stability of the peptide. During drying, it was possible to discriminate the effect of the different excipients used. In particular, it was seen that trehalose dihydrate and 92 kDa sodium hyaluronate led to the stabilisation of the peptide in this phase. These formulations, in particular, could represent a valid strategy in the administration of this peptide by the pulmonary route offering an alternative and non-invasive strategy to subcutaneous administration.

General conclusions

In conclusion, the thesis work has resulted in the development of three powders for inhalation administration. In the first part of this work, the dissolution of the spray-dried CsA was improved. The design of experiment led to the selection of the mannitol and ethanol content used for the powder formulation. This powder, containing 20% (*w*/*w*) of mannitol and 45% (*w*/*v*) of ethanol, has also shown to have antiviral effects against Sars-CoV-2 and anti-inflammatory effects in *in vitro* tests. This formulation would be useful both in the context of preventing transplant rejection and containing the inflammatory process and viral activity in patients affected by Covid-19.

In the second part of the work, CsA has loaded into calcium phosphate-coated liposomes with the aim of potentially increasing cell uptake and reducing the dose required for the prevention of lung rejection. In this study, the presence of the coating was demonstrated using different methods such as the variation of the Z-potential, the effect of reconstitution in buffers at different pH, direct observation by cryo-TEM, and calcium titration. Subsequently, the liposomal dispersion was transformed into a powder using mannitol as a bulking agent. This formulation led to an increased anti-inflammatory effect compared to the raw CsA, demonstrating the increased efficacy due to the liposomal system combined with the coating.

In the latter part of this thesis, a pramlintide-containing inhalation powder was formulated for blood glucose control in diabetic patients and potentially to obtain weight reduction in patients with obesity. The powder was produced using non-reducing sugars (trehalose and raffinose) or sodium hyaluronate at 92 and 804 kDa to stabilize the solid-state formulation. It was observed that trehalose dihydrate and 92 kDa sodium hyaluronate led to better stabilization of the peptide compared to other excipients used. The inhalation powder could represent an interesting alternative strategy for the administration of this peptide, which is currently only administered subcutaneously.

Overall, the development of these inhalation powders represents a promising step toward improving drug delivery of the selected peptides. Further *in vivo* studies are needed to evaluate the efficacy and safety of these powders.

Acknowledgements

First of all, I would like to thank my supervisor Professor Francesca Buttini for giving me the opportunity to have this experience and always guiding me in the realization of this project. I would like to thank my co-supervisor, Professor Fabio Sonvico and Professor Bettini, for all the helpful advice and support I received during this period.

I would also like to thank Professor Simona Bertoni's group at the University of Parma for carrying out the experiments concerning the ELISA and viability assays and Professor Vittorio Sambri's group of Microbiology Unite of Cesena for carrying out the analyses with SARS-CoV-2. I also thank the research group of the University of Copenhagen, in particular Professor Mingshi Yang, for giving me the opportunity to carry out the last part of my doctoral project in his laboratories.

I also thank my colleagues Doctor Eride Quarta, Giada Varacca, Stefania Glieca, Giulia Carretta, Fabiola Guareschi, and Gianluca Bazzoli for all the support and daily help received.

6. REFERENCES

1. Anderson PJ (2005) History of Aerosol Therapy : Liquid Nebulization to MDIs to DPIs Ceramic Inhalers (19th Century). Respir Care 50:1139–1149
2. Rospond B, Krakowska A, Muszynska B, Opoka Wł (2022) The history, current state and perspectives of aerosol therapy. Acta Pharm 72:225–243
3. de Boer AH, Hagedoorn P, Hoppentocht M, Buttini F, Grasmeijer F, Frijlink HW (2017) Dry powder inhalation: past, present and future. Expert Opin Drug Deliv. https://doi.org/10.1080/17425247.2016.1224846
4. Hickey AJ (2020) Emerging trends in inhaled drug delivery. Adv Drug Deliv Rev 157:63–70
5. Fröhlich E, Mercuri A, Wu S, Salar-Behzadi S (2016) Measurements of deposition, lung surface area and lung fluid for simulation of inhaled compounds. Front Pharmacol 7:1–10
6. Wang YB, Watts AB, Peters JI, Williams RO (2014) The impact of pulmonary diseases on the fate of inhaled medicines - A review. Int J Pharm 461:112–128
7. Patton JS, Fishburn CS, Weers JG (2004) The lungs as a portal of entry for systemic drug delivery. Proc Am Thorac Soc 1:338–344
8. Borghardt JM, Kloft C, Sharma A (2018) Inhaled Therapy in Respiratory Disease: The Complex Interplay of Pulmonary Kinetic Processes. Can Respir J. https://doi.org/10.1155/2018/2732017
9. Wright J, Brocklebank D, Ram F (2002) Inhaler devices for the treatment of asthma and chronic obstructive airways disease (COPD). Qual Saf Heal Care 11:376–382
10. Hickey AJ, da Rocha SR. (2019) Pharmaceutical Inhalation Aerosol Technology, Third Edit.
11. Weibel ER (1963) Morphometry of the Human Lung With a Foreword.
12. Lansley AB (1993) Mucociliary clearance and drug delivery via the respiratory tract. Adv Drug Deliv Rev 11:299–327
13. Todoroff J, Vanbever R (2011) Fate of nanomedicines in the lungs. Curr Opin Colloid Interface Sci 16:246–254
14. Ke WR, Chang RYK, Chan HK (2022) Engineering the right formulation for enhanced drug delivery. Adv Drug Deliv Rev 191:114561
15. Haagsman HP, Diemel R V. (2001) Surfactant-associated proteins: Functions and structural variation. Comp Biochem Physiol - A Mol Integr Physiol 129:91–

16. Bernhard W (2016) Lung surfactant: Function and composition in the context of development and respiratory physiology. Ann Anat 208:146–150

17. Pérez-Gil J (2008) Structure of pulmonary surfactant membranes and films: The role of proteins and lipid-protein interactions. Biochim Biophys Acta - Biomembr 1778:1676–1695

18. Tonnis WF, Lexmond AJ, Frijlink HW, De Boer AH, Hinrichs WLJ (2013) Devices and formulations for pulmonary vaccination. Expert Opin Drug Deliv 10:1383–1397

19. Rossi I, Spagnoli G, Buttini F, et al (2021) A respirable HPV-L2 dry-powder vaccine with GLA as amphiphilic lubricant and immune-adjuvant. J Control Release 340:209–220

20. Fathe K, Ferrati S, Moraga-Espinoza D, Yazdi A, D.C. Smyth H (2016) Inhaled Biologics: From Preclinical to Product Approval. Curr Pharm Des 22:2501–2521

21. Zhou Q, Gengenbach T, Denman JA, Yu HH, Li J, Chan HK (2014) Synergistic antibiotic combination powders of colistin and rifampicin provide high aerosolization efficiency and moisture protection. AAPS J 16:37–47

22. FDA (2019) Inactive ingredient search for approved drug products. FDA Approv. drug Prod.

23. Islam N, Gladki E (2008) Dry powder inhalers (DPIs)—A review of device reliability and innovation. Int J Pharm 360:1–11

24. Dal Negro RW (2015) Dry powder inhalers and the right things to remember: A concept review. Multidiscip Respir Med 10:2–5

25. Clark AR, Weers JG, Dhand R (2020) The Confusing World of Dry Powder Inhalers: It Is All about Inspiratory Pressures, Not Inspiratory Flow Rates. J Aerosol Med Pulm Drug Deliv 33:1–11

26. Scherließ R, Bock S, Bungert N, Neustock A, Valentin L (2022) Particle engineering in dry powders for inhalation. Eur J Pharm Sci. https://doi.org/10.1016/j.ejps.2022.106158

27. Vehring R (2008) Pharmaceutical particle engineering via spray drying. Pharm Res 25:999–1022

28. Maikawa CL, D'Aquino AI, Lal RA, Buckingham BA, Appel EA (2021) Engineering biopharmaceutical formulations to improve diabetes management. Sci Transl Med 13:1–12

29. Mensink MA, Frijlink HW, van der Voort Maarschalk K, Hinrichs WLJ (2017) How sugars protect proteins in the solid state and during drying (review): Mechanisms of stabilization in relation to stress conditions. Eur J Pharm

Biopharm 114:288–295

30. Chew NYK, Chan H (2006) Use of Solid Corrugated Particles to Enhance Powder Aerosol Performance. Pharm Res 18:1570–1577

31. Mitchell MJ, Billingsley MM, Haley RM, Wechsler ME, Peppas NA, Langer R (2021) Engineering precision nanoparticles for drug delivery. Nat Rev Drug Discov 20:101–124

32. Bassetti M, Vena A, Russo A, Peghin M (2020) Inhaled Liposomal Antimicrobial Delivery in Lung Infections. Drugs 80:1309–1318

33. Cipolla D, Blanchard J, Gonda I (2016) Development of liposomal ciprofloxacin to treat lung infections. Pharmaceutics 8:1–31

34. Alton EWFW, Armstrong DK, Ashby D, et al (2015) Repeated nebulisation of non-viral CFTR gene therapy in patients with cystic fibrosis: a randomised, double-blind, placebo-controlled, phase 2b trial. Lancet Respir Med 3:684–691

35. Wittgen BPH, Kunst PWA, Van Der Born K, Van Wijk AW, Perkins W, Pilkiewicz FG, Perez-Soler R, Nicholson S, Peters GJ, Postmus PE (2007) Phase I study of aerosolized SLIT cisplatin in the treatment of patients with carcinoma of the lung. Clin Cancer Res 13:2414–2421

36. Olivier KN, Griffith DE, Eagle G, et al (2017) Randomized trial of liposomal amikacin for inhalation in nontuberculous mycobacterial lung disease. Am J Respir Crit Care Med 195:814–823

37. Tagami T, Ando Y, Ozeki T (2017) Fabrication of liposomal doxorubicin exhibiting ultrasensitivity against phospholipase A2 for efficient pulmonary drug delivery to lung cancers. Int J Pharm 517:35–41

38. Khatib I, Tang P, Ruan J, Cipolla D, Dayton F, Blanchard JD, Chan HK (2020) Formation of ciprofloxacin nanocrystals within liposomes by spray drying for controlled release via inhalation. Int J Pharm 578:119045

39. Chougule M (2007) Nano-liposomal dry powder inhaler of tacrolimus : Preparation , characterization , and pulmonary pharmacokinetics. 2434187:675–688

40. Berton P, Mishra MK, Choudhary H, Myerson AS, Rogers RD (2019) Solubility Studies of Cyclosporine Using Ionic Liquids. ACS Omega 4:7938–7943

41. Sonvico F, Chierici V, Varacca G, Quarta E, D'Angelo D, Forbes B, Buttini F (2021) Respicelltm: An innovative dissolution apparatus for inhaled products. Pharmaceutics 13:1–18

42. Langenbucher F (1972) Letters to the Editor: Linearization of dissolution rate curves by the Weibull distribution. J Pharm Pharmacol 24:979–981

43. Li Y, Su R, Chen J, Li Y, Su R, Chen J (2020) Co-culture Systems of Drug-

Treated Acute Myeloid Leukemia Cells and T Cells for In Vitro and In Vivo Study. STAR Protoc 1:1–19

44. Burnett L, McQueen MJ, Jonsson JJ, Torricelli F (2007) IFCC Position Paper: Report of the IFCC Taskforce on Ethics: Introduction and framework. Clin Chem Lab Med 45:1098–1104

45. Sato H, Kawabata Y, Yuminoki K, Hashimoto N, Yamauchi Y (2012) Comparative studies on physicochemical stability of cyclosporine A-loaded amorphous solid dispersions. Int J Pharm 426:302–306

46. Yamasaki K, Kwok PCL, Fukushige K, Prud'Homme RK, Chan HK (2011) Enhanced dissolution of inhalable cyclosporine nano-matrix particles with mannitol as matrix former. Int J Pharm 420:34–42

47. Leung SSY, Wong J, Guerra HV, Samnick K, Prud'homme RK, Chan HK (2017) Porous mannitol carrier for pulmonary delivery of cyclosporine A nanoparticles. AAPS J 19:578–586

48. Sato H, Suzuki H, Yakushiji K, Wong J, Seto Y, Prud'homme RK, Chan HK, Onoue S (2016) Biopharmaceutical Evaluation of Novel Cyclosporine A Nano-matrix Particles for Inhalation. Pharm Res 33:2107–2116

49. Corcoran TE, Smaldone GC, Dauber JH, Smith DA, McCurry KR, Burckart GJ, Zeevi A, Griffith BP, Iacono AT (2004) Preservation of post-transplant lung function with aerosol cyclosporin. Eur Respir J 23:378–383

50. Iacono AT, Johnson BA, Grgurich WF, et al (2006) A randomized trial of inhaled cyclosporine in lung-transplant recipients. N Engl J Med 354:141–150

51. Iacono A (2021) Capitalizing on the concept of local immune suppression by inhalation for lung transplant recipients. Am J Transplant 9–11

52. Neurohr C, Kneidinger N, Ghiani A, et al (2022) A randomized controlled trial of liposomal cyclosporine A for inhalation in the prevention of bronchiolitis obliterans syndrome following lung transplantation. Am J Transplant 22:222–229

53. Behr J, Zimmermann G, Baumgartner R, et al (2009) Lung deposition of a liposomal cyclosporine a inhalation solution in patients after lung transplantation. J Aerosol Med Pulm Drug Deliv 22:121–129

54. Wu X, Zhang W, Hayes D, Mansour HM (2013) Physicochemical characterization and aerosol dispersion performance of organic solution advanced spray-dried cyclosporine A multifunctional particles for dry powder inhalation aerosol delivery. Int J Nanomedicine 8:1269–1283

55. Suzuki H, Ueno K, Mizumoto T, Seto Y, Sato H, Onoue S (2017) Self-micellizing solid dispersion of cyclosporine A for pulmonary delivery: Physicochemical, pharmacokinetic and safety assessments. Eur J Pharm Sci 96:107–114

56. Yang TT, Wen BF, Liu K, Qin M, Gao YY, Ding DJ, Li WT, Zhang YX, Zhang WF (2018) Cyclosporine A/porous quaternized chitosan microspheres as a novel pulmonary drug delivery system. Artif Cells, Nanomedicine Biotechnol 46:552–564

57. Anderson S, Atkins P, Bäckman P, et al (2022) Inhaled Medicines: Past, Present, and Future. Pharmacol Rev 74:50–118

58. Sosnik A, Seremeta KP (2015) Advantages and challenges of the spray-drying technology for the production of pure drug particles and drug-loaded polymeric carriers. Adv Colloid Interface Sci 223:40–54

59. Belotti S, Rossi A, Colombo P, Bettini R, Rekkas D, Politis S, Colombo G, Balducci AG, Buttini F (2014) Spray dried amikacin powder for inhalation in cystic fibrosis patients: A quality by design approach for product construction. Int J Pharm 471:507–515

60. Guisado-Vascoa P, Valderas-Ortegab S, Carralòn-Gonzalez MM, et al (2020) Clinical characteristics and outcomes among hospitalized adults with severe COVID-19 admitted to a tertiary medical center and receiving antiviral , antimalarials , glucocorticoids , or immunomodulation with tocilizumab or cyclosporine : A retrospective o. EClinicalMedicine 28:1–10

61. Buttini F, Quarta E, Allegrini C, Lavorini F (2021) Understanding the importance of capsules in dry powder inhalers. Pharmaceutics 13:1–15

62. Wheeler DS, Misumi K, Walker NM, Vittal R, Combs MP, Aoki Y, Braeuer RR, Lama VN (2021) Interleukin 6 trans-signaling is a critical driver of lung allograft fibrosis. Am J Transplant 21:2360–2371

63. Rose-John S, Winthrop K, Calabrese L (2017) The role of IL-6 in host defence against infections: Immunobiology and clinical implications. Nat Rev Rheumatol 13:399–409, 10.1038/nrrheum.2017.83.

64. Zhou J, He W, Liang J, Wang L, Yu X, Bao M, Liu H (2021) Association of Interleukin-6 Levels with Morbidity and Mortality in Patients with Coronavirus Disease 2019 (COVID-19). 293–298

65. Reisi Nassab P, Blazsó G, Nyári T, Falkay G, Szabó-Révész P (2008) In vitro and in vivo investigations on the binary meloxicam-mannitol system. Pharmazie 63:319–320

66. Blumberg EA, Noll JH, Tebas P, et al (2022) A phase I trial of cyclosporine for hospitalized patients with COVID-19. JCI Insight 7:1–11

67. de Wilde AH, Zevenhoven-Dobbe JC, van der Meer Y, Thiel V, Narayanan K, Makino S, Snijder EJ, van Hemert MJ (2011) Cyclosporin A inhibits the replication of diverse coronaviruses. J Gen Virol 92:2542–2548

68. Prasad K, Ahamad S, Kanipakam H, Gupta D, Kumar V (2021) Simultaneous

Inhibition of SARS-CoV-2 Entry Pathways by Cyclosporine. ACS Chem Neurosci 12:930–944

69. Czogalla A (2009) Oral cyclosporine A - The current picture of its liposomal and other delivery systems. Cell Mol Biol Lett 14:139–152

70. Ammerman N, Beier-Sexton M, Azad A (2009) Growth and Maintenance of Vero Cell Lines. Curr Protoc Microbiol APPENDIX:1–10

71. Lei C, Yang J, Hu J, Sun X (2020) On the Calculation of TCID50 for Quantitation of Virus Infectivity. Virol Sin. https://doi.org/10.1007/s12250-020-00230-5

72. Reed LJ, Muench H (1938) A simple method of estimating fifty per cent endpoints. Am J Epidemiol 27:493–497

73. Jiang X, Zhao Y, Guan Q, Xiao S, Dong W, Lian S, Zhang H, Liu M, Wang Z, Han J (2022) Amorphous solid dispersions of cyclosporine A with improved bioavailability prepared via hot melt extrusion: Formulation, physicochemical characterization, and in vivo evaluation. Eur J Pharm Sci 168:1–9

74. Benetti AA, Bianchera A, Buttini F, Bertocchi L, Bettini R (2021) Mannitol polymorphs as carrier in dpis formulations: Isolation characterization and performance. Pharmaceutics 13:1–21

75. Adi H, Young PM, Chan HK, Agus H, Traini D (2010) Co-spray-dried mannitol-ciprofloxacin dry powder inhaler formulation for cystic fibrosis and chronic obstructive pulmonary disease. Eur J Pharm Sci 40:239–247

76. Iacono A, Wijesinha M, Rajagopal K, Murdock N, Timofte I, Griffith B, Terrin M (2019) A randomised single-centre trial of inhaled liposomal cyclosporine for bronchiolitis obliterans syndrome post-lung transplantation. ERJ Open Res 5:1–11

77. Bangham AD, Horne RW (1964) Negative staining of phospholipids and their structural modification by surface-active agents as observed in the electron microscope. J Mol Biol 8:660–668

78. Mehta PP, Ghoshal D, Pawar AP, Kadam SS, Dhapte-Pawar VS (2020) Recent advances in inhalable liposomes for treatment of pulmonary diseases: Concept to clinical stance. J Drug Deliv Sci Technol 56:101509

79. Kim E, Jeong H (2021) Liposomes : Biomedical Applications. 27–35

80. Ali A, Khaled K, Almatroodi SA, Almatroudi A, Husain A (2020) Recent strategies towards the surface modification of liposomes : an innovative approach for different clinical applications. 3 Biotech 10:1–15

81. Hamill RJ (2013) Amphotericin B formulations: A comparative review of efficacy and toxicity. Drugs 73:919–934

82. Slobbe L, Boersma E, Rijnders BJA (2008) Pulmonary Pharmacology &

Therapeutics Tolerability of prophylactic aerosolized liposomal amphotericin-B and impact on pulmonary function : Data from a randomized placebo-controlled trial. 21:855–859

83. Loo AS, Muhsin SA, Walsh TJ (2013) Toxicokinetic and mechanistic basis for the safety and tolerability of liposomal amphotericin B. Expert Opin Drug Saf 12:881–895

84. Liu JC, Modha DE, Gaillard EA (2013) What is the clinical significance of filamentous fungi positive sputum cultures in patients with cystic fibrosis? J Cyst Fibros 12:187–193

85. Esposti LD, Carella F, Adamiano A, Tampieri A, Iafisco M (2018) Calcium Phosphate-Based Nanosystems for Advanced Targeted Nanomedicine. Drug Dev Ind Pharm 44:1223–1238

86. Thakkar HP, Baser AK, Parmar MP, Patel KH, Ramachandra Murthy R (2012) Vincristine-sulphateloaded liposome-templated calcium phosphate nanoshell as potential tumor-targeting delivery system. J Liposome Res 22:139–147

87. Ingvarsson PT, Yang M, Nielsen HMø, Rantanen J, Foged C (2011) Stabilization of liposomes during drying. Expert Opin Drug Deliv 8:375–388

88. Ziaee A, Albadarin AB, Padrela L, Ung MT, Femmer T, Walker G, O'Reilly E (2020) A rational approach towards spray drying of biopharmaceuticals: The case of lysozyme. Powder Technol 366:206–215

89. Vehring R, Foss WR, Lechuga-Ballesteros D (2007) Particle formation in spray drying. J Aerosol Sci 38:728–746

90. Danaei M, Kalantari M, Raji M, Samareh Fekri H, Saber R, Asnani GP, Mortazavi SM, Mozafari MR, Rasti B, Taheriazam A (2018) Probing nanoliposomes using single particle analytical techniques: effect of excipients, solvents, phase transition and zeta potential. Heliyon 4:e01088

91. Notices G, Methods H, Spectrochemistry P, Spectrochemistry P (2021) Anhydrous Dibasic Calcium Phosphate. 4–6

92. Stewart PL (2017) Cryo-electron microscopy and cryo-electron tomography of nanoparticles. Wiley Interdiscip Rev Nanomedicine Nanobiotechnology 9:1–16

93. Li Y, Su R, Chen J (2020) Co-culture Systems of Drug-Treated Acute Myeloid Leukemia Cells and T Cells for In Vitro and In Vivo Study. STAR Protoc 1:100097

94. Danaei M, Dehghankhold M, Ataei S, Hasanzadeh Davarani F, Javanmard R, Dokhani A, Khorasani S, Mozafari MR (2018) Impact of particle size and polydispersity index on the clinical applications of lipidic nanocarrier systems. Pharmaceutics 10:1–17

95. Rytting E, Nguyen J, Wang X, Kissel T (2008) Biodegradable polymeric

nanocarriers for pulmonary drug delivery. Expert Opin Drug Deliv 5:629–639

96. Chen M, Liu X, Fahr A (2011) Skin penetration and deposition of carboxyfluorescein and temoporfin from different lipid vesicular systems : In vitro study with finite and infinite dosage application. Int J Pharm 408:223–234

97. Konate K, Josse E, Viv E, Deshayes S (2021) Peptide-Based Nanoparticles for Therapeutic Nucleic.

98. Services H (2018) Liposome Drug Products Guidance for Industry Liposome Drug Products.

99. Shrestha S, Wang B, Dutta P (2020) Nanoparticle processing : Understanding and controlling aggregation. Adv Colloid Interface Sci 279:102162

100. Pochapski DJ, Carvalho Dos Santos C, Leite GW, Pulcinelli SH, Santilli CV (2021) Zeta Potential and Colloidal Stability Predictions for Inorganic Nanoparticle Dispersions: Effects of Experimental Conditions and Electrokinetic Models on the Interpretation of Results. Langmuir 37:13379–13389

101. Quarta E, Sonvico F, Bettini R, et al (2021) Inhalable microparticles embedding calcium phosphate nanoparticles for heart targeting: The formulation experimental design. Pharmaceutics. https://doi.org/10.3390/pharmaceutics13111825

102. Pilcer G, Amighi K (2010) Formulation strategy and use of excipients in pulmonary drug delivery. Int J Pharm 392:1–19

103. Poursina N, Vatanara A, Rouini MR, Gilani K, Rouholamini Najafabadi A (2015) Systemic delivery of parathyroid hormone (1?34) using spray freeze-dried inhalable particles. Pharm Dev Technol 00:1–7

104. Steckel H, Bolzen N (2004) Alternative sugars as potential carriers for dry powder inhalations. Int J Pharm 270:297–306

105. Chimote G, Banerjee R (2005) Lung surfactant dysfunction in tuberculosis : Effect of mycobacterial tubercular lipids on dipalmitoylphosphatidylcholine surface activity. 45:215–223

106. Mueller M, Brandenburg K, Dedrick R, Schromm AB, Seydel U (2005) Phospholipids Inhibit Lipopolysaccharide (LPS)-Induced Cell Activation: A Role for LPS-Binding Protein. J Immunol 174:1091–1096

107. Kuronuma K, Mitsuzawa H, Takeda K, Nishitani C, Chan ED, Kuroki Y, Nakamura M, Voelker DR (2009) Anionic pulmonary surfactant phospholipids inhibit inflammatory responses from alveolar macrophages and U937 cells by binding the lipopolysaccharide-interacting proteins CD14 and MD-2. J Biol Chem 284:25488–25500

108. Komalla V, Allam VSRR, Kwok PCL, et al (2020) A phospholipid-based

formulation for the treatment of airway inflammation in chronic respiratory diseases. Eur J Pharm Biopharm 157:47–58

109. Aronne LJ, Halseth AE, Burns CM, Miller S, Shen LZ (2010) Enhanced weight loss following coadministration of pramlintide with sibutramine or phentermine in a multicenter trial. Obesity 18:1739–1746

110. Young A (2005) Inhibition of Glucagon Secretion. Adv Pharmacol 52:151–171

111. Reda TK, Geliebter A, Pi-Sunyer FX (2002) Amylin, food intake, and obesity. Obes Res 10:1087–1091

112. Ryan GJ, Jobe LJ, Martin R (2005) Pramlintide in the treatment of type 1 and type 2 diabetes mellitus. Clin Ther 27:1500–1512

113. McQueen J, Bonk ME (2005) Pramlintide acetate. Am J Heal Pharm 62:2363–2372

114. Chapman I, Parker B, Doran S, et al (2005) Effect of pramlintide on satiety and food intake in obese subjects and subjects with type 2 diabetes. Diabetologia 48:838–848

115. Chapman I, Parker B, Doran S, et al (2007) Low-dose pramlintide reduced food intake and meal duration in healthy, normal-weight subjects. Obesity 15:1179–1186

116. Carpenter JF, Crowe Jhon H. (1988) Modes of stabilization of a protein by organic solutes during desiccation.

117. Carpenter JF, Crowe JH (1989) An infrared spectroscopic study of the interactions of carbohydrates with dried proteins. Biochemistry 28:3916–3922

118. Chang LL, Pikal MJ (2009) Mechanisms of protein stabilization in the solid state. J Pharm Sci 98:2886–2908

119. Arakawa T, Prestrelski SJ, Kenney WC, Carpenter JF (2001) Factors affecting short-term and long-term stabilities of proteins. Adv Drug Deliv Rev 46:1–8

120. Crowe JH, Carpenter JF, Crowe LM (1998) The role of vitrification in anhydrobiosis. Annu Rev Physiol 60:73–103

121. Ógáin ON, Li J, Tajber L, Corrigan OI, Healy AM (2011) Particle engineering of materials for oral inhalation by dry powder inhalers. i - Particles of sugar excipients (trehalose and raffinose) for protein delivery. Int J Pharm 405:23–35

122. Mero A, Campisi M (2014) Hyaluronic acid bioconjugates for the delivery of bioactive molecules. Polymers (Basel) 6:346–369

123. Martinelli F, Balducci AG, Kumar A, Sonvico F, Forbes B, Bettini R, Buttini F (2017) Engineered sodium hyaluronate respirable dry powders for pulmonary drug delivery. Int J Pharm 517:286–295

124. Wan F, Maltesen MJ, Andersen SK, Bjerregaard S, Baldursdottir SG, Foged C, Rantanen J, Yang M (2014) Modulating protein release profiles by incorporating hyaluronic acid into PLGA microparticles via a spray dryer equipped with a 3-fluid nozzle. Pharm Res 31:2940–2951

125. Surendrakumar K, Martyn GP, Hodgers ECM, Jansen M, Blair JA (2003) Sustained release of insulin from sodium hyaluronate based dry powder formulations after pulmonary delivery to beagle dogs. J Control Release 91:385–394

126. Alhajj N, O'Reilly NJ, Cathcart H (2021) Leucine as an excipient in spray dried powder for inhalation. Drug Discov Today 26:2384–2396

127. Li L, Sun S, Parumasivam T, Denman JA, Gengenbach T, Tang P, Mao S, Chan HK (2016) L-Leucine as an excipient against moisture on in vitro aerosolization performances of highly hygroscopic spray-dried powders. Eur J Pharm Biopharm 102:132–141

128. Wang H, John W (1987) Particle Density Correction for the Aerodynamic Particle Sizer. Aerosol Sci Technol. https://doi.org/10.1080/02786828708959132

129. Chen BT, Cheng YS, Yeh HC (1985) Performance of a TSI aerodynamic particle sizer. Aerosol Sci Technol 4:89–97

130. Pinto JT, Faulhammer E, Dieplinger J, Dekner M, Makert C, Nieder M, Paudel A (2021) Progress in spray-drying of protein pharmaceuticals: Literature analysis of trends in formulation and process attributes. Dry Technol 39:1415–1446

131. Taylor LS, York P (1998) Characterization of the Phase Transitions of Trehalose Dihydrate on Heating and Subsequent Dehydration. J Pharm Sci 87:347–355

132. Kajiwara K, Franks F (1997) Crystalline and amorphous phases in the binary system water-raffinose. J Chem Soc - Faraday Trans 93:1779–1783

133. Moura Ramos JJ, Pinto SS, Diogo HP (2005) Molecular mobility in raffinose in the crystalline pentahydrate form and in the amorphous anhydrous form. Pharm Res 22:1142–1148